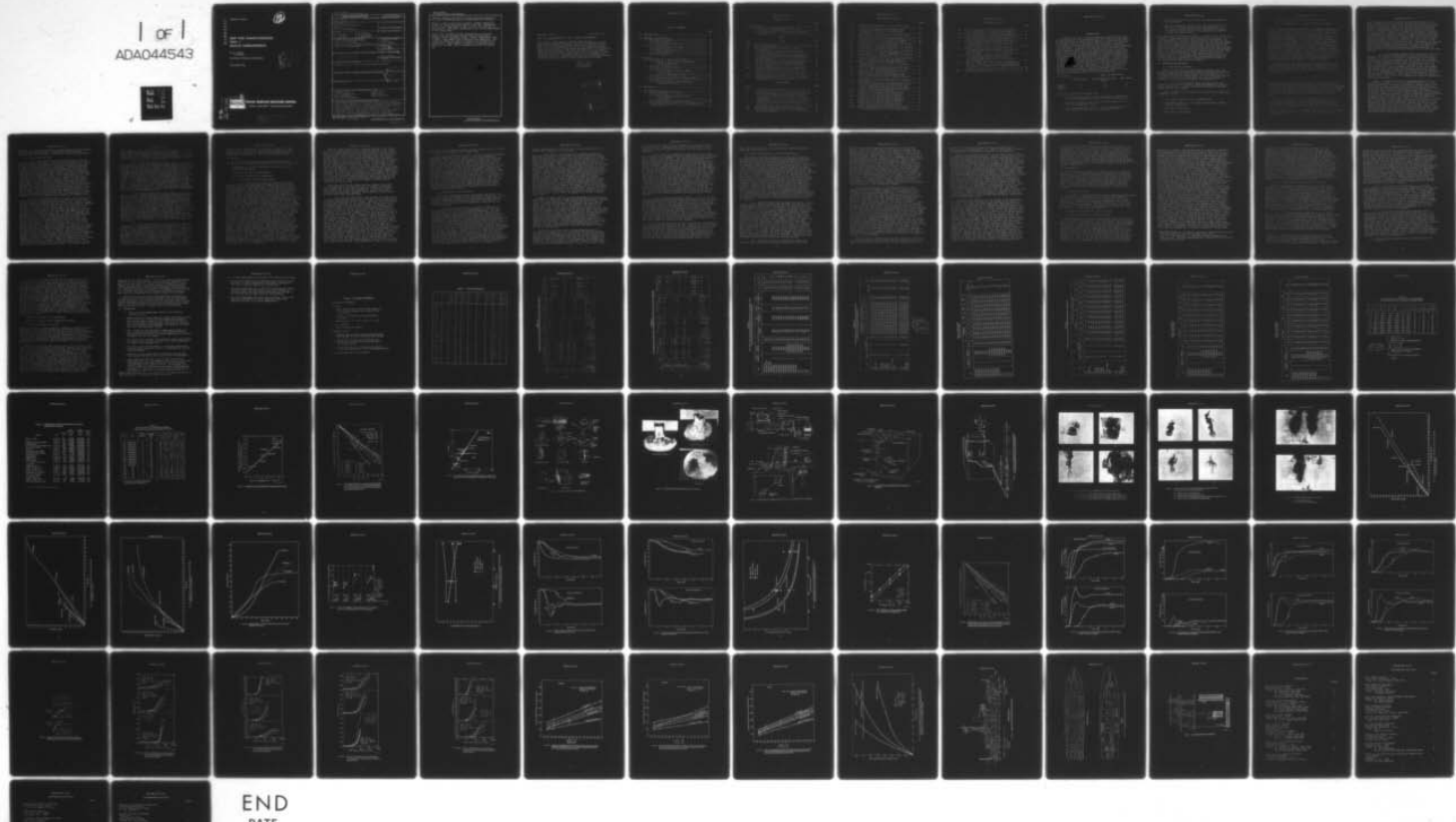


AD-A044 543 NAVAL SURFACE WEAPONS CENTER WHITE OAK LAB SILVER SP--ETC F/G 20/2
SHIP FIRE CHARACTERISTICS. PART 1. SEALED COMPARTMENTS, (U)
NOV 76 R S ALGER, S J WIERSMA, R G MCKEE
UNCLASSIFIED NSWC/WOL/TR-76-125 NL

1 of 1
ADA044543



END
DATE
FILED
10-77
DDC

ADA 044543

NSWC/WOL TR 76-125

19
B-5

SHIP FIRE CHARACTERISTICS

PART 1

SEALED COMPARTMENTS

BY R. S. ALGER
S. J. WIERSMA

RESEARCH & TECHNOLOGY DEPARTMENT

10 NOVEMBER 1976

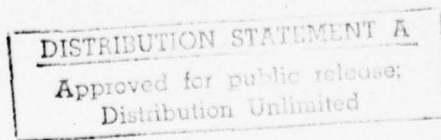


AD NO.
DDC FILE COPY



NAVAL SURFACE WEAPONS CENTER

Dahlgren, Virginia 22448 • Silver Spring, Maryland 20910



UNCLASSIFIED

SECURITY CLASSIFICATION OF THIS PAGE (When Data Entered)

REPORT DOCUMENTATION PAGE		READ INSTRUCTIONS BEFORE COMPLETING FORM
1. REPORT NUMBER <i>(14) NSWC/WOL/TR-76-125</i>	2. GOVT ACCESSION NO.	3. RECIPIENT'S CATALOG NUMBER
4. TITLE (and Subtitle) <i>(6) Ship Fire Characteristics, Part 1. Sealed Compartments,</i>	5. TYPE OF REPORT & PERIOD COVERED	
7. AUTHOR(s) <i>(10) R. S. Alger W. H. Johnson S. J. Wiersma F. I. Laughridge R. G. McKee L. L. Wiltshire</i>	6. PERFORMING ORG. REPORT NUMBER	
9. PERFORMING ORGANIZATION NAME AND ADDRESS <i>Naval Surface Weapons Center White Oak Laboratory White Oak, Silver Spring, Maryland 20910</i>	8. CONTRACT OR GRANT NUMBER(s)	
11. CONTROLLING OFFICE NAME AND ADDRESS	10. PROGRAM ELEMENT, PROJECT, TASK AREA & WORK UNIT NUMBERS <i>(11) 63514N ; 0 ; SSL32 ; WR 4831 ;</i>	
14. MONITORING AGENCY NAME & ADDRESS (if different from Controlling Office) <i>(16) SSL32</i>	12. REPORT DATE <i>10 Nov 1976</i>	
	13. NUMBER OF PAGES <i>75</i>	
	15. SECURITY CLASS. (of this report) <i>Unclassified</i>	
	15a. DECLASSIFICATION/DOWNGRADING SCHEDULE	
16. DISTRIBUTION STATEMENT (of this Report) Approved for public release; distribution unlimited	17. DISTRIBUTION STATEMENT (of the abstract entered in Block 20, if different from Report) <i>(17) DDC-PAK/ENCL SEP 26 1977</i>	
18. SUPPLEMENTARY NOTES		
19. KEY WORDS (Continue on reverse side if necessary and identify by block number) Shipboard Fire Sealed Compartments Fuel Parameters Ventilation Parameters	Oxygen Index Suppression Damage Threshold	
20. ABSTRACT (Continue on reverse side if necessary and identify by block number) To optimize weight and cost of fire protection for aluminum ships, it is essential to know the characteristics of the fire threat. Fire behavior is a function of the fuel and environment, particularly of ventilation; therefore, fire characteristics are studied as a function of typical conditions aboard Navy ships. This report covers the first part of a series of experiments dealing with various ventilation conditions. Fire characteristics such as burning rate, fuel		

UNCLASSIFIED

SECURITY CLASSIFICATION OF THIS PAGE(When Data Entered)

consumed, temporal and spatial heating patterns, and the O₂, CO₂, and CO concentrations at extinction were measured.

With all class A and B fuels examined, flaming combustion stopped at oxygen concentrations of 10-to 15%. Factors such as pool size, compartment volume, and fire location had as much effect on the oxygen concentration for self-extinguishment as the oxygen index.

Because fuel consumed has been proportional to available oxygen, the heat released and the thermal hazard can be estimated from compartment volume. Sealed compartments offer a simple, light weight form of passive fire protection. The concept of spaces too small to flashover is explored with a simple model. This approach to passive fire protection is applied to the PHM-1 and to components suitable for general use.

UNCLASSIFIED

SECURITY CLASSIFICATION OF THIS PAGE(When Data Entered)

NSWC/WOL/TR 76-125

10 November 1976

SHIP FIRE CHARACTERISTICS - PART 1 SEALED COMPARTMENTS

This report is the result of a joint effort of the Naval Surface Weapons Center and the Stanford Research Institute under contract N60921-75-C-0184. The work is sponsored by the Naval Sea Systems Command and the Naval Ship Engineering Center under Task Area S4643. This report represents part of a continuing effort to define problems associated with fires in light weight aluminum ship structures. This is the first of a series of reports which will deal with the phenomenology of the environment and recommend structural designs and procedures to minimize the problem. The first author was, until recently, employed at the NSWC.

Paul R. Wessel
PAUL R. WESSEL
By direction

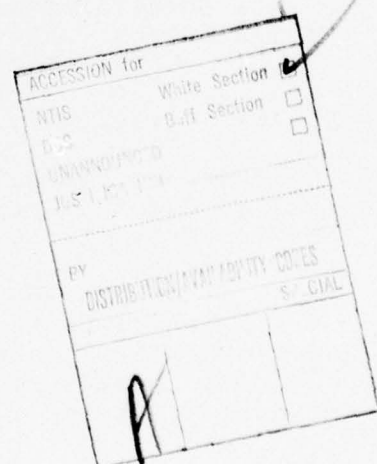


TABLE OF CONTENTS

	Page
1.0 INTRODUCTION.....	1
2.0 APPARATUS AND PROCEDURE.....	2
2.1 Experimental Variables.....	2
2.1.1 Fuel Parameters.....	2
2.1.2 Environmental Chambers.....	4
2.2 Fire Characteristics.....	5
2.2.1 Ignition and Fire Buildup.....	5
2.2.2 Burning Rates.....	5
2.2.3 Flame Characteristics.....	6
2.2.4 Thermal Fields.....	6
2.2.5 Gas Analysis.....	6
3.0 RESULTS.....	7
3.1 Fire Behavior in Sealed Compartments.....	7
3.1.1 Effects of Fuel and O ₂ Concentration on Flame Appearance.....	7
3.1.2 Burning Rates.....	8
3.2 Conditions for Extinguishment.....	9
3.2.1 Fuel Effects.....	9
3.2.2 Effects of Burning Rate on Oxygen Consumption.....	10
3.2.3 Effect of Compartment Volume.....	11
3.2.4 CO ₂ and CO Production.....	11
3.3 Energy Considerations and the Thermal Threat.....	12
3.3.1 Energy Released.....	12
3.3.2 Energy Arriving at and Absorbed by Compartment Surfaces.....	12
4.0 DISCUSSION.....	15
4.1 Non-Serious Fires.....	15
4.2 Sealed Compartments and Passive Fire Protection.....	17
4.2.1 Sealed Compartment Possibilities on the PHM-1.....	17
4.2.2 Sealed Bunks.....	18
4.2.3 Sealed Electronic Spacing Consoles.....	18
4.3 Thermal Insults Appropriate for Testing Materials and Structures.....	18

CONTENTS (Cont.)

	Page
5.0 CONCLUSIONS.....	20
5.1 Fires in Sealed Compartments Exhibit the Following Characteristics.....	20
5.2 Sealed Compartments as a Passive Fire Protection Technique.....	21

Tables

Table	Title	Page
2.0	Experimental Parameters.....	22
2.1	Fuel Characteristics.....	23
3.0	Burning Characteristics of Fuels in Sealed Compartments.....	24
3.1	Gas Concentrations When Fires are Suffocated in Sealed Compartments.....	25
3.2	Fuel Spray Fire Burning Characteristics and Gas Concentrations When the Fires are Suffocated in Sealed Chambers.....	26
3.3	Maximum Temperatures of Aluminum Panels Reached Before Fires in Sealed Room Self Extinguish.....	27
3.4	Time for Aluminum Panels to Reach Temperatures Listed in Table 3.3.....	29
4.0	Average Thermoflux Incident on the Chamber Walls Calculated According to the Simple Adiabatic Model.....	32
4.1	Comparison of Fire Hazard on PHM-1 by Available Oxygen Versus Fuel Loading.....	33
4.2	Maximum Thermoflux Incident on Sealed Compartment Bulkheads During Spray Fuel Fires.....	34

ILLUSTRATIONS

Figure		Page
2.0	Theoretical Oxygen Requirements to Burn Various Fuels.....	35
2.1	Relationship Between Total Energy Available per Ft^3 of Air and The Oxygen Concentration at Extin- guishment for Various Fuels Burning in a Sealed Compartment.....	36
2.2	Relation Between Liquid Burning Rates at Large Pool Diameters and a Thermochemical Properties of the Fuel.....	37
2.3	Various Solid Fuel Configurations.....	38
2.4	Melting and Flow Patterns of Plastic Samples.....	39
2.5	Experimental Arrangement for the 1.19, 7.94, and 102.4 Ft^3 Chambers.....	40

ILLUSTRATIONS (Cont.)

	Page
2.6 Experimental Arrangement for the 1050 Ft ³ Test Cell.....	41
2.7 Fuel Nozzle Arrangement for the Spray Fires and a Block Diagram of the Gas Analysis Equipment.....	42
3.0 Flame Geometry and Turbulence for Various Pool Sizes.....	43
3.1 Flame Structures at Various Stages During a 5 3/4" Dia JP-4 Pool Fire in the 102.4 Ft ³ Chamber.....	44
3.2 JP-4 Spray Fires in the 1050 Ft ³ Test Cell.....	45
3.3 Burning Rate, i.e., Weight Loss Curve, for 3" Dia. Pool Fires in 7.94 Ft ³ Compartment.....	46
3.4 Burning Rate, i.e., Weight Loss Curve, for 18" Pool Fires and in 1050 Ft ³ Test Cell.....	47
3.5 Burning Rate, i.e., Weight Loss Curve, for Class A Fires Burning in 7.94 Ft ³ Compartment.....	48
3.6 Burning Rate, i.e., Weight Loss Curve, for Class A Fire in 1050 Ft ³ Test Cell.....	49
3.7 Effect of Chamber Volume and Fire Pool Diameter on the O ₂ Concentration at Extinguishment.....	50
3.8 Effect of Nozzle Location and Spray Rate on Extinguishment O ₂ Concentration for JP-4 and Methanol Fires.....	51
3.9 Variation in O ₂ Concentration During JP-4 Spray Fires in 1050 Ft ³ Sealed Test Cell.....	52
3.10 Variation in O ₂ Concentration During Methanol Spray Fires in 1050 Ft ³ Test Cell.....	53
3.11 Effect of Spray Rate on Extinguishment Time for JP-4 and Methanol Fires in Sealed 1050 Ft ³ Test Cell.....	54
3.12 Fuel Burned in a Sealed Compartment as a Function of Chamber Size.....	55
3.13 Comparison of Theoretical and Experimental Values for the Available Energy per Ft ³ of Air in a Sealed Compartment When Burning Various Fuels.....	56
3.14 Variation in CO Concentration During JP-4 Spray Fires in 1050 Ft ³ Sealed Chamber.....	57
3.15 Variation in CO Concentrations During MeOH Spray Fires in 1050 Ft ³ Sealed Chamber.....	58
3.16 Variation in CO ₂ Concentration During JP-4 Spray Fires in 1050 Ft ³ Sealed Chamber.....	59
3.17 Variation in CO ₂ Concentration During MeOH Spray Fires in 1050 Ft ³ Sealed Chamber.....	60
3.18 Burning Rates and Total Energy Release as Obtained from Weight Loss Measurements.....	61
3.19A Spatial and Temporal Characteristics of Various Sized Methanol Fires in a Sealed Compartment.....	62

ILLUSTRATIONS (Cont.)

	Page
3.19B Spatial and Temporal Characteristics of Constant Area Methanol Fires in Sealed Compartments.....	63
3.20A Spatial and Temporal Characteristics of Various Sized Hexane Fires in a Sealed Compartment.....	64
3.20B Spatial and Temporal Characteristics of Constant Area Hexane Fires in Sealed Compartments.....	65
3.21 Effect of Chamber Volume to Surface Ratio on the Maximum Temperatures Reached by the Various Aluminum Panels of Fig. 2.5 and 2.6 During Hexane Fires.....	66
3.22 Effect of Chamber Volume to Surface Ratio on the Maximum Temperatures Reached by the Various Aluminum Panels of Fig. 2.5 and 2.6 During Acetone Fires.....	67
3.23 Effect of Chamber Volume to Surface Ratio on the Maximum Temperatures Reached by the Various Aluminum Panels of Fig. 2.5 and 2.6 During Methanol Fires.....	68
4.0 Effect of Chamber Size and the Heat Liberated by Burning a Cubic Foot of Air on the Thermal Insult Arriving at the Boundaries of a Simple Adiabatic Chamber.....	69
4.1 Compartment Arrangements for the PHM-1.....	70
4.2 Enclosed Bedding Techniques.....	72

INTRODUCTION

Shipboard fires are a long-standing Navy problem particularly during wartime when increased weapon and fuel loads, hurried tempos, and the potential for enemy action augment the normal hazards which in peacetime lead to an average of about 10 serious fires per year, i.e., damages in excess of \$100,000, and about four reportable fires per week. In recent years the fire problem has been compounded by the extensive application of aluminum in the construction of high performance craft and in the superstructures of conventional ships. The susceptibility of aluminum to fire damage coupled with lower manning levels prompts the demand for "more fire protection" and the design factors responsible for the switch to aluminum are responsible for the postscript "With less weight." Current efforts to improve the passive and active fire protection in aluminum ship structure are beset with uncertainties about the thermal insults to be expected and how the various fire characteristics respond to shipboard fuels and their environments. In order to dispel some of this uncertainty, the "characteristics of compartment fires" part of the fire protection program was designed to show how the three classes of common shipboard fuels burn under the various degrees of confinement listed in the following matrix:

Fuel Category	Degree of Confinement		
	sealed compts.	ventilation controlled compts.	open compts.
Class A	2	5	8
Class B	1	4	7
Class C	3	6	9

Particular questions of interest are:

- o In sealed volumes should hazard evaluations be based only on the fuel loadings or consider also the available oxygen?
- o What are the spatial and temporal heating characteristics of sealed compartment fires?
- o Under what conditions should a burning compartment be sealed or ventilated to optimize fire suppression efforts?

- o How do the thermal loads vary with the amount and pattern of ventilation?
- o What are appropriate thermal insult characteristics to be employed in testing ship materials and structures, i.e., do the fire characteristics differ sufficiently to permit a significant weight saving if the protection is based on a family of heating curves?

This report deals with matrix elements 1, 2, and 3, i.e., the various classes of sealed compartment fires and as such is the first of a trilogy planned to cover the three degrees of confinement. The scope examines the first two questions in detail and lays the groundwork for the remaining three. Simple models based on the available oxygen and the compartment volume to surface ratio provide a new approach to evaluating fire hazards and the conditions where serious fires cannot occur. Design principles based on these limited oxygen models are then applied to the passive fire protection of such ship areas as storage compartments, crews' quarters, and critical electrical cables. The temporal and spatial descriptions of the thermal input to the compartment walls also provide guidance for the most effective application of thermal insulation to protect the aluminum compartment structural members.

2.0 APPARATUS AND PROCEDURE

2.1 Experimental Variables

Table 2.0 classifies the experimental parameters under two categories, namely, the controlled variables pertaining to the fuel and environment and the measured quantities that describe the resulting fire and its extinguishment. In this section we consider the factors involved in the choice of fuels and environment to satisfy the first column of the matrix in section 1.0.

2.1.1 Fuel Parameters--Three characteristics were considered in selecting the fuels, chemical composition, physical state, and quantity. In each case fuels were picked to provide a wide range of the variable.

Table 2.1 summarizes the factors of interest from a combustion standpoint, namely,

- o The oxygen required to burn a pound of fuel
- o The oxygen index, i.e., the oxygen concentration needed to maintain combustion.
- o The heat of combustion
- o The heat of vaporization

- o Typical burning rates for liquids in open pools
- o Type of combustion, i.e., flaming, glowing, or both.

The stoichiometric oxygen requirements for a complete chemical reaction (column 3) vary by a factor of 3.5 from the fuels richest in hydrogen to sulfur. When this theoretical oxygen requirement is plotted as a function of the heat of combustion, i.e., (Figure 2.0), the energy released is almost linearly proportional to the oxygen requirement, i.e., the heat liberated is about 5.8 KBTU per lb of oxygen or on a volume basis about 110 BTU per ft³ of air if all the oxygen were to be consumed. When allowance is made for the oxygen index, i.e., about 15, which means only about 28% of the oxygen will be burned before self-extinguishment, the available energy per ft³ of air is reduced to about 31 BTU. For a specific fuel, the departure from this average will depend both on the displacement from the line in Figure 2.0 and the actual fraction of the oxygen consumed. Therefore, fuels were selected to cover extremes in both of these quantities. The straight lines in Figure 2.1 show the total energy available per cubic foot of air for various fuels as a function of the oxygen concentration at extinguishment, where the emphasis is on the word total.

Thermal effects also depend on the rate of energy release or delivery; therefore, for a given geometry and amount the burning rates for the various fuels are important. Burgess et al found that the burning rate (V) for liquid pool fires depended on the ratio (γ) of the net heat of combustion over the sensible heat of vaporization, i.e.,

$$V = 0.0076 \gamma \text{ cm min}^{-1}$$

Figure 2.2 shows his data augmented with values from Table 2.1 for some additional fuels of practical interest. The selected fuels provide good coverage of the available burning rate values. Column #9 in Table 2.1 indicates the type of combustion involved, i.e., flaming or glowing. The glowing combustion is expected to continue to lower oxygen concentrations with an associated potential for a large total energy release; however, the rate of release is apt to be modest.

The physical state of the fuel provides the basis for identifying fires as Class A or B; however, the more important factors are the changes in the combustion process and burning rate that result from the rigid structure of solids. Most of the liquids were burned as two dimensional fuel arrays, i.e., as pools. A few

¹ Burgess, D. S., Scrasser A. and Grumer, "Defusive Burning of Liquid Fuels or Open Trays" Fire Research Abstracts and Reviews, 3, 177, 1961.

wick and spray fires were included but most of the data are for pools. Solid fuels were burned in various configurations as illustrated in Figure 2.3. Paper, wood, charcoal and vulcanized rubber maintain their general shape until all the material is consumed while the polyethylene, Delrin, and PVC melt and burn much like liquids. Thermal reinforcement is required to maintain combustion in the larger fuel elements; therefore, various groves or stacking arrangements were required. Figure 2.4 shows the melted and burned areas on several of the plastic samples after the fires were extinguished by oxygen starvation. Obviously the burning area changed dramatically during the course of these fires in contrast to the liquid pools where the area remained fixed. Consequently the burning rate was a controlled variable only in the liquid fuel experiments where the pool diameters were varied as indicated in Table 2.0. In the spray fires, burning rates were altered by changing the number of spray nozzles to provide discharges of 550, 1100, and 2200 cm³/min.

2.1.2 Environmental Chambers--As indicated in Table 2.0, the four test chambers covered about a three decade range of air volumes, i.e., from 1.19 to 1050 ft³; therefore, the total energy available from burning the oxygen also should span three decades. In the simple adiabatic chamber model, this energy is shared equally with all the compartment surfaces and the energy input per unit area is proportional to the volume to surface ratio. For simple cubes covering the range of volumes involved in these experiments, each decade increase in volume approximately doubles the thermal load on the compartment surfaces. The chambers actually employed were of the thermally leaky variety and included various cylindrical and rectangular geometries. Nevertheless, the volume to surface ratios of .17, .35, .77, and 1.66 respectively follow the approximate doubling relationship.

Figure 2.5 shows the physical arrangement employed with the three smaller chambers. All of the sensing elements, i.e., the weighing platform, thermocouples, photocell, and gas sampling tube along with the igniter and pressure control bag were mounted on a water sealed base plate that served all three chambers. The 1050 ft³ chamber was a separate cement and concrete block chamber as shown in Figure 2.6. For convenience, water seals were employed in all four chambers; therefore, a plastic expansion bag was attached to each system to maintain the internal pressure at atmospheric throughout the burn. These bags ranged in size from about 2 to 2000 ft³; however, these volumes and surface areas were not included in the above calculations because the bags were collapsed at the beginning of each test and the small opening near the base of the chamber permitted relatively little heat to escape. This small opening restricted air circulation between bag and chamber. Since the oxygen concentration of the air initially entering the bag was relatively normal, the chambers were kept sealed after the fires had extinguished themselves until the gasses cooled, the bags

deflated, and the oxygen monitoring equipment observed the formation of an equilibrium atmosphere. Usually the change in oxygen concentration resulting from this procedure was barely perceptible.

2.2 Fire Characteristics

2.2.1 Ignition and Fire Buildup--Ignition procedures varied according to the fuel. All of the liquid fuels, i.e., pool, wick, and spray, were ignited directly with an electric arc from a 15 KV, 1 MA sign transformer. In order to avoid the formation of explosive mixtures in the sealed chambers, the fuel pans were sealed with a thin film of saran or polyethylene that would melt under the electric arc and permit ignition. Figure 2.5 shows the electrode film arrangement. Small solid samples were ignited with the electric arc applied directly to thin fuel sections, i.e., the ignition points indicated in Figure 2.3. Wood cribs and rubber tires were quickly ignited with a small quantity of JP-4 applied to the finely divided kindling elements. With liquid fuels, the flames spread quickly and full involvement was achieved within a few seconds. With the solid fuels, particularly the thermoplastics, the rate of buildup frequently stretched over many minutes, e.g., 10 to 20, depending on the geometry and the melting pattern of the fuel element. While the rate of buildup appeared to have little effect on the total oxygen consumed, the "thermally leaky" chambers could lose considerable heat during these slow buildup conditions; thereby, minimizing the temperatures reached by the chamber walls.

2.2.2 Burning Rates--All of the pool, wick, and class A fires were built on weighing platforms so that the burning rates could be continuously observed by the weight loss. Figure 2.5 shows the beam balance arrangement employed with the three smaller chambers. The water seal permitted the beam to move with relatively little friction. In operation, all weights other than the fuel to be burned were counter-balanced with buckshot; consequently, the load cell felt only the weight of the fuel which was added in measured increments to calibrate the load cell. A similar arrangement was employed with the 1050 ft³ chamber except that the weight platform was supported by a cable from overhead as shown in Figure 2.6. Again a water seal in the overhead provided a low friction exit to the outside world. Bicycle wheels were used for large radius low friction pulleys to direct the support cables to the counter-balance and load cell. The load cell capacities were 0 to 1 lb in Figure 2.5 and 0 to 100 lbs for Figure 2.6. All load cell signals were recorded on a multichannel visicorder simultaneously with the other electrical data. While some control over the burning rates for pools and solid fuels can be achieved through the selection of the fuel type, and the burning surface area, various environmental factors influence the heat feedback from combustion zone to fuel. Therefore, some variations between nominally duplicate runs are normally observed. In contrast, spray fire burning rates are readily controlled by a valve. Figure 2.7 shows the spray fire nozzle arrangements and the provisions for burning rate control. In the lower position the nozzles sprayed up while in the upper position

the sprays were down. Fuel flow rates were controlled by the fuel tank nitrogen pressure which was adjusted to establish the desired flow. With this arrangement, methanol and JP-4 were easily burned at the same rate, a condition that requires time consuming adjustments with pool fires. The range of rates selected extended from about 1/2 to 3 times the largest JP-4 pool value.

2.2.3 Flame Characteristics--Flame sizes and geometries were observed visually and recorded photographically; therefore, some non-smoking fuels were selected to permit observations throughout the burn. In the two smaller chambers, the fires were viewed from below through the transparent base plate and weighing platform. The smoke did not obscure these observations and there was never any question when the flames were extinguished. With the two larger chambers, the flames were observed through windows in the sides of the chamber and smoke obscuration frequently limited the observations from these points. In addition to the smoke, water vapor from the fire condensed on the windows adding further to the obscuration; however, the problem was minimized by coating the windows with a wetting agent, i.e., AFFF solution. Time lapse super 8mm cameras recorded the flames at 1 second intervals and simultaneously registered a fiducial mark on the visicorder records to synchronize the electrical and photographic data.

2.2.4 Thermal Fields--The thermal energy arriving at various positions on the compartment walls was measured by an array of thermocouples, radiometers, and calorimeters. In Figure 2.5 one t.c. monitors the air temperature near the top of the chamber and 4 t.c.'s attached to the 1/32" thick aluminum panels measure the temperature rise resulting from the thermal load. These temperatures provide an indication of the spatial heating pattern within the chamber but the main function is to show when such thin sections can be expected to encounter damage in the fires. Because of their unknown reflection and loss characteristics, these panels are unsuited for calorimetric measurements of the incident heat flux. In Figure 2.6 the bare Hy-Cal radiometers record the combined instantaneous convective and radiative thermal input while the calorimeter integrates the input and indicates the total energy received. Again the aluminum panels indicate the effect of the thermal insult on thin sections.

2.2.5 Gas Analysis--Figure 2.7 also shows the sampling arrangement, instrumentation, and calibrating provisions for monitoring the concentrations of CO, CO₂, and O₂ in the combustion chamber. About five minutes are required to analyze a sample with the gas chromatograph; therefore, on short burns, the first sample was inspected immediately after the flames self-extinguished. Subsequent samples were grabbed at approximately 5-minute intervals. With long burning fires, additional samples were collected during the burn. All gas concentration determinations are based on peak heights normalized to the N₂ which is assumed to remain unchanged throughout the burn. Several times during a burn day all of the gas measuring instruments were calibrated with standard gas mixtures

injected at the sampling port as indicated in Figure 2.7. With the three small chambers, gas analysis was limited to the gas chromatography grab samples. Both continuous analysis and grab samples were obtained for the fires in the 1050 ft³ system.

3.0 RESULTS

The results are principally concerned with three areas of information and the temporal and spatial history in each case, i.e.,

- o Dependence of the fire characteristics on the fuel and environmental factors.
- o Conditions for self-extinguishment
- o The thermal threat to the compartment.

3.1 Fire Behavior in Sealed Compartments

3.1.1 Effect of Fuel and O₂ Concentration on Flame Appearance--The visual appearance of flames covers such factors as color, geometry, size, and flicker. These characteristics are described for three situations, namely, liquid pool fires, spray fires and burning solids. With the liquid fuels, the flame color is predominantly a characteristic of the fuel and secondarily, a function of the burning rate, e.g., at the nominal burning rates listed in Table 2.1, MeOH burns with a blue flame, ETOH has some pink mixed with the blue and the rest of the fuels burn with luminous yellow-orange flames. However, near the extinguishment point, as the flames are dying down and the burning rate is decreasing, some of the normally luminous flames become blue and pink, e.g., acetone, hexane, etc. The geometry of the flame structure ranged from predominantly laminar for the 1" dia. pools to completely turbulent for the 3' fires. Most of the pool sizes were in the transition region. Figure 3.0 shows typical flame structures for several fire sizes. Views A and B show the flames as observed from below, i.e., looking up through the fuel. C and D indicate the substantial increase in turbulence accompanying a change from 5 3/4 to 9" dia. pools. In addition to color changes, the stability of the flames also provides an indication when extinguishment is about to occur. In the small chambers where observations were made through the water-filled base plate, the pulsating flame would generate ripples in the water at the start of the burn. Some time later the ripples usually stopped and the combustion column would become quite steady. However, shortly before extinguishment the flames become unstable again, generate ripples on the water surface, and no longer cover the fuel surface uniformly. Figure 3.1 shows four views during the cycle of a 5 3/4" dia. JP-4 fire as seen from above. In views (a) and (b) the flames are building up from ignition to the maximum burning rate, in (c) the burning rate is dropping off slightly probably accompanied by a cessation of ripples on the H₂O. Finally at (d) the flames are reaching here and there in search of oxygen just before the fire is extinguished.

With the spray fuel fires, the changes observed in the flames during a burn concerned the color, capacity and size of the flames. Again, low oxygen concentrations caused the colors to shift toward the pink. Furthermore, blue fringes developed in JP-4 shortly before extinguishment. With methanol, the luminous flames that develop at the higher burning rates subsided and became blue just before extinguishment. Figure 3.2 shows a typical JP-4 fire for two nozzles. The fuel spraying out of the nozzle travels an appreciable distance before reaching a well defined flame front. As the oxygen is used up the flames appear to blow off and reflash several times before remaining extinguished. Under the smokeless conditions of a methanol fire, extinguishment is well defined, but visual timing becomes difficult when the reflashes are occurring in a smoke-filled compartment; consequently, these times were determined by a radiometer that sensed the heat. When the spray was downward from the overhead, the length of the flames increased toward the deck as oxygen was depleted and the region around the nozzles became obscured in smoke and buoyant combustion products. Increasing the number of nozzles merely shortened the burning time.

With the class A fuels, flame size was strongly influenced by fuel geometry and the opportunities for thermal reinforcement. Occasionally with a poor fuel arrangement, a class A fire would go out before the oxygen was depleted, but usually the flames persisted and exhibited a spasmodic dance similar to their liquid brethren just before extinguishment.

3.1.2 Burning Rates--With class B fuels, the experimental variables affecting the burning rate are type of fuel, surface area of the pool and perhaps the air volume. Table 3.0 lists the maximum burning rates observed for the liquid fuels. These values cannot be compared directly to the values in Figure 2.2 because of the pool size effect. The rates plotted in the figure correspond to an infinite diameter where V^∞ is attained empirically by fitting burning rate data (V) to the expression $V = V^\infty (1 - e^{-kd})$ where k is a constant and is the pool diameter. Since this expression neglects convective and conductive heat transfer, it does not apply to the small pools, i.e., 1, 3, and 5 in diameter where the container rim effects are prominent. When the 11-, 18-, and 36-inch pool results are compared to the data used to evaluate V^∞ , the values for MeOH are in fair agreement; however, the hexane values are about 25% low. Similarly, the JP-4 and JP-5 burning rates are only about 1/2 to 3/4 the values obtained in open burns. While it is tempting to suggest that burning rates do not reach their open burn values because of reduced oxygen, the combination of pool sizes and chamber volumes in Table 3.0 does not permit this facet to be evaluated. Figures 3.3 and 3.4 show typical weight loss curves for 3-inch and 18-inch dia. pools respectively. The near linearity of the curves suggests an essentially constant burning rate. In the spray fuel burns the burning rates were the same as the spray rates during most of the fire; however, near the extinguishing point, some of the spray would settle out without burning. The maximum spray rates, i.e., slightly

over 1700 grams per minute exceeded the pool burning rates by factors of 3.2 and 2.6 for MeOH and JP-4 respectively.

With the class A fuels, the effect of fuel arrangement frequently masked the importance of the material. With the arrangements indicated in Figure 2.3, the paper rolls and wooden cribs achieved burning rates on a weight basis comparable to the largest liquid pools. However, Table 3.0 shows that on an energy scale the heat release rate for the liquids was several times greater than for the solids. Figures 3.5 and 3.6 show weight loss curves for various class A fuels in the 7.94 ft³ and 1050 ft³ chambers respectively. In contrast to the liquid fuel curves included for reference, each solid fuel curve exhibits a period of buildup that frequently delays the period of maximum burning rate until the liquid fires have suffocated themselves. With the thermoplastics, i.e., polyethylene, PVC, and Delrin the fuel would melt in the region of the flames and then flow according to the dictates of gravity. When the flow was onto a cool surface the fuel sometimes solidified and extinguished that part of the fire for lack of thermal reinforcement. Such behavior contributes to the random behavior of the class A weight loss curves and complicates the process of establishing standard thermal insult curves.

3.2 Conditions for Extinguishment

Assuming extinguishment results from oxygen starvation, this section is concerned primarily with the effects of fuel type, burning rate, and compartment volume on the extinguishing oxygen concentration. Since CO₂ and CO concentrations also were measured, the production of these gases will be examined as a function of the burning conditions.

3.2.1 Fuel Effects--Tables 3.1 and 3.2 summarize the gas chromatographic analyses of the atmospheres in the various chambers after the fires had extinguished themselves. The range of oxygen concentrations observed with each fuel indicates that an extinguishment concentration is not unique to each type of fuel. Burning conditions mask oxygen index effects and cause a general overlapping of the results. For fuels that exhibit flaming combustion the minimum extinguishment concentrations were between 10 and 12%. Usually these values were obtained with small fires in small chambers; e.g., in the 1050 ft³ chamber the minimum values for pool fires were between 12 and 15%. Generally the alcohols, methanol and ethanol are on the lower side of the distribution for a particular combination of pool size and chamber volume; however, the parafins occasionally gave equally low values. With the spray fires, both the size of the fire and the position had as much effect as the difference in the two fuels, MeOH and JP-4. Again the range was from 10 to 15%. Similarly with the class A fuels, the extinguishment O₂ concentration varied from about 9 to 18 percent depending on the burning conditions, particularly the degree of reinforcement. The glowing combustion of charcoal continued well beyond the limits for flames, i.e.,

values ranging from 3 to 6 percent were observed depending on the number and arrangement of the brickets.

3.2.2 Effects of Burning Rate on Oxygen Consumption-- Systematic variations in the burning rates were limited to class B pool and spray fires. In going from a 3-inch dia pool to a 3-foot pool, the surface area increases by a factor of 144, thus, the total burning rates recorded in Table 3.0 cover a range of at least two orders of magnitude. However, it was impractical to burn all pool sizes in each chamber, e.g., a 3-inch dia pool could burn in the 1050 ft³ chamber for about 8 hours. Therefore, three or four sizes were selected to give burning times less than about 20 minutes in each chamber. Figure 3.7 shows the general tendency for the larger pools to be extinguished at slightly higher oxygen concentrations but the effect is not very large. Burning rates for the spray fires were varied by a factor of four by changing the number of nozzles. Table 3.2 and the scattergram in Figure 3.8 show the behavior of methanol and JP-4 fires. Nozzle position had a substantial effect on the methanol results, i.e., when fuel sprayed down from above the fuel extinguished itself at higher O₂ concentration than when the nozzles were on the bottom of the chamber. With JP-4 the effect was much less pronounced, and the O₂ concentration at extinguishment was essentially independent of the burning rate. Figures 3.9 and 3.10 show the O₂ concentration as a function of time after ignition. The three curves in each figure correspond to the three indicated spray rates.

Figure 3.8 shows that the JP-4 extinguishment O₂ concentrations reach about the same value irrespective of the burning rate. Methanol shows a bit more dispersion. The standard gas curve included in Figure 3.9 shows the relatively slow response time exhibited by the O₂ cell when standard gas is introduced at the inlet of the sample take, i.e., it can take a minute or so to reach the new equilibrium value. This resolution undoubtedly limits the measurement of abrupt concentration changes such as the four nozzle top position curves in Figures 3.9 and 3.10. Irrespective of the possible distortions, the minimum concentrations observed about a minute after ignition indicate substantial nonuniformities in the oxygen concentration throughout the chamber during these large fires. Under such conditions the observed values become sensitive to the sampling tube location. In these measurements the inlet was always outside the flame envelope but with the overhead nozzles more combustion products were probably collected than when the nozzles pointed up from the deck.

Figure 3.11 shows the time to extinguishment plotted as a function of the spray rate. If the fraction of the fuel consumed was constant irrespective of the spray rate, the data points would fall on a family of hyperbolas that give the inverse relationship between time and rate for each total fuel value. For example, the hyperbolas sketched in Figure 3.11 correspond to the average fuel burned for the various nozzle orientations. While the data points follow the general hyperbolic pattern, the fit is not close. Some

of this dispersion stems from the spasmodic fire behavior during suffocation, i.e., reflashes occur over various periods of time thereby obscuring the actual burning time and the amount of fuel consumed.

3.2.3 Effect of Compartment Volume--Figure 3.12 shows the effect on fuel consumption when the compartment volume is changed over a range of three decades. The vertical displacement between lines reflects the differing oxygen requirements set forth in Figure 2.0; however, the close fit between the experimental points and the 45-degree lines shows that the fuel burned and thus, the energy released is almost directly proportional to the compartment volume. If the oxygen concentrations for pool fire extinguishments are segregated according to compartment volume as shown in Figure 3.7, the values increase only slightly with volume and pool size. From the results in Figures 3.7 and 3.13 it is apparent that the total energy release is controlled primarily by the available oxygen and only secondarily by the type of fuel and surface area involved. Additional fuel beyond the amount required to satisfy the available oxygen has no effect on the total heat release. Figure 3.13 is a reproduction of Figure 2.1 with experimental points added for a variety of fuels and environments. As previously mentioned, the flames self-extinguish before half the oxygen is consumed and the available energies fall in the range from about 30 to 60 BTU ft^{-3} of air. Therefore, as a rough rule of thumb, we can multiply the air volume in a sealed compartment by these values to obtain the range of total energies available from various fuels burning therein.

3.2.4 CO₂ and CO Production--Tables 3.1 and 3.2 list the maximum observed CO and CO₂ concentrations along with some CO₂ values calculated from the O₂ consumed. With small class B fires in the three smaller chambers, the CO production was below the measurement threshold for the gas chromatography unit; therefore, CO values are tabulated only for the larger class B fires and the class A fuels. When all the fuels and chambers are included, the range of CO₂ concentrations extends from about 2 to 11%; however, the larger class B fires gave values in the 4 to 7% range. CO₂ concentrations measured in the 1.19 and 7.94 ft^3 chambers were consistently lower for a given concentration than the values obtained from the two larger chambers. Some of the CO₂ may have been absorbed in the water that formed the bottom of these chambers.

In the JP-4 and methanol spray fires, substantial concentrations of CO were generated along with the CO₂. Figures 3.14 to 3.17 show the temporal behavior of the CO and CO₂ concentrations for the same nozzle configurations employed in the oxygen depletion curves in Figures 3.9 and 3.10. With four nozzles in the overhead position both the CO and CO₂ curves show transient humps corresponding to the dips found in the oxygen curves thereby supporting the picture of non-uniform gas concentrations particularly during the early part of the fire. Again the CO₂ concentrations reach 5 to 6%.

Under these conditions the CO concentrations reached substantial levels of .5 to over 1%.

3.3 Energy Considerations and the Thermal Threat

The temporal and spatial history of a fire can be examined from several points of view depending on the parameters measured. One approach concentrates on energy production as in Figure 3.18 where the rate and total yield are plotted as functions of time. In converting weight loss measurements to energy units, it was assumed that handbook values for the heat of combustion applied to these fires. The total energy released provides a basis for estimating the fire hazard associated with various fuel loadings and the heat-release rate determines the amount of some agents required to suppress the fire. The second viewpoint focuses on the energy arriving at the various surfaces in the compartment, i.e., the incident heat. Most of this energy is transported by radiation and convection with only a minor fraction going by conduction. At any point the radiation contribution depends on the view factor and the convection component is controlled by the flow of hot gases and combustion products; therefore, the incident energy varies with both time and position. Finally, the behavior of materials and the structures exposed to the fire will depend on the fraction of the incident energy actually absorbed. In the sealed compartments employed in these experiments, all the energy is trapped but the amount absorbed at a particular position will depend on the heat transfer coefficient as well as the incident flux. The ten panels in Figure 2.6 provide an indication of the pattern of absorbed energy when the receiver is aluminum.

3.3.1 Energy Released--The two aspects of energy release, namely, the rate and the total amount have been covered under the related subjects of burning rates section 3.1.2 and conditions for extinguishment section 3.2.3. For example, the weight loss curves in Figures 3.3 to 3.6 are readily converted to energy release values through the use of the appropriate heats of combustion. Maximum burning rates are controlled by the fuel type and configuration while the available oxygen determines the values of total energy listed in Tables 3.0 and 3.2. For example, with the pool fires the maximum rates of energy release listed in Table 3.0 ranged from about 25 to 28,000 BTU per minute depending on the fuel type, burning area, and compartment. Higher rates up to 75,000 BTU per minute are encountered in the spray fires of Table 3.2. Applying the rule of thumb from section 3.2.3, i.e., an average available heat of 45 BTU ft^{-3} of air, leads to a total release of about 54 BTU in the 1.19 ft^3 chamber or enough energy to boil about 3/4 of a cup of tea. In contrast, the 1050 ft^3 chamber can release 47,000 BTU or enough heat to melt 110 lbs of aluminum. Actually no water boiled or aluminum melted because the surface to volume ratios kept the absorbed energy density below the destruction point.

3.3.2 Energy Arriving at and Absorbed by Compartment Surfaces--Both the temporal and spatial characteristics of the

absorbed energy are illustrated in Figures 3.19 and 3.20 and Tables 3.3 and 3.4 as functions of fuel type, air volume, and burning rate. In the three chambers of Figures 3.19 and 3.20 the thermocouples T.C.-1 through T.C.-3 are attached to aluminum panels which in turn were equally spaced up the bulkhead. T.C.-4 is on an overhead panel. Hot air still rises; consequently, the overhead and upper positions of the bulkheads reach the highest temperatures and would require the most thermal protection. Burning times ranged from 90 sec for hexane in the smallest chamber to about an hour for methanol in the 102.4 ft³ volume. The logarithmic time scale visually accentuates the period of about 10 seconds between ignition and a detectable temperature rise in the aluminum panels. As expected, methanol burns slower than hexane, and the burning times increase with air volume, and decrease with pool diameter. None of the temperatures exceeded the safe limits for aluminum and the 102.4 ft³ wooden chamber was never in danger of igniting. The actual peak temperatures depended on the combined effects of fuel, fire size, air volume, and rate of heat loss from the chamber. For example, the temperatures in Figures 3.19b and 3.20b for the small fires in the large chamber reached equilibrium at values below those encountered in the intermediate chamber.

The special distribution of the energy impinging on the compartment walls and contents depends also on the location and geometry of the fuel. Simple symmetrical arrangements were used throughout the experiments reported here, i.e., the fires were centered in the floor area, but the elevation above the floor was one of the variables. No flames impinged on the bulkheads and the amount of flame contact with the overhead varied substantially according to the fire area, type of fuel, and its elevation. Table 3.3 shows the heating pattern in the 1050 ft³ chamber. Panels 1, 2, 3, 4 overhead and 6 and 9 at the 6 ft level on the bulkheads exceeded 400°F for the larger fires particularly when the fuel was 50 inches off the floor but all plates remained well below the melting point. The highest heat load was received by the calorimeter located in the flames directly over the fuel bed. When these thermal loads are translated into temperatures for a 1/4-inch thick aluminum plate, many of the values are in the damaging range, particularly for the elevated fires. Temperatures calculated from the calorimeter measurements were based on 100% heating efficiency, i.e., no energy was lost to the surroundings. Such energy losses undoubtedly reduce the maximum temperatures reached by Plates 1-9; therefore, the last column in the Table represents the worst possible case. These heating patterns confirm our past recommendation that in weight critical ships, insulation for passive fire protection should be applied according to the thermal loading and not uniformly over the compartment surface; e.g., no insulation would be required in the lower one-half of the bulkheads in his 1000 ft³ room unless the prospective fire was in direct contact.

Burning rates are controlled by the fuel surface area and can vary from an explosion with suitably vaporized liquids to the stable long burning fires of Figures 3.19 and 3.20. Both extremes are

possible in shipboard situations and must be considered in a decision to seal compartments; e.g., blow-out panels may be required to accommodate the overpressure generated in the explosion.

Table 3.0 lists the surface area for the liquid fuels and the corresponding maximum burning rates. Figure 3.18 shows that constant burning rates reached by the liquids within the first minute are maintained throughout most of the fire, e.g., 1960 BTU per minute for methanol and 2620 BTU per minute for ethanol. In contrast, the wood required about 9 minutes to reach the maximum burning rate of about 4410 BTU per minute. The shape of these burning curves becomes an important factor in establishing the test to evaluate the thermal effect on structural members and practical insulation requirements for passive protection of aluminum members. Table 3.4 shows times when maximum temperatures were reached in the large chamber. Since each fuel and burning area tends to generate a different heat-release-rate curve, the possibilities become infinite and the task of specifying a suitable rate for evaluation tests at first appears quite formidable. Fortunately, when viewed from the temperature rise in the exposed plates, the situation is simplified when the rate of heat loss is slow compared with the rate of arrival. Under such conditions, the temperature rise depends more on the total thermal exposure and less on the rate of arrival. The modest burning rates employed on the JP-4 test 105, 112, and 113 illustrates this point. In Table 3.0 the burning rate increased by a factor of 32 between Tests 113 and 105; however, in Table 3.3, the corresponding temperatures in the overhead aluminum panels increased by factors ranging from 2 and 3.

As described in section 2.1.2, the various sized compartments were selected to show the effect of air volume on the heating of the walls. The simple adiabatic compartment model predicts that the specific thermal input at the boundaries should be proportional to the volume to surface ratio. However, the thermal leaks in the experimental chambers and the insulation between the aluminum panels perturb this simple picture, i.e., in Table 3.3, the panels do not reach a common temperature and in Figures 3.19 and 3.20 the temperatures tend to level off or decrease as the losses overtake the thermal input. A precise check of the heating model would require eliminating the heat leaks. Since this approach was inconvenient with the available chambers, the sizes of some fires were increased in a rough proportion to the chamber volume so that the burning times would be about equal, thereby keeping the heat leaks roughly comparable. Figures 3.21, 3.22 and 3.23 show aluminum panel temperatures as a function of chamber volume to surface ratios for hexane, acetone and methanol fires where the burning times were relatively constant for each fuel. The approximate linearity of the curves demonstrates the usefulness of the model even for leaky chambers. Applying the rule of thumb for the energy available in a cubic foot of air and assuming a value of 30 BTU per ft^3 on the basis of the Table 3.0 values for hexane and acetone, leads to the dotted curve in Figures 3.21 through 3.23. In calculating this

curve it was assumed that the energy required to heat the air to an average value, i.e., 150, 175, 250, and 375°F, respectively for the smallest to the largest chambers, did not contribute to the aluminum panel heating. With hexane and methanol this simple estimating procedure leads to reasonable average temperatures, i.e., about midway between the maximum overhead and minimum bulkhead temperatures. With acetone the estimated temperatures are above those observed in the large chamber; however, the acetone pot size resulted in burning times 50 to 100% longer than for MeOH and hexane, and the attendant heat leaks could easily account for the lower observed temperatures.

4.0 DISCUSSION

The introduction (section 1.0) listed a series of questions pertaining to fire characteristics and suppression countermeasures under various conditions of ventilation. This report on fires in sealed compartments is the first of a trilogy planned to cover the three general categories of ventilation indicated in that matrix; therefore, it is premature to present general conclusions about when to seal and when to ventilate all compartments. However, some of the present observations can be applied to passive fire protection in ship design without waiting until all the results are in.

4.1 Non-Serious Fires

A principle assumption behind the sealed compartment measurements is "that there is a compartment size too small to accommodate a serious fire." Consequently, the fire characteristics and fire effects were examined as a function of compartment size to help establish when serious fires developed and how size could be used as a fire protection measure. This line of reasoning calls for a definition of "serious fires" and immediately, we enter the realm of opinions. Two approaches are obvious:

- o Judge the seriousness by the fire effects
- o Catalog the fire by its characteristics.

Operationally, a non-serious fire will not impair the ship's ability to perform its mission. Such a definition leads to a different sized fire for each space; e.g., a dry storage space presumably could tolerate a much larger fire than a critical electronics space. Structurally, the non-serious fire does not weaken the material or stress the members to the damage point. For example, it is commonly stated that typical aluminum members should not be heated above about 400°F. These are the important definitions but they are very difficult to employ in ship design; therefore, we will attempt a transition to a fire characteristic that can be specified ultimately in terms of the fuel and environment. Unfortunately, fire behavior varies widely during the build up and spread period following ignition, depending on the type of fuel and its mode of

application. However, the flashover point is generally recognized as characteristic of a serious fire because at that point all of the combustibles in the space become involved. While the boundary between serious and non-serious fires will undoubtedly occur under conditions of less complete involvement in some crucial spaces, we will use the flashover point to illustrate the application of compartment size considerations in ship design. The mechanism of flashover and the prerequisites for its occurrence have been developed in a series of test burns at IITRI² and NBS;³ namely, the thermal radiation from the heated overhead, the layer of hot gasses, and the flames reaching the ignition threshold for the remaining uninvolved combustible materials in the compartment. Following the approach outlined in section 3.3, the conditions for flashover can be stated in terms of (1) the radiation field required to ignite the combustible materials, (2) the overhead temperatures required to generate the radiation field or (3) the heat release rate required to maintain the overhead temperatures and the radiation field. This third approach is the most convenient for evaluating the flashover potential exhibited by a particular combination of fuel and air volume. For example, in the ventilated NBS 10' x 10' x 7' chamber employed in berthing compartment fire tests, a heat release rate of about 38,000 BTU min⁻¹ was required to maintain the ceiling air temperature of about 1290°F which was sufficient for flashover. A direct comparison to the 1050 ft³ sealed compartment is complicated by the ventilation heat losses, the smaller size of the NBS chamber, and the transient burning characteristics as oxygen is depleted in the sealed chamber. However, the energy release rates listed in Table 3.0 and the temperatures in Table 3.3 fall short of the NBS flashover requirements and indeed, no flashovers were observed. According to section 3.3 the thermal insult imposed on the compartment surfaces increases with compartment size, consequently, some volume exists where the supply of oxygen is adequate to produce flashover. At present the provision for scaling flashover requirements to different sized chambers are not adequate to provide reliable values, particularly for transient fires. However, some very rough estimates can be obtained by applying the "rule of thumb" for energy available in the confined air in the adiabatic chamber model. Figure 4.0 shows a family of thermal insult curves for available energies of 30, 45, and 60 BTU per ft³ of air enclosed in square chambers 8 feet high and 1 foot on a side. Table 4.0 lists the calculations and indicates the other simplifying assumptions, namely, the energy stored in the air and the average uniform heat input to all surfaces. In Table 3.0 the available energies in the 1050 ft³ chamber are in the 30 to 45 BTU ft⁻³ range except

² Waterman, Thomas E., IIT Research Institute, "Sealed Room Flashover," Technical Report on Dash 20-70-C-0308, April 1971

³ Lee, B. T. and Parkes, W. J., NBS Report "Naval Shipboard Fire Risk Criteria - Berthing Compartment Fire Study and Fire Performance Guidelines," April 1976

in several cases where slow burning rates increased the fuel consumed but reduced the rate of heat release and thus, the temperatures reached near the deck. Also, the average thermal input assumption imposes higher energies near the deck than the temperature curves of Figures 3.19 and 3.20 suggest; consequently, the real threat probably rests between the 30 and 45 BTU ft⁻³ lines. Fine fuels such as newspapers and upholstery materials require about 70 BTU ft⁻² for ignition, therefore, Figure 4.0 indicates that flashover cannot be achieved in a sealed compartment the size of our test chamber, in fact, a considerably larger volume would be required if the actual heat release was near 30 BTU ft⁻³. This ability to prevent a serious fire by limiting the available oxygen has been combined with the correlating approach based on fuel limitations to form the third of the Ten Commandments for ship fire protection,⁴ i.e., "starve and imprison unwanted fires; minimize fire buildup and flashover by restricting the fuel loading and oxygen availability. Confine the fire to the point of origin with frequent fuel breaks and adequate fire barriers."

4.2 Sealed Compartments and Passive Fire Protection

Many ship compartments already are or could be made smaller than the size required for a serious fire when the ventilation is sealed off; therefore, commandment III provides a simple method of achieving passive fire protection with a minimum penalty in weight and money. No single countermeasure will be sufficient for all fire emergencies; therefore, the guiding design philosophy should embrace a sequence of steps beginning with prevention, and retreating through detection, confinement, control and extinguishment (commandment I). Admittedly, the sealed compartment technique fails when enemy action breaches the seal with a large hole, but for the many self-inflicted fires or action fires with small holes, the third commandment can provide another element of protection at essentially no penalty in cost and weight. The third commandment was demonstrated⁴ with three applications of sealed compartments.

4.2.1 Sealed Compartment Possibilities on the PHM-1-- Figure 4.1 shows the PHM-1 layout and Table 4.1 compares the potential thermal insult obtained by a conventional hazard analyses based on fuel loadings⁵ to the heat available when the compartment air is burned. The values for combustion of the air are obtained from the same floor areas employed in reference 5 with the additional assumptions of an 8-foot clearance to the overhead and an available energy of 45 BTU ft⁻³ from combustion of the enclosed air. In the last column, the ratios of heating potentials indicate that ventilated compartments where all the fuel is burned can liberate

4 Alger, R.S., Protection for Aluminum Ships from Fuel Fires," Published in the Proceedings at the Navy Workshop on Shipboard Fire Protection Research and Development, March 1976

5 Butler, F. and Kaysen, H. D., Gibbs and Cox, Inc. "PHM Fire Protection Study for the Naval Ship Engineering Center" September 1975.

50-200 times more heat than the corresponding sealed space. Only the pilot house and the CIC compartments contain enough oxygen to exceed the heat released in the 1050 ft⁻³ test chamber of Figure 2.6; therefore, the laboratory burns are directly applicable to this ship. While the ship arrangement is not conducive to sealing all of the areas, several good opportunities to apply the technique are marked with asterisks in Table 4.1. With a little insulation overhead, fires in these compartments could be allowed to burn themselves out without damage to the ship. The heating potential ratios for the storage compartments illustrate an interesting reversal of design philosophy that emerges when the available air determines the thermal insult. In a conventional hazard analysis, based on fuel loadings, storage spaces inherently exhibit a large heating potential which coupled with a history of frequent fires leads to a potentially hazardous rating. However, when evaluated according to the available air volume, the hazard decreases as the fuel loading increases. Consequently, storage spaces should be designed for a maximum packing density in order to minimize the air content and thus, the heat that can be released.

4.2.2 Sealed Bunks--The recent Okinawa fire provides a good example of the problems that can be generated by a few burning foam mattresses. Although these mattresses were in storage, other more disastrous bedding fires are on record, e.g., the USS EXCELL fire of 1973 and the FORRESTAL fire in 1972. Since a foam mattress contains sufficient fuel to flashover small berthing compartments, it represents a potentially serious fire hazard when stowed in the conventional manner. Pullman and others in the mobile bed business have reduced the mattress fire hazard in unoccupied bunks by folding up the beds in containers that limit the available combustion air. Figure 4.2 shows three metal enclosure arrangements for storing unoccupied bedding in compliance with commandment III, i.e., the pullman, hide-a-bed and stack arrangements.

4.2.3 Sealed Electronic Spaces and Consoles--The VI Commandment "protect thy vital parts"⁴ applies particularly to the ship's vital electrical cables. Most of the ship functions, i.e., both weapon systems and the platforms are controlled electrically; consequently, fires that cause little structural damage can easily put a ship out of action electronically. All too frequently, fires in trivial spaces feeding on non-essential combustibles have destroyed important cables that rendered whole systems inoperative and compromised the ship. Rule VI along with III suggests that at a minimum, the most important cables should be enclosed in conduits that limit the available air and provide a measure of heat protection, e.g., hollow structural elements. Also, electronic cabinets should be sealed and preferably inserted with nitrogen to limit the oxygen available for ignition and combustion.

4.3 Thermal Insults Appropriate for Testing Materials and Structures

A decision to provide a measure of fire protection in ships immediately leads to questions about tests to obtain design information and procedures for evaluating and certifying performance, e.g., What fire characteristics are appropriate and what material or structural properties should be tested? A pertinent example involves the passive protection of structural elements and cables by thermal insulation. Where weight and cost are minor considerations, a significant safety factor can be applied by designing to meet the worst case fire. However, where aluminum structures are involved weight is important and the insulation materials must be selected and distributed so as to provide the maximum protection per lb. for the anticipated thermal insult. Conventionally, such decisions have been based on the results of ASTM E-119 tests; therefore, it is of interest to compare the heating curves followed in the E-119 test against the thermal load generated by various fires in sealed compartments. Since the environments and the controlled and measured parameters are quite different, a number of reservations and assumptions are involved in such a comparison. In section 3.3 the discussion of thermal energy was approached from three points of view:

- o The heat released in the compartment
- o The heat incident on the compartment surfaces
- o The heat absorbed at a surface

and in each case the energy exhibits a temporal and spatial pattern. In contrast, the E-119 curve expresses the average temperature sampled at a plane between the furnace source and the test specimens. For materials that do not burn or release significant amounts of heat, the test provides an essentially reproducible incident heat flux that can be measured and compared to the thermal flux generated in the sealed compartments. NBS has provided some unpublished thermal flux data measured during inert material tests with their E-119 furnace.

Such heat flux values fall fairly close to the radiation levels predicted for a black emitter following the standard time-temperature curve. The significant differences between this incident energy and the thermal fluxes measured by the radiometers in the 1050 ft³ sealed chamber are the relatively slow buildup and the long duration of the E-119 curve. Particularly with class B fires, the thermal insult reaches its maximum value and the flames are extinguished within a minute or two, i.e., before the E-119 curve really gets underway. Table 4.2 shows some maximum heat flux values recorded by the radiometers during sprayed fuel fires in the 1050 ft³ sealed compartment. Since these sensors are outside the flames and the burning times are short, i.e., 1 to 6 minutes, the heat fluxes remain in the modest range from 1 to 5 BTU ft⁻² sec⁻¹. A square wave heating curve or a E-119 furnace preheated to 1300°F would provide a more realistic rendition of the heating pattern to be

expected for the class B fires. In areas of flame impingement flux levels of 10 or 11 BTU $\text{ft}^{-2} \text{ sec}^{-2}$ may be reached; therefore, this more severe case the E-119 furnace should be preheated to about 1700°F. Similar abrupt initiation patterns are anticipated for the standard ventilation and the open compartment fires; however, the increased availability of oxygen will lengthen the burning time, i.e., increase the total energy released and probably alter the heat flux level depending on the energy trapped in the chamber.

Conclusions regarding the maximum amplitudes and durations of tests to allow for the possible increase in threat introduced by ventilation will have to await the next series of tests but in sealed compartments, where the integrity of the seal can be assured, passive insulation protection can be tested adequately with simple heat sources that provide a constant flux for a few minutes.

5.0 CONCLUSIONS

5.1 Fires in Sealed Compartments Exhibit the Following Characteristics:

- Flaming combustion stops when the oxygen concentration falls within the range of 10 to 15% and smoldering combustion can continue down to about 6% O_2 .* Within this range of self-extinguishment concentrations, the value for a particular fire depends on the secondary influences of fuel type, fire size and compartment volume.
- Over a range of three decades in compartment volume, the fuel consumed was proportional to the available oxygen; therefore, the fire hazard in sealed compartments is readily estimated from the air volume.
- As a useful rule of thumb, the available energy from burning the oxygen with a variety of fuels in a closed compartment is about 30 to 60 BTU per ft^3 .
- The time to self-extinguishment is inversely proportional to the burning rate which in turn is controlled by the fuel type and geometry.
- Depletion of the oxygen does not cause the burning rate to decrease dramatically until just before extinguishment.
- Under conditions where the rate of heat loss from the compartment walls is slow compared with the rate of arrival, the temperature rise depends more on the total thermal exposure than on the rate of arrival. For example, in a series of 1050 ft^3 compartment tests where the burning was increased by a factor of 32, the overhead aluminum panels increased in temperature by factors ranging from 2 to 3.

*These concentrations are in agreement with some unpublished work at NRL on burning α - cellulose in sealed enclosures.

5.2 Sealed Compartments as a Passive Fire Protection Technique.

- o Fires cannot develop to the flashover point with the oxygen available in small compartments; therefore, compartment size can be used for passive fire protection.
- o Aluminum compartments up to 10^3 ft³ can tolerate the energy released by the available oxygen with little damage and the requirements for protective insulation are limited to the overhead and the upper areas of the bulkheads.
- o The third Commandment for ship fire protection "starve and imprison unwanted fires" can be applied to many ship components as well as to whole compartments.

TABLE 2.0 EXPERIMENTAL PARAMETERS

I CONTROLLED VARIABLES

(a) FUEL

- Type, Methanol, Ethanol, Hexane, Acetone, Benzene, JP-4, JP-5, Cellulose, Polyethylene, Delrin, Charcoal, Rubber, Sulfur and PVC.
- Geometry, Liquid Pools, Wood Cribs, Plastic Chunks and Sheets.
- Pool Diameter 1", 3", 5-3/4", 9-1/8", 11", 18", 36".

(b) AIR VOLUMES

- 1.19, 7.94, 102.4, and 1050 ft³.

II MEASURED VALUES

- (a) BURNING RATE, BY WEIGHT LOSS TO EVALUATE THE HEAT RELEASE RATE AND THE TOTAL HEAT RELEASE.
- (b) SPATIAL AND TEMPORAL HEATING PATTERN, BY RADIOMETERS, CALORIMETERS, ALUMINUM PANELS AND THERMOCOUPLES.
- (c) OXYGEN DEPLETION AND COMBUSTION PRODUCTS, BY I.R. ANALYSIS, CONDUCTIVITY CELL AND CHROMATOGRAPHY.
- (d) FLAME GEOMETRY, BY PHOTOGRAPHY.

TABLE 2.1 FUEL CHARACTERISTICS

#1 Fuel	#2 Formula	#3 Pounds of O ₂ Required to Burn Pound of Fuel	#4 Oxygen Index %	#5 Pounds of Air Required to Burn Pound of Fuel	#7 Heat of Combustion BTU/g	#8 Heat of Vaporization BTU/g	#9 Specific Burning Rate for Large Pools mm/min	#10 Type of Combustion	#6 Ft ³ of Air Required to Burn Pound of Fuel
Methanol wick pool spray	CH ₃ OH	1.5		6.47	21.9	1.13	1	Flaming	79.8
Ethanol pool	C ₂ H ₅ OH	2.08		8.97	28.3	.81		Flaming	110.7
Acetone pool	C ₃ H ₆ O	2.21	16	9.53	29.2	.53	3	Flaming	117.6
Benzene pool	C ₆ H ₆	3.08	16.4	13.28	39.8	.42	6	Flaming	163.9
Hexane pool	C ₆ H ₁₄	3.53	15.4	15.22	44.1	.35	7.3	Flaming	187.8
JP-4 pool spray	~ C ₈ H ₁₈	3.51	~ 16	15.13	44.2	.29	6	Flaming	186.8
JP-5 pool	~ C ₁₀ H ₂₂	3.49	~ 16	15.04	44.2	.28	4.3	Flaming	185.7
Cellulose paper wood	C ₆ H ₁₀ O ₅	.83		3.78	17.5			Flaming and Glowing	44.2
Polyethylene stick sheet	~ C _n H _{2n+2}	~ 3.44	17.5	14.83				Flaming	183.1
Delrin round bar			15					Flaming	
Charcoal brickets	C	2.67	56	11.51	28.8			Glowing	142.1
Rubber tires					13.3			Flaming and Glowing	
Sulfur powder	S	1	13.6	4.31	8.7			Flaming	53.2
PVC sheet			47						

TABLE 3.0
BURNING CHARACTERISTICS OF FUELS IN SEALED COMPARTMENTS

NSWC/WOL/TR 76-125

TABLE 3.1
GAS CONCENTRATIONS WHEN FIRES ARE SUFFOCATED IN SEALED CHAMBERS

FUEL SIZE: G/A	LOCATION: ABOVE FLOOR	CHAMBER VOLUME = 1.19 FT ³				CHAMBER VOLUME = 7.94 FT ³				CHAMBER VOLUME = 102.4 FT ³				CHAMBER VOLUME = 1060 FT ³							
		TEST % =	O ₂ % =	CO ₂ % =	MAX BURN TIME SEC	TEST % =	O ₂ % =	CO ₂ % =	MAX BURN TIME SEC	TEST % =	O ₂ % =	CO ₂ % =	MAX BURN TIME SEC	TEST % =	O ₂ % =	CO ₂ % =	MAX BURN TIME SEC				
METHANOL	3'WICK	10.11	11.811.0	5.553	—	210.226	360.388	30.31	10.310.7	5.661	—	260.360	214.267	68	12.7	5.9	—	140			
	3' POOL	0	20.21	11.312.3	5.354	—	440.480	37	26.37	11.312.0	4.553	—	370.400	90.91	71	13.8	5.4	—	220		
	5'3" POOL	0													73	15.4	4.5	—	310		
	9'1" POOL	0																	578		
	18" POOL	0																	114		
	18" POOL	5"																	13.2		
	36" POOL	0																	11.1		
	36" POOL	5"																	15.9		
ETHANOL	T' POOL	0	6.7	10.310.7	5.559	—	270.278	141.154											11.0		
	T' POOL	12"																	14.6		
HEXANE	T' POOL	0	4.5	11.0	5.4	—	278.286	69.90										100			
	T' POOL	12"	14.15	11.1	5.556	—	1360.1440	118.121										114			
	T' POOL	0	18.19	12.112.2	4.145	—	630.640	22.23	26	27	11.711.8	4.345	—	330.340	97.106	67	16.2	3.9	—	200	
	T' POOL	12"	24.26	13.313.5	2.53.0	—	560.790	17.24	34	35	12.5	3.83.9	—	560	36.39	72	16.0	3.5	—	100.3	
	5'3" POOL	0																	500		
	9'1" POOL	0																	94		
	18" POOL	0																	375		
ACETONE	T' POOL	0	2.3	11.011.3	5.153	—	228.240	109.127											116		
	T' POOL	12"	12.13	11.411.6	5.159	—	131.133												117		
	T' POOL	0	16.17	11.211.6	5.456	—	550.980	23.24	28.29	29	12.512.6	4.446	—	300.320	119.126					14.8	
	T' POOL	12"						32.33	12.6	4.24.3	—	480.900	47						4.9	—	1100
BENZENE	T' POOL	0	8.9	12.312.4	5.051	—	260	95.109											120		
	T' POOL	12"	22.23	11.412.5	3.14.1	—	480.900	22.25											115		
	5'2"R	0																	15.2		
	T' POOL	0																	5.6		
	11"	0																	—		
	18"	0																	300		
	18"	5"																			
	36"	0																			
	36"	5"																			
CELLULOSE	PAPER	0	59.60	12.112.4	4.35.7	0.20.5	280.370	106.112	46.47	14.615.7	1.12.7	—	140.240	122.154	75	18.7	1.0	—	100		
	PAPER	0																	784		
	WOOD	0	65	11.5	3.8	0.1	200	217	38.38.40	12.213.6	3.13.7	—	200.230	319.430	81.82	16.16.7	4.7	0.270.32	220.260		
	POLYETHYLENE STICK	0	57.58	8.8.9.0	9.4.9.9	0.2	220.230	315.352	44.45	13.513.6	2.22.9	—	120.250	360.960	74.80	17.17.8	2.5.2.9	0.30.4	100.130		
	DELINX ROUND DISK	0	54.05.56	2.8.3.2	7.3.4.6	0.6.1.4	230.260	1290	42.43	11.511.9	6.6.6.9	—	140.160	990.1111	120	13.9	7.1	0.39	72.0		
	CHARCOAL BRICKETS	0	66	11.1	5.1	5.1(SO ₂)	0.1	360	66	52.53	6.0.6.4	1.1.5.11.7	1.0.1.1	140.160	900.1100	83	6.2	1.1	1.6	40000	
	NATURAL RUBBER SHEET	0	61.62	10.510.7	10.310.5	—	160.170	432.489	50.51	10.610.6	10.710.6	—	160.170	170.257							
	SULFUR POWDER	0																	1300.1460		
	PHC SHEET	0	63.64	13.712.6	0.52.4	—	140.270	21.40											110		

TABLE 3.2
FUEL SPRAY FIRE BURNING CHARACTERISTICS AND GAS CONCENTRATIONS
WHEN THE FIRES ARE SUFFOCATED IN SEALED CHAMBERS

FUEL	NO. OF NOZZLES	NOZZLE LOCATION	TEST #	SPRAY RATE CC/MIN	HEAT RELEASE RATE BTU/MIN	BURN TIME MIN	TOTAL HEAT RELEASE BTU	O ₂ %	CO ₂ %	CO %
WOOD (CRIB)			127					9.0	10.5	2.0
METHANOL POOL			128					12.5	6.6	-
RUBBER TIRES			129					13.2	5.9	-
METHANOL	4	DECK	131	2198	2.23	82840	9.8	6.2	1.8	.40
METHANOL	4	DECK	132	2198	1.57	58330	9.3	6.4	1.1	
METHANOL	2	DECK	133	1132	19130	2.48	47440	11.4	5.8	.12
METHANOL	2	DECK	134	1132	19130	2.93	56050	12.7	4.8	.46
METHANOL	2	DECK	135	1132	19130	2.88	55090	11.9	5.6	.09
METHANOL	1	DECK	136	559	9447	5.12	48370	12.8	5.9	.05
METHANOL	4	DECK	137	2198	37150	1.68	62410	12.6	7.6	.9
METHANOL	4	OVERHEAD	138	2198	37150	1.10	40870	13.9	7.8	.03
METHANOL	4	OVERHEAD	139	2198	37150	1.27	47180	14.4	6.8	.05
METHANOL	2	OVERHEAD	140	1132	19130	3.30	63130	13.3	6.2	.06
METHANOL	1	OVERHEAD	141	559	9447	6.0	56680	-	-	-
METHANOL	1	OVERHEAD	142	559	9447	5.98	56490	13.4	5.7	.02
JP-4	1	OVERHEAD	143	559	19170	2.72	52140	10.6	6.1	.4
JP-4	2	OVERHEAD	144	1132	38830	1.27	49310	10.7	6.6	.4
JP-4	4	OVERHEAD	145	2198	75390	1.03	77650	11.5	5.4	1.2
JP-4	4	DECK	146	2198	75390	.97	73130	11.2	4.5	1.9
JP-4	2	DECK	147	1132	38830	1.78	69120	10.5	5.8	1.5
JP-4	1	DECK	148	559	19170	2.72	52140	10.4	6.4	.6

TABLE 3.3
MAXIMUM TEMPERATURES OF AI PANELS REACHED BEFORE
FIRES IN SEALED ROOM SELF EXTINGUISH

FUEL	POOL DIA. IN.	LOCATION ABOVE FLOOR IN.	TEST #	TEMPERATURES OF 1/32" THICK AI PANELS 1' x 2'												$\Delta T_{\% AL}$ °F	
				OVERHEAD			BOT.			MID.			TOP				
				1 °F	2 °F	3 °F	4 °F	5 °F	6 °F	7 °F	8 °F	9 °F	10 °F	11 °F	12 °F		
JP-4	36	0	104	480	560	535	490	283	277	372	333	442	410	>1200	327	454	
JP-4	36	0	105	635	500	540	490	287	285	340	462	409	1300	970	1350		
METHANOL	36	0	111	485	420	500	450	290	300	400	372	438	418	810	231	322	
JP-4	18	0	112	365	340	350	345	185	191	272	267	319	300	630	432	604	
JP-4	11	0	113	230	225	230	230	138	139	180	179	214	208	250	505	705	
METHANOL	18	0	114	265	255	270	260	166	169	229	220	248	238	330	577	804	
ACETONE	18	0	115	360	340	363	350	200	206	290	284	325	320	360	346	481	
HEXANE	11	0	116	266	253	260	253	153	152	202	194	243	233	370	288	402	
HEXANE	18	0	117	505	470	540	530	250	255	372	360	441	447	1120	336	470	
ETHANOL	18	0	118	280	270	290	280	169	169	233	229	258	243	375	471	655	
JP-5	18	0	119	358	330	360	335	199	200	268	255	318	290	600	336	470	
POLYETHYLENE	0	120	126	128	134	135	107	108	122	120	128	127	160	125	174		
WOOD	0	121	375	360	365	360	184	190	255	253	310	305	720	674	935		
JP-5	36	0	122	565	470	540	480	280	284	384	353	460	414	1120	288	402	
JP-4	36	48	106	590	565	618	630	146	148	229	209	443	440	1500	826	1150	
JP-4	11	48	107	290	285	286	287	115	115	146	138	224	211	700	1015	1410	
JP-4	18	48	108	490	545	468	535	145	150	211	200	368	381	1060	1250	1740	
METHANOL	18	48	109	418	360	410	375	148	149	200	178	324	310	850	1515	2100	
METHANOL	36	48	110	570	560	580	580	161	160	233	215	455	455	1470	962	1340	

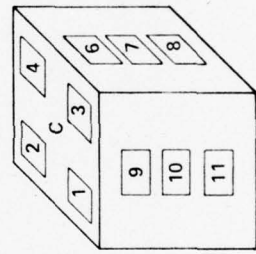


TABLE 3.3 (CONTINUED)
(SPRAY FUEL FIRES)

FUEL	NO OF NOZZLES	NOZZLE LOCATION	TEST #	OVERHEAD				BOT.			MID.			TOP			C BTU/FT ²
				1 °F	2 °F	3 °F	4 °F	11 °F	8 °F	10 °F	7 °F	9 °F	6 °F				
METHANOL	4	DECK	131	725	676	783	817	167	158	342	361	549	561	4.86			
METHANOL	4	DECK	132	617	666	759	849	187	163	342	347	505	590	5.2			
METHANOL	2	DECK	133	543	581	617	689	180	147	289	289	430	502	3.4			
METHANOL	2	DECK	134	514	451	590	617	158	140	257	255	421	473	2.8			
METHANOL	2	DECK	135	612	633	675	709	180	162	302	307	486	520	4.4			
METHANOL	1	DECK	136	403	491	444	522	147	140	199	210	333	347	.95			
METHANOL	4	DECK	137	550	675	689	880	162	162	316	343	473	597	3.3			
METHANOL	4	OVERHEAD	138	446	752	410	696	127	131	250	273	361	441	2.1			
METHANOL	4	OVERHEAD	139	437	689	428	698	126	129	243	270	356	473	2.0			
METHANOL	2	OVERHEAD	140	423	523	363	487	118	95	174	176	289	351	1.5			
METHANOL	1	OVERHEAD	141	302	415	286	327	90	97	138	136	237	264	.61			
METHANOL	1	OVERHEAD	142	306	442	302	365	113	104	153	158	257	286	.56			
JP-4	1	OVERHEAD	143	430	541	451	759	145	154	205	232	376	523	2.1			
JP-4	2	OVERHEAD	144	491	730	588	851	198	192	297	324	414	581	3.9			
JP-4	4	OVERHEAD	145	518	734	500	804	181	185	302	345	426	590	2.4			
JP-4	4	DECK	146	549	631	507	756	174	163	289	313	399	496	4.6			
JP-4	2	DECK	147	504	636	525	784	192	180	313	320	419	489	4.0			
JP-4	1	DECK	148	547	761	486	649	187	174	284	284	397	450	2.1			

TABLE 3.4
TIME FOR AI PANELS TO REACH TEMPERATURES LISTED IN TABLE 3.3

FUEL	POOL DIA. IN.	LOCATION ABOVE FLOOR IN.	TEST #	TIME FOR PANELS TO REACH MAX. TEMP.										AIR SEC.		
				OVERHEAD				BOT.				MID.		TOP		
				1 SEC.	2 SEC.	3 SEC.	4 SEC.	11 SEC.	8 SEC.	10 SEC.	7 SEC.	9 SEC.	6 SEC.	5 SEC.		
JP-4	36	0	104	80	76	76	76	80	85	87	87	81	87	~ 40		
JP-4	36	0	105	73	77	74	77	85	89	87	89	79	86	51		
METHANOL	36	0	111	200	200	190	190	220	210	220	210	220	200	200	70	
JP-4	18	0	112	340	350	345	345	350	345	350	350	355	345	350	120	
JP-4	11	0	113	1195	1195	1195	1195	1250	1195	1210	1210	1210	1240	1240	210	
METHANOL	18	0	114	940	940	940	940	990	980	980	980	990	990	990	550	
ACETONE	18	0	115	300	310	300	290	330	330	330	320	310	300	300	90	
HEXANE	11	0	116	850	850	850	850	850	850	850	860	860	860	860	240	
HEXANE	18	0	117	120	130	120	120	150	150	150	140	140	134	130	66	
ETHANOL	18	0	118	500	500	500	500	530	525	525	525	525	525	525	285	
JP-5	18	0	119	360	370	370	370	370	370	360	390	380	370	390	220	
POLYETHYLENE	0	120	1350	1350	1350	1350	1350	1450	1460	1450	1450	1450	1450	1450	810	
WOOD	0	121	240	230	230	210	210	330	330	290	300	270	270	250	154	
JP-5	36	0	122	124	133	127	137	134	137	132	135	130	134	134	44	
JP-4	36	48	106	245	211	235	221	253	253	273	234	228	224	224	36	
JP-4	36	48	107	1580	1580	1570	1580	1650	1600	1620	1640	1540	1560	1560	180	
JP-4	36	48	108	270	270	280	273	420	420	410	420	400	400	400	53	
METHANOL	18	48	109	1060	1130	1150	1150	1220	1210	1210	1210	1150	1060	1060	290	
METHANOL	36	48	110	160	140	140	140	280	280	220	230	170	160	160	50	

TABLE 3.4 (CONTINUED)
(SPRAY FUEL FIRES)

FUEL	NO. OF NOZZLES	NOZZLE LOCATION	TEST	OVERHEAD				BOT.	MID.	TOP	C SEC.	
				1 SEC.	2 SEC.	3 SEC.	4 SEC.					
METHANOL	4	DECK	131	73	75	64	104	101	100	97	98	138
METHANOL	4	DECK	132	80	70	65	96	91	89	88	80	100
METHANOL	2	DECK	133	147	146	146	148	148	147	147	147	160
METHANOL	2	DECK	134	158	156	156	163	163	156	158	159	180
METHANOL	2	DECK	135	161	161	161	170	167	167	165	161	173
METHANOL	1	DECK	136	305	287	281	310	310	310	310	303	317
METHANOL	4	DECK	137	81	73	82	58	97	97	87	85	83
METHANOL	4	OVERHEAD	138	67	61	67	62	70	70	67	60	65
METHANOL	4	OVERHEAD	139	68	64	68	64	74	74	72	72	69
METHANOL	2	OVERHEAD	140	185	184	185	179	186	185	186	185	196
METHANOL	1	OVERHEAD	141	310	311	310	322	311	321	311	312	367
METHANOL	1	OVERHEAD	142	314	314	314	314	321	320	320	320	358
JP-4	1	OVERHEAD	143	174	171	177	172	179	177	176	180	174
JP-4	2	OVERHEAD	144	71	77	76	66	80	83	79	80	85
JP-4	4	OVERHEAD	145	63	59	65	60	77	71	71	70	70
JP-4	4	DECK	146	31	51	51	42	57	57	58	55	54
JP-4	2	DECK	147	100	100	99	67	101	101	105	99	110
JP-4	1	DECK	148	146	135	150	150	154	154	150	153	154

TABLE 3.4 (CONTINUED)
(SPRAY FUEL FIRES)

FUEL	NO. OF NOZZLES	NOZZLE LOCATION	TEST #	OVERHEAD			BOT.			MID.			TOP			C SEC.
				1 SEC.	2 SEC.	3 SEC.	4 SEC.	5 SEC.	6 SEC.	7 SEC.	8 SEC.	9 SEC.	10 SEC.	11 SEC.		
METHANOL	4	DECK	131	73	75	64	104	101	100	97	98	98	138			
METHANOL	4	DECK	132	80	70	65	62	96	91	89	88	80	75			100
METHANOL	2	DECK	133	147	146	146	146	148	148	147	147	147	147			160
METHANOL	2	DECK	134	158	156	156	156	163	163	156	158	159	159			180
METHANOL	2	DECK	135	161	161	161	170	167	167	167	165	161	170			173
METHANOL	1	DECK	136	305	287	281	310	310	310	310	310	310	303			317
METHANOL	4	DECK	137	81	73	82	58	97	97	87	85	84	83			120
METHANOL	4	OVERHEAD	138	67	61	67	62	70	70	67	60	67	65			70
METHANOL	4	OVERHEAD	139	68	64	68	64	74	74	72	72	72	69			75
METHANOL	2	OVERHEAD	140	185	184	185	179	186	185	186	185	185	185			196
METHANOL	1	OVERHEAD	141	310	311	310	310	322	311	321	311	312	311			367
METHANOL	1	OVERHEAD	142	314	314	314	314	321	320	321	320	320	314			358
JP-4	1	OVERHEAD	143	174	171	177	172	179	177	176	180	177	174			200
JP-4	2	OVERHEAD	144	71	77	76	66	80	83	79	80	78	75			85
JP-4	4	OVERHEAD	145	63	59	65	60	77	71	71	70	69	63			70
JP-4	4	DECK	146	31	51	51	42	57	57	58	55	54	54			63
JP-4	2	DECK	147	100	100	99	67	101	101	105	99	96	101			110
JP-4	1	DECK	148	146	135	150	150	154	154	150	153	154	154			160

TABLE 4.0
AVERAGE THERMAL FLUX INCIDENT ON THE CHAMBER WALLS
CALCULATED ACCORDING TO THE SIMPLE ADIABATIC MODEL

X FT	V FT ³	Q ₃₀ BTU	Q ₄₅ BTU	Q ₆₀ BTU	ΔT °F	A FT ²	q ₃₀ BTU FT ⁻²	q ₄₅ BTU FT ⁻²	q ₆₀ BTU FT ⁻²
2	32	960	1440	1920	150	72	12	19	25
4	128	3840	5760	7680	175	106	21	33	45
6	288	8640	12960	17280	250	264	27	44	60
8	512	15360	23040	30720	300	384	32	52	72
10	800	24000	36000	48000	375	520	35	58	81
12	1152	34560	51840	69120	382	672	38	64	90
14	1568	47040	70560	94080	390	840	41	69	97
16	2048	61440	92160	122880	395	1024	44	74	104
18	2592	77760	116640	155520	400	1224	47	78	110
20	3200	96000	144000	192000	405	1440	49	82	115

$$V = \text{VOLUME} = 8X^2$$

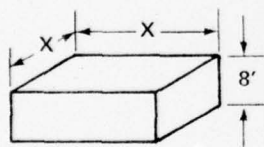
$$A = \text{SURFACE} = 2X^2 + 32X$$

Q = ENERGY AVAILABLE IN COMPARTMENT AIR

$$Q_{30} = 30 \circ V \text{ BTU}$$

$$Q_{45} = 45 \circ V \text{ BTU}$$

$$Q_{60} = 60 \circ V \text{ BTU}$$



ΔT = INCREASE IN AIR TEMPERATURE ASSUMED
BASED ON TABLES 3.0 AND 3.3

$$Q_{\text{AIR}} = 0.75 \circ V \circ \Delta T$$

q = SPECIFIC HEAT FLUX INCIDENT ON WALLS

$$q = \frac{Q - Q_{\text{AIR}}}{A}$$

TABLE 4.1 COMPARISON OF FIRE HAZARD ON PHM-1 BY AVAILABLE
 O_2 VERSUS FUEL LOADING

SPACE	NO.	AREA ft ²	O_2 ENERGY Btu _D	FUEL ENERGY Btu _F	RATIO Btu _F / Btu _C
PILOT HOUSE	01-9-0-C	184	66,240	3,264,800	49
CIC	1-9-0-C	399	143,640	9,012,800	63
COMMUNICATIONS ROOM	1-14-2-C	78.7	28,332	2,353,600	83*
PASSAGE NO. 4	1-15-1-L	79.6	28,656	3,160,800	110
ELECTRONICS EQUIPMENT RM.	1-17-2-C	130	46,800	2,545,600	54*
CO STATE ROOM	1-18-1-L	96.8	34,848	2,736,800	78*
GALLEY	2-9-1-Q	74.0	26,640	1,255,200	47
CREW AND CPO MESS	2-9-2-L	121.8	43,848	4,007,200	91
OFFICERS BUNK ROOM	2-11-1-L	116	41,760	5,000,000	120*
PASSAGE NO. 1	2-13-2-L	21.5	7,740	848,800	110
WARDROOM	2-13-4-L	45	16,200	1,370,400	85
PASSAGE NO. 2	2-15-0-L	65.6	23,616	1,230,400	52
COP LIVING	2-15-1-L	77.8	28,008	4,504,000	161*
OFF. AND COP WR, WC, AND SH	2-15-2-L	70.7	25,452	2,026,400	80
PASSAGE NO. 3	2-18-01-L	60.2	21,672	2,844,000	131
CREW LIVING NO. 1	2-18-0-L	30.2	10,872	2,242,400	206
CREW LIVING NO. 2	2-18-1-L	61.9	22,284	5,375,200	241*
CREW LIVING NO. 3	2-18-1-L	63.8	22,968	5,420,000	236*
CREW WR, WG AND SH	2-21-1-L	95.6	34,416	3,560,000	103
EOS AND DAMAGE CONTROL STA.	2-21-2-C	95.6	34,416	3,580,000	104
BOSON STRM NO. 1	3-C-1-A	12.6	4,536	1,128,800	249*
BOSON STRM NO. 2	3-C-2-A	12.6	4,536	1,175,200	260*
DRY PROVISIONS STRM	3-4-0-Q	43	15,480	1,977,600	128*

*Suitable for Sealed Compartment Fire Protection.

TABLE 4.2
MAXIMUM THERMAL FLUX INCIDENT ON SEALED
COMPARTMENT BULKHEADS DURING SPRAY FUEL FIRES

TEST #	FUEL	NO OF NOZZLES	BURNING TIME SEC.	R ₁	R ₂	R ₃	R ₄	R ₅
				BTU	FT ⁻²	SEC ⁻¹		
131	METHANOL	4 †	134	3.4	3.2	2.5	1.4	1.7
132	METHANOL	4 †	94	3.6	3.2	2.3	1.6	1.8
133	METHANOL	2 †	149	2.0	2.1	1.3	1.0	1.0
134	METHANOL	2 †	176	2.0	2.0	1.2	.8	1.0
135	METHANOL	2 †	173	1.8	1.9	1.2	—	1.0
136	METHANOL	1 †	307	.9	.9	.5	.4	.5
137	METHANOL	4 †	101	3.8	—	2.5	1.7	2.7
138	METHANOL	4 x	66	1.5	2.1	1.4	1.6	2.1
139	METHANOL	4 x	76	1.7	2.1	1.3	1.5	1.9
140	METHANOL	2 x	198	1.0	1.2	.7	.7	.9
141	METHANOL	1 x	360	.7	.8	.5	.4	.6
142	METHANOL	1 x	359	.7	.7	.5	.4	.7
143	JP-4	1 x	163	1.3	1.8	.8	.7	1.2
144	JP-4	2 x	76	3.0	3.2	1.6	1.4	2.2
145	JP-4	4 x	62	3.5	4.1	2.4	1.6	2.1
146	JP-4	4 †	58	5.0	4.6	3.0	2.7	3.4
147	JP-4	2 †	107	2.9	2.7	1.4	1.6	2.3
148	JP-4	1 †	163	1.3	1.4	.8	.8	1.2

x NOZZLES OVERHEAD POINTED DOWN

† NOZZLES ON DECK POINTED UP

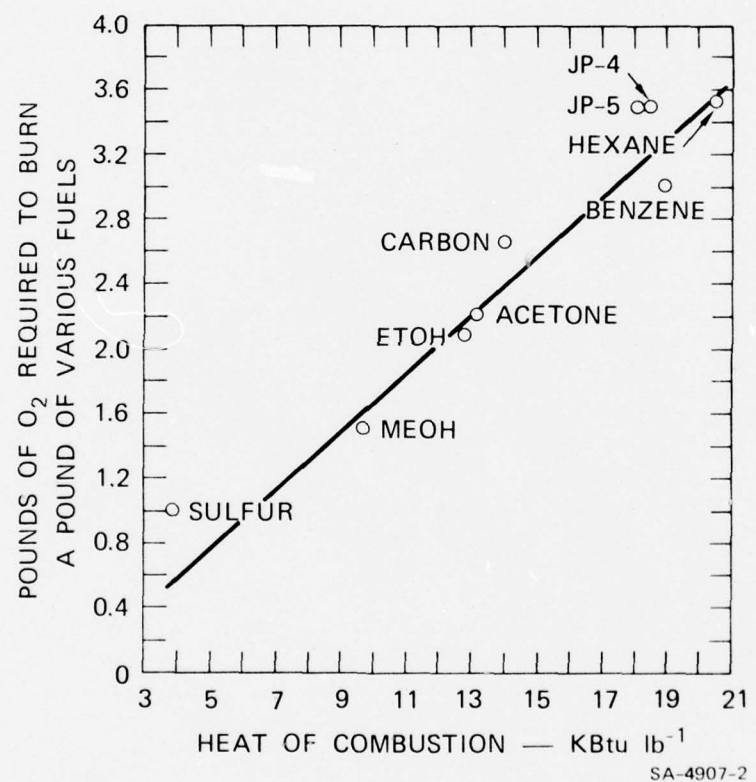


FIG. 2.0 THEORETICAL O₂ REQUIREMENTS TO BURN VARIOUS FUELS

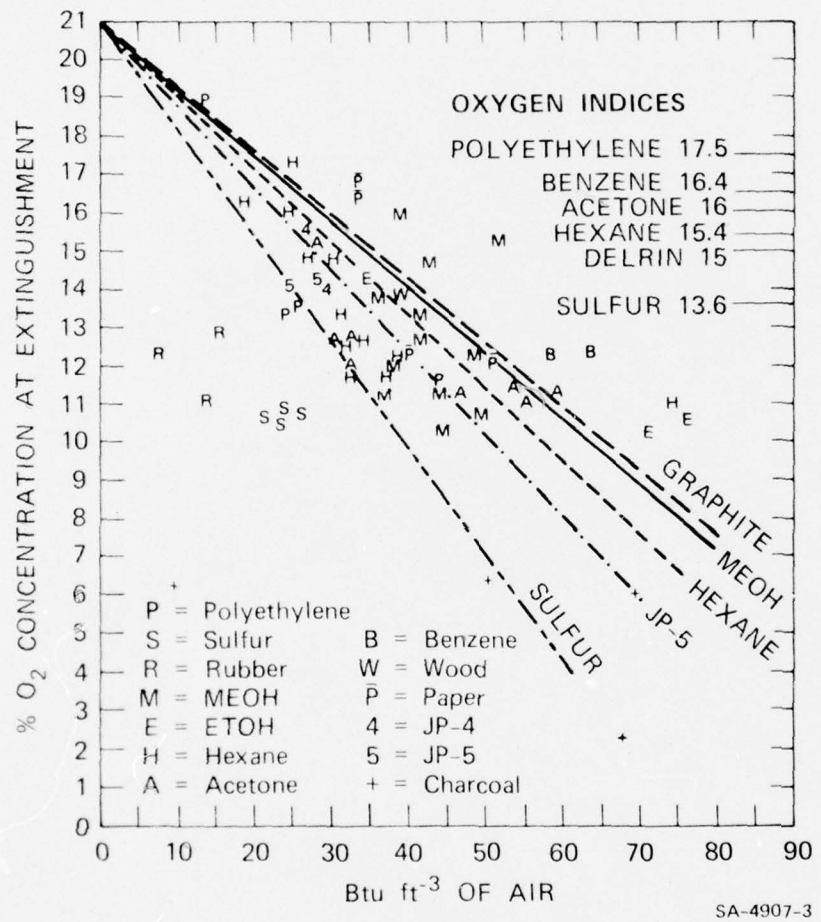


FIG. 2.1 RELATIONSHIP BETWEEN TOTAL ENERGY AVAILABLE PER FT³ OF AIR AND THE OXYGEN CONCENTRATION AT EXTINGUISHMENT FOR VARIOUS FUELS BURNING IN A SEALED COMPARTMENT

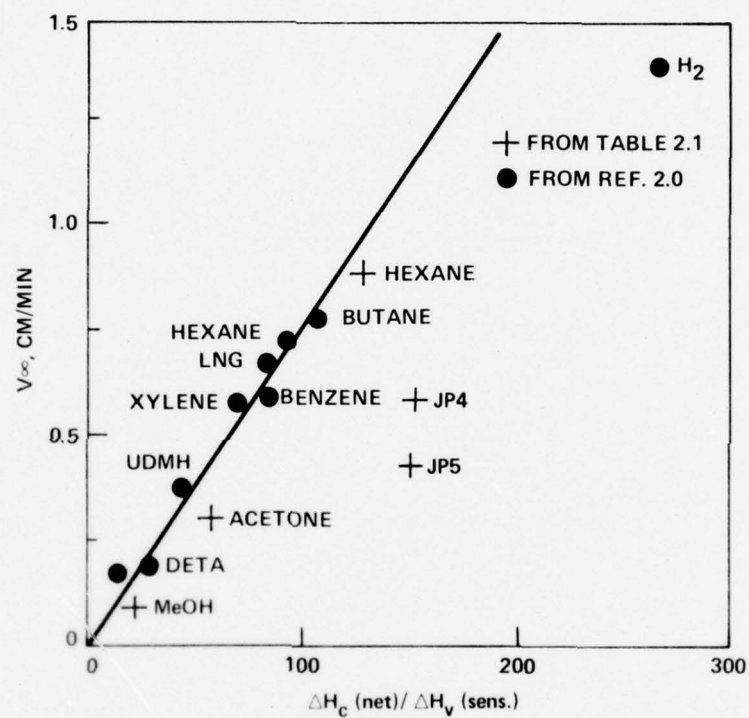


FIG. 2.2 RELATION BETWEEN LIQUID BURNING RATES AT LARGE POOL DIAMETER AND THERMOCHEMICAL PROPERTIES OF THE FUELS

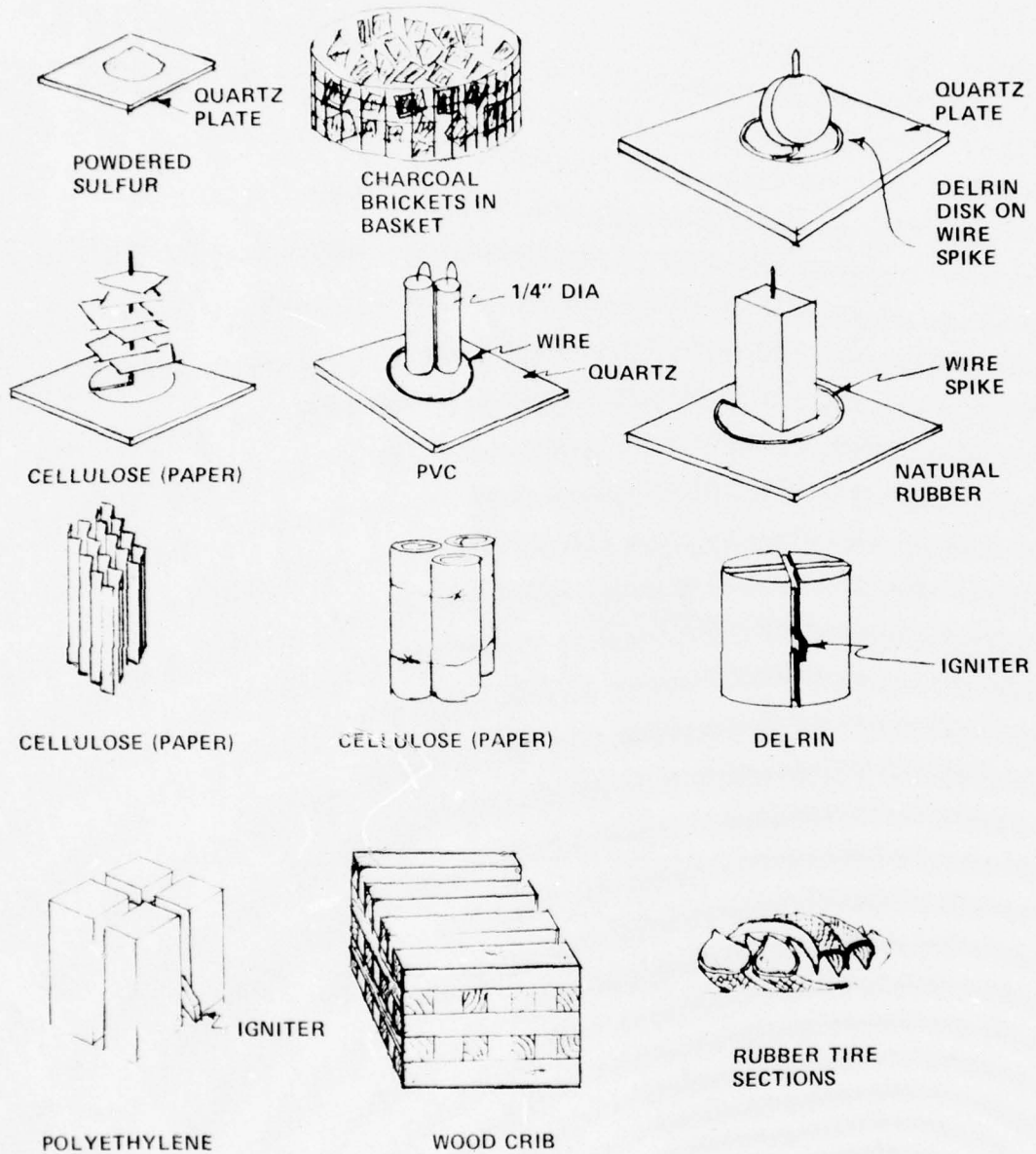
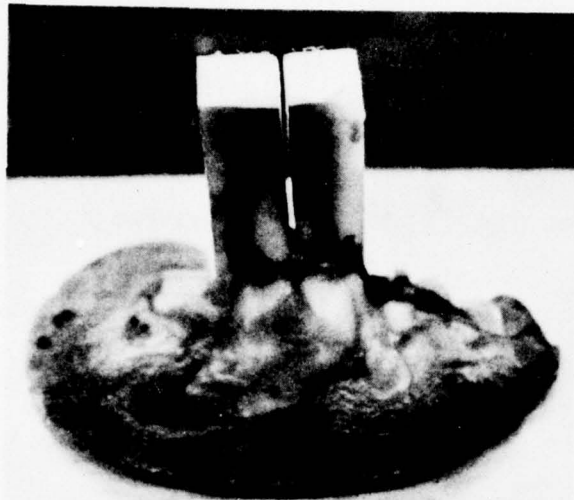
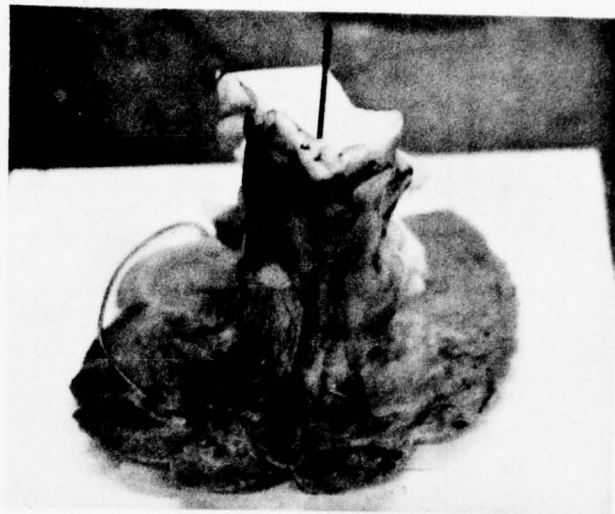


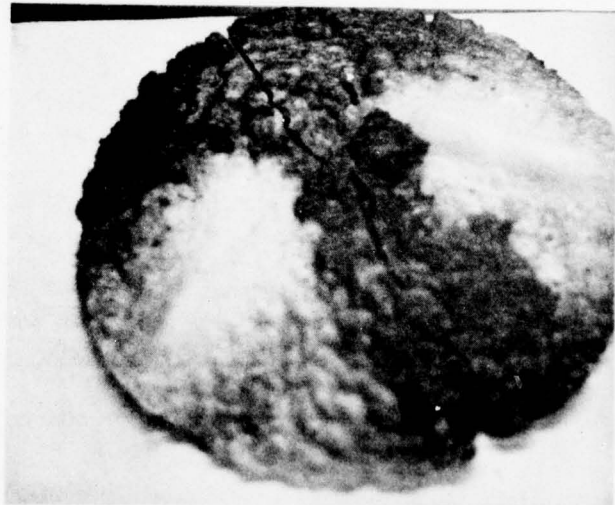
FIG. 2.3 VARIOUS SOLID FUEL CONFIGURATIONS



POLYETHYLENE TEST #81

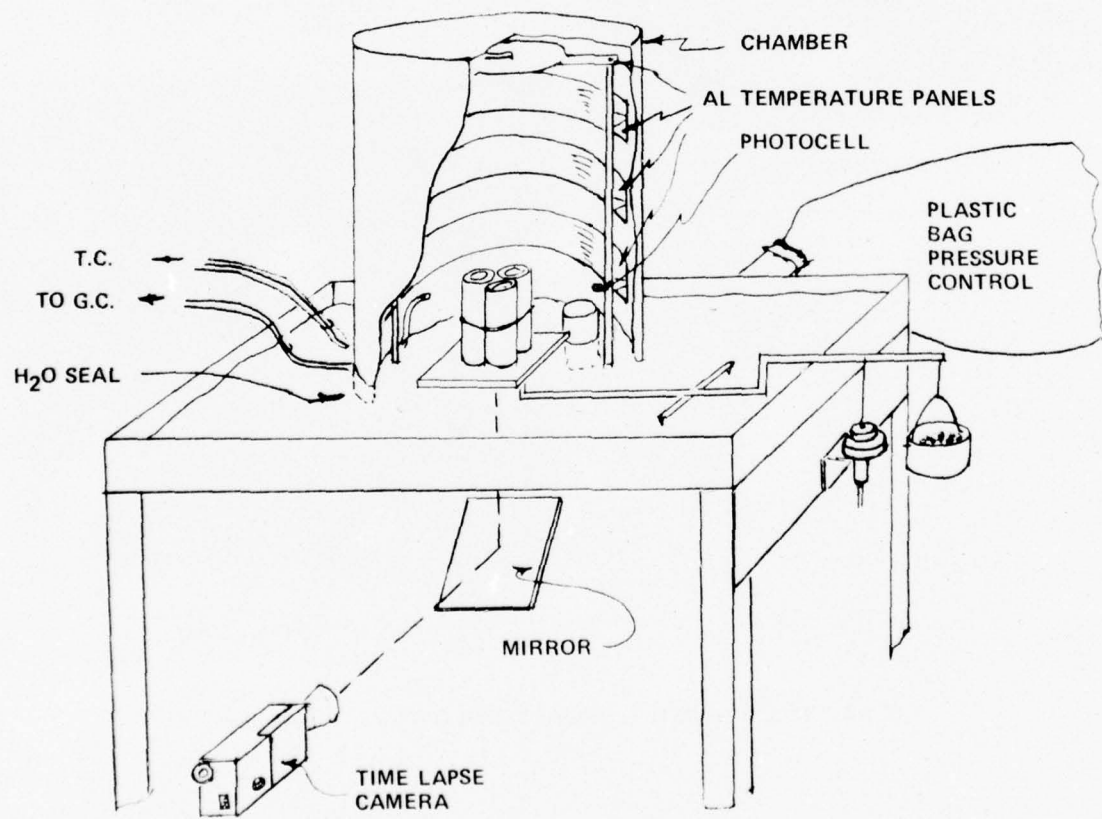
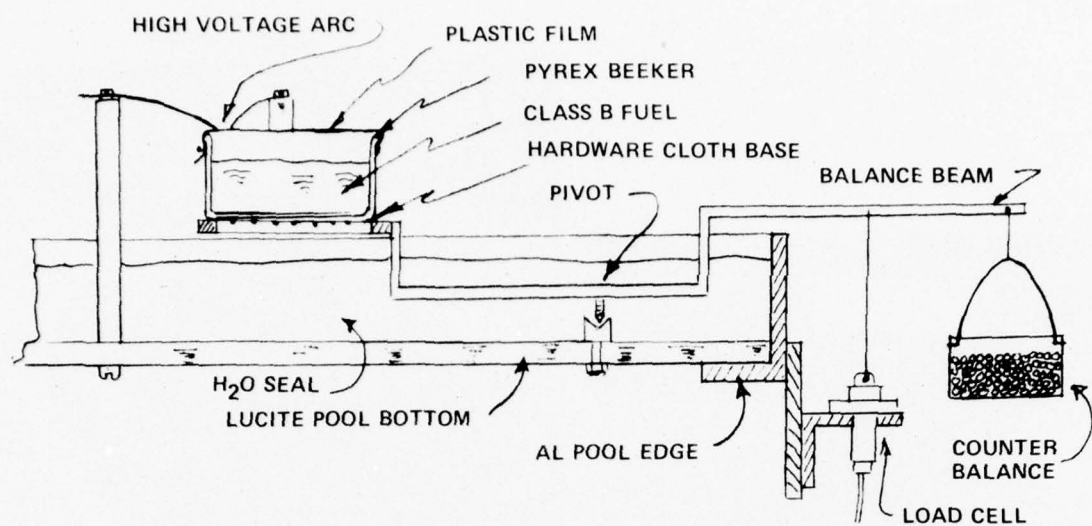


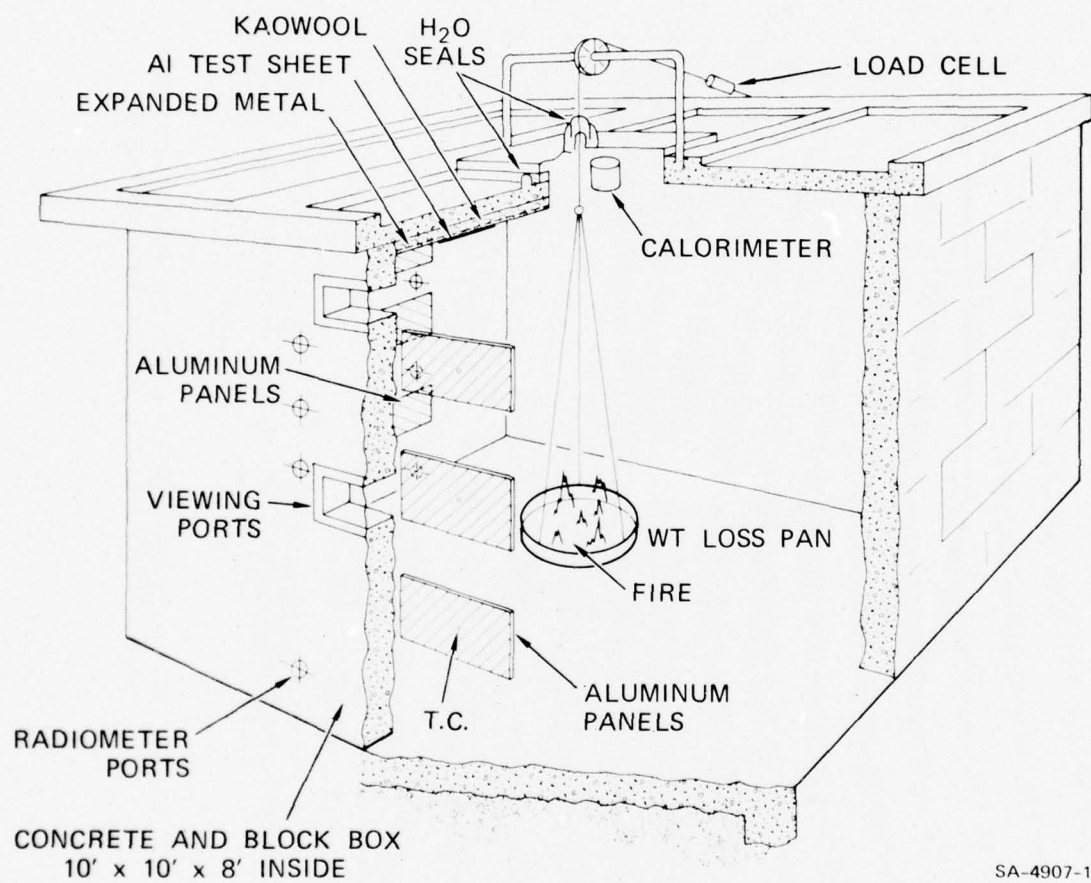
POLYETHYLENE TEST #82



DELRIN #80

FIG. 2.4 MELTING AND FLOW PATTERNS OF PLASTIC SAMPLES

FIG. 2.5 EXPERIMENTAL ARRANGEMENT FOR THE 1.19, 7.94, AND 102.4 FT³ CHAMBERS



SA-4907-1

FIG. 2.6 EXPERIMENTAL ARRANGEMENT FOR THE 1050 FT³ TEST CELL

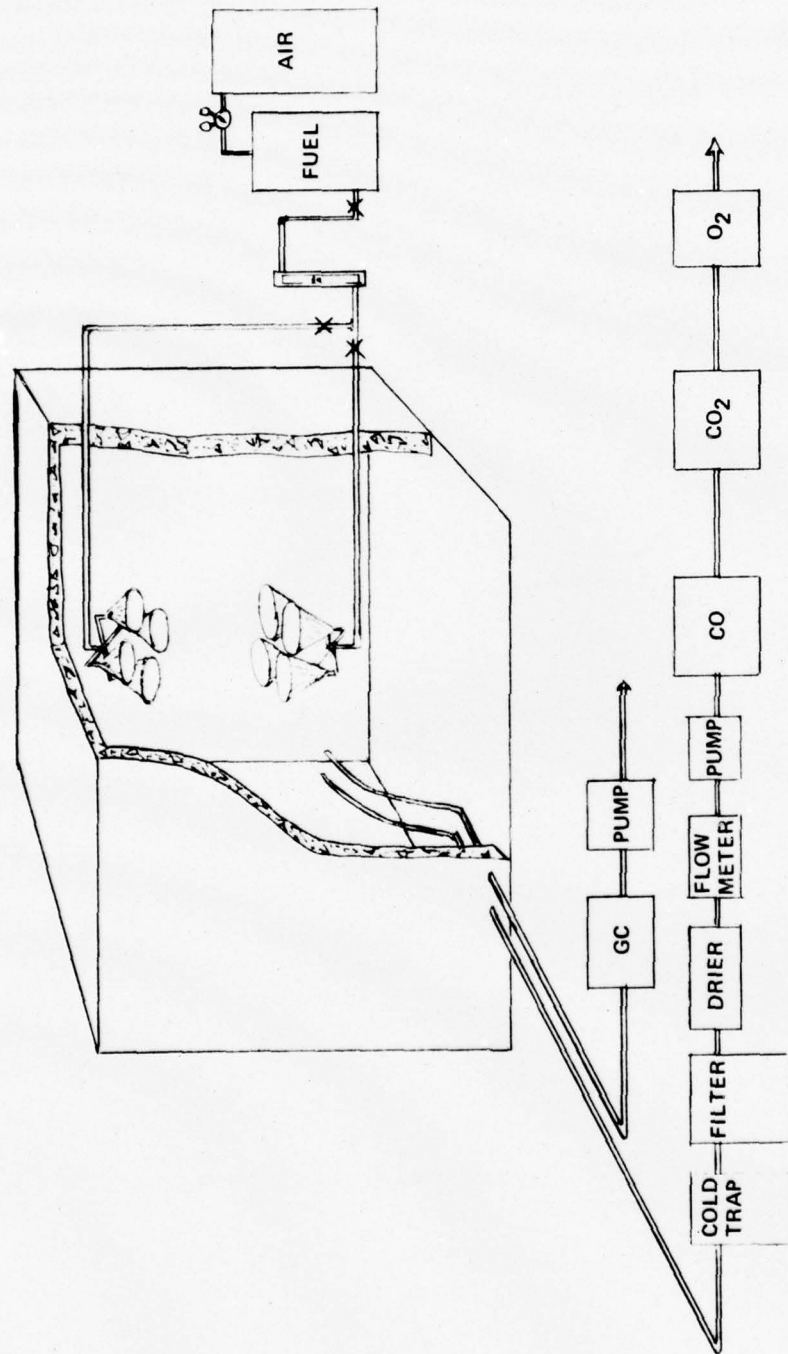
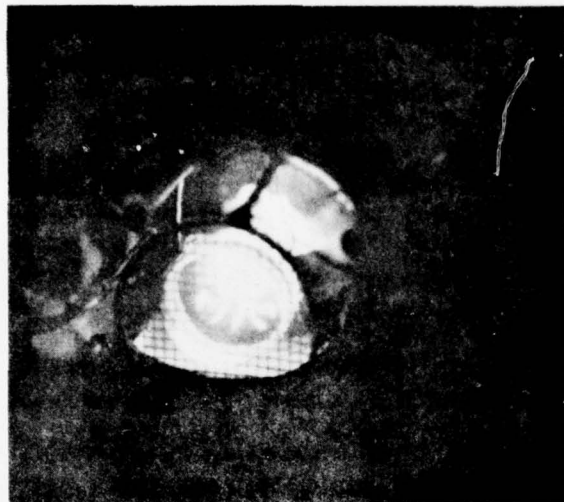
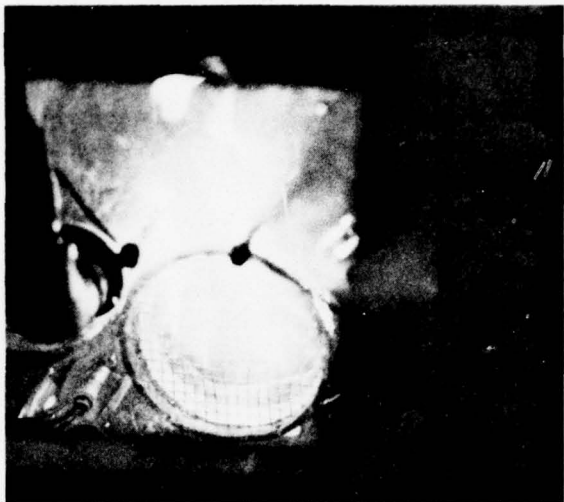


FIG. 2.7 FUEL NOZZLE ARRANGEMENT FOR THE SPRAY FIRES AND
A BLOCK DIAGRAM OF THE GAS ANALYSIS EQUIPMENT



(a)



(b)



(c)



(d)

FIG. 3.0 FLAME GEOMETRY AND TURBULENCE FOR VARIOUS POOL SIZES

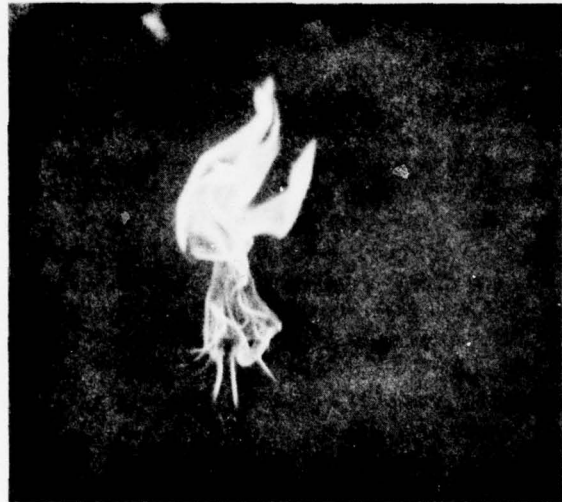
- (a) 3" DIA. JP-4 FIRE IN 1.19 FT^3 CHAMBER VIEWED FROM BELOW
- (b) 5 3/4" DIA. HEXANE FIRE IN 7.94 FT^3 CHAMBER VIEWED FROM BELOW
- (c) 5 3/4" DIA. HEXANE FIRE IN 102.4 FT^3 CHAMBER VIEWED FROM ABOVE
- (d) 9 1/4" DIA. HEXANE FIRE IN 102.4 FT^3 CHAMBER VIEWED FROM ABOVE



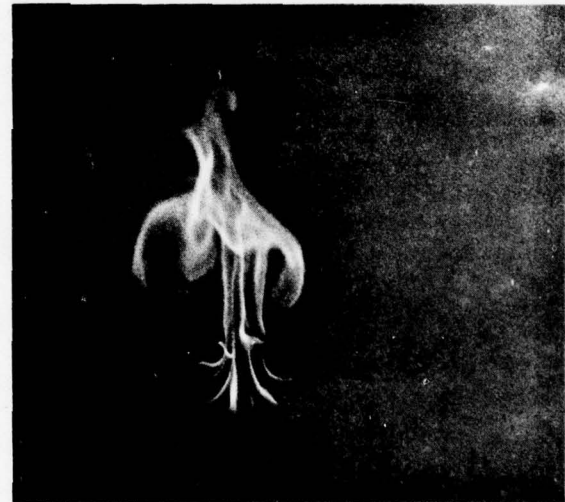
(a)



(b)



(c)



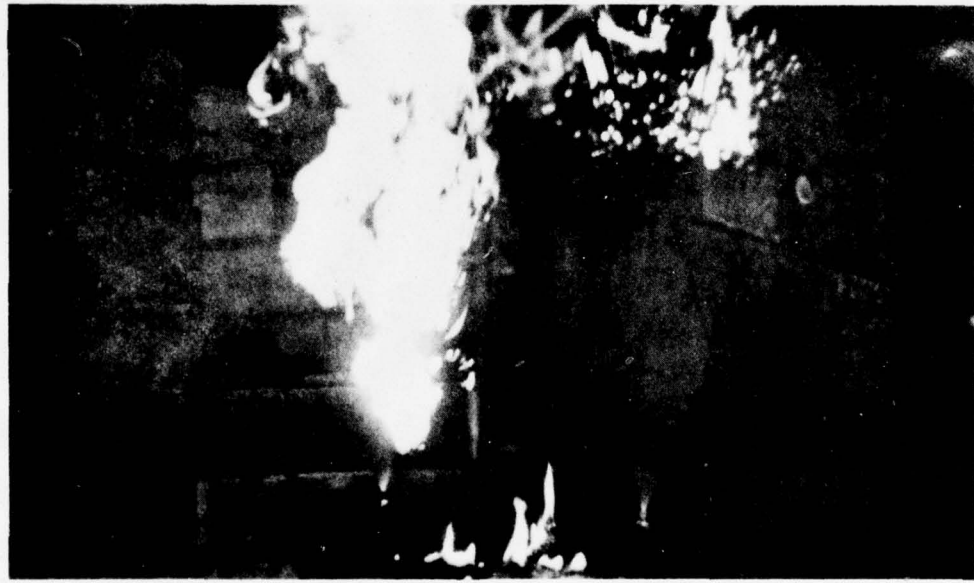
(d)

FIG. 3.1 FLAME STRUCTURES AT VARIOUS STAGES DURING A 5 3/4" DIA.
JP-4 POOL FIRE IN THE 102.4 FT³ CHAMBER

- (a) IMMEDIATELY AFTER IGNITION
- (b) DURING PEAK BURNING RATE PERIOD
- (c) AFTER THE PEAK BURNING RATE WHEN STARTING TO RUN OUT OF O₂
- (d) DYING FLAME JUST BEFORE EXTINGUISHMENT



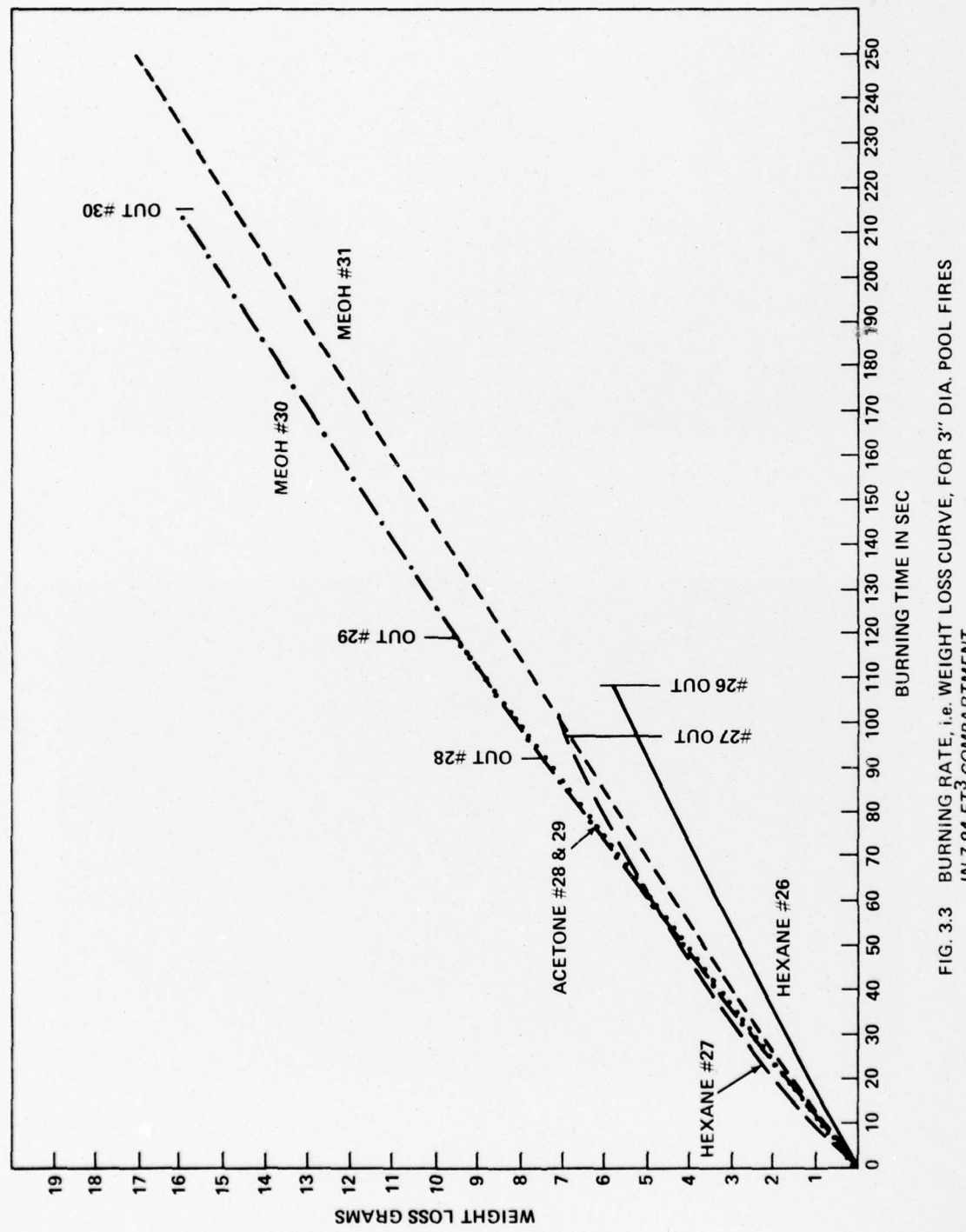
(a)



(b)

FIG. 3.2 JP-4 SPRAY FIRES IN THE 1050 FT³ TEST CELL

- (a) NORMAL COMBUSTION
- (b) JUST BEFORE EXTINGUISHMENT



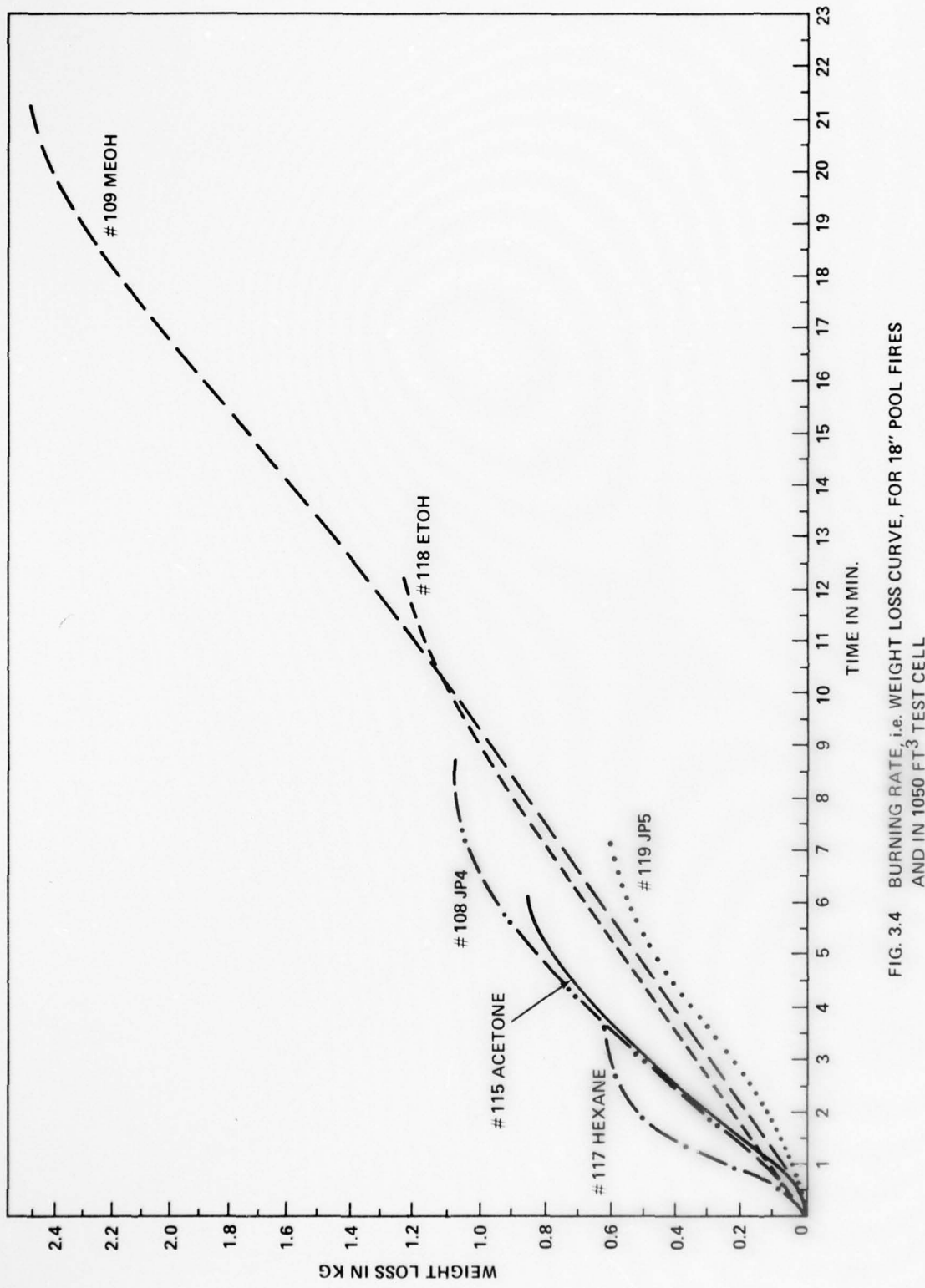


FIG. 3.4 BURNING RATE, i.e. WEIGHT LOSS CURVE, FOR 18" POOL FIRES
AND IN 1050 FT³ TEST CELL

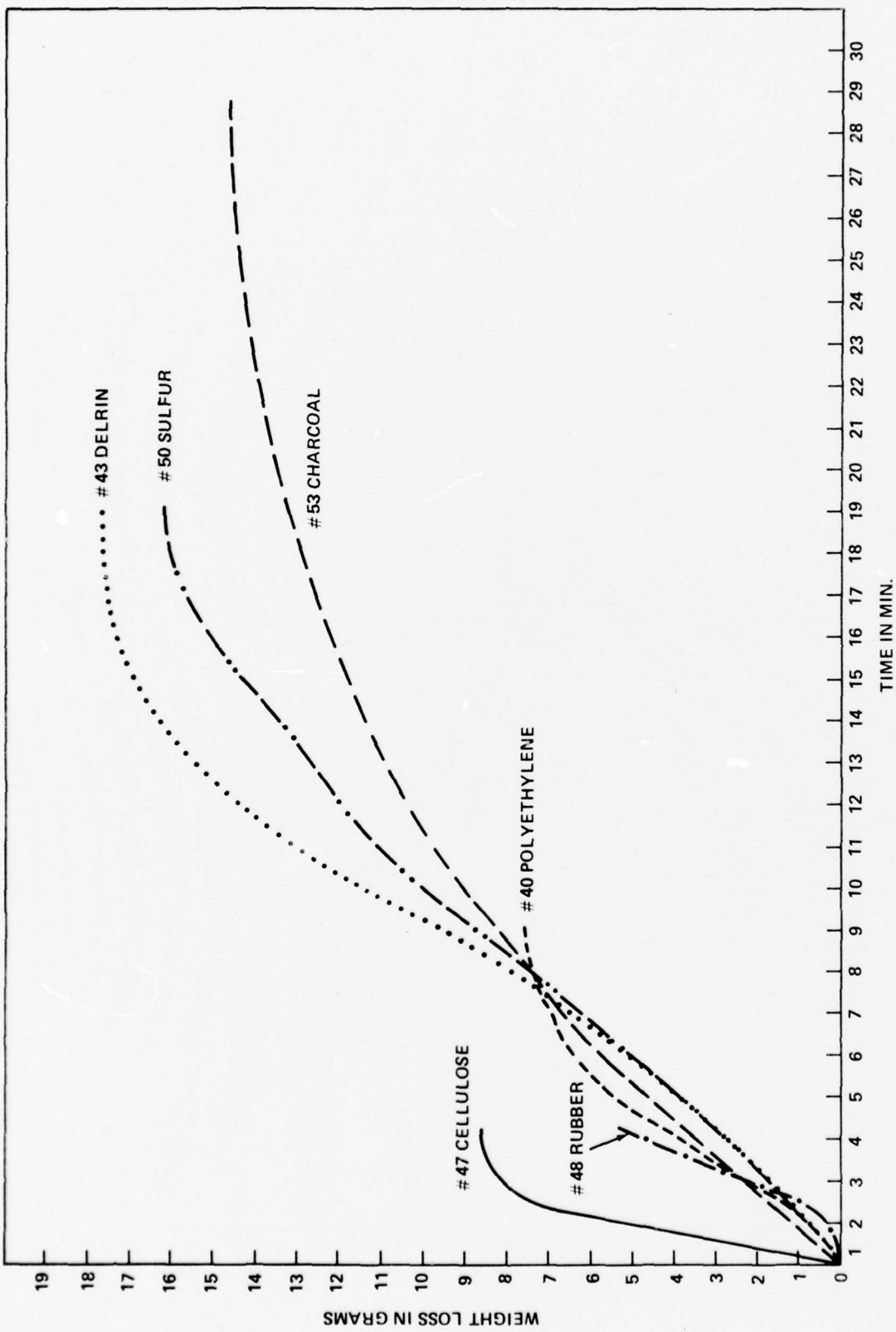


FIG. 3.5 BURNING RATE, i.e. WEIGHT LOSS CURVE FOR CLASS A FIRES
BURNING IN 7.94 FT³ COMPARTMENT

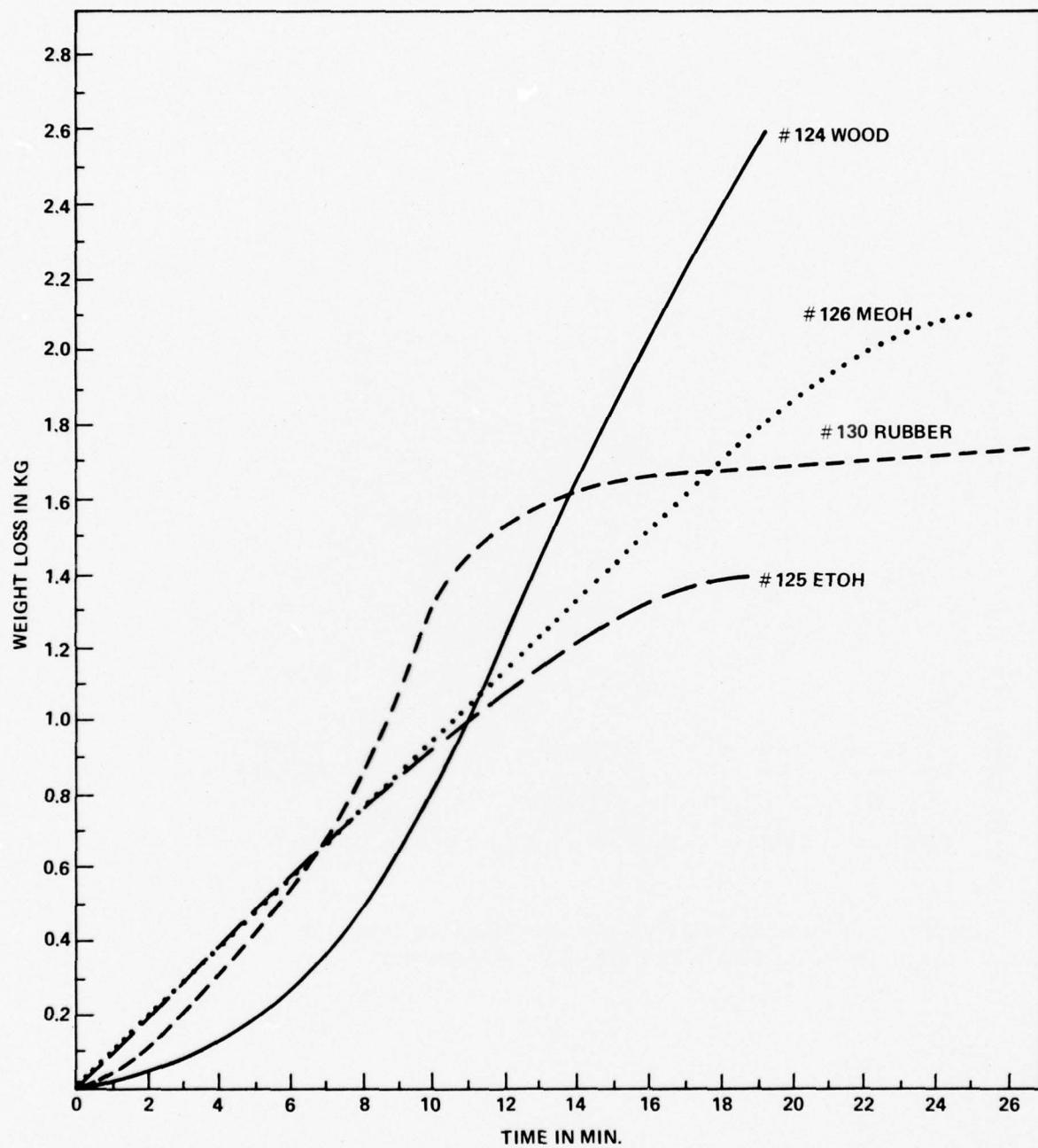


FIG. 3.6 BURNING RATE, i.e. WEIGHT LOSS CURVE, FOR CLASS A FIRE
IN 1050 FT³ TEST CELL

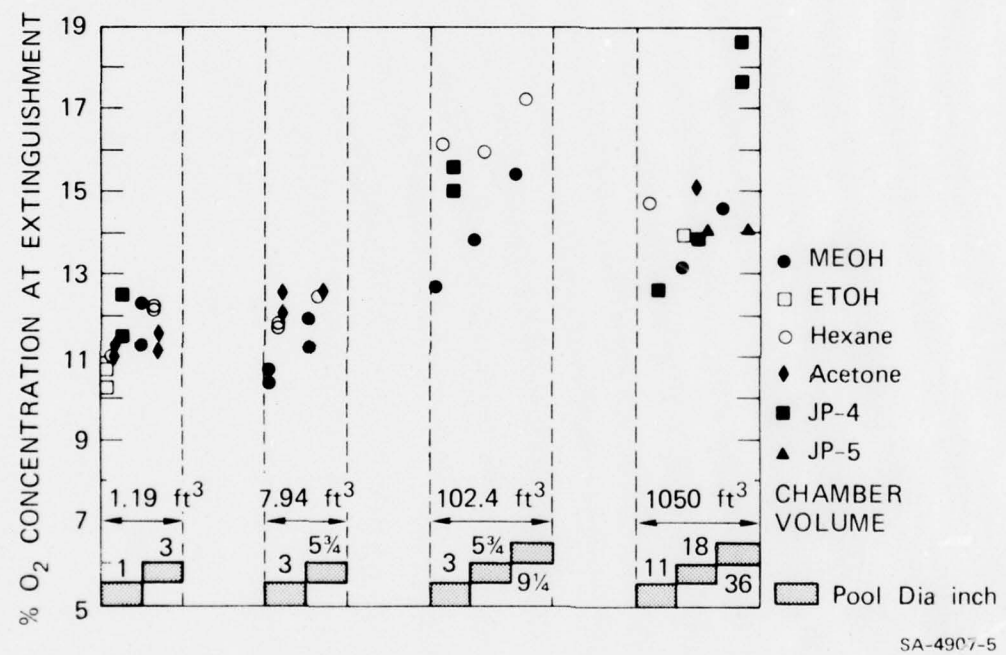


FIG. 3.7 EFFECT OF CHAMBER VOLUME AND FIRE POOL DIAMETER
ON THE O₂ CONCENTRATION AT EXTINGUISHMENT

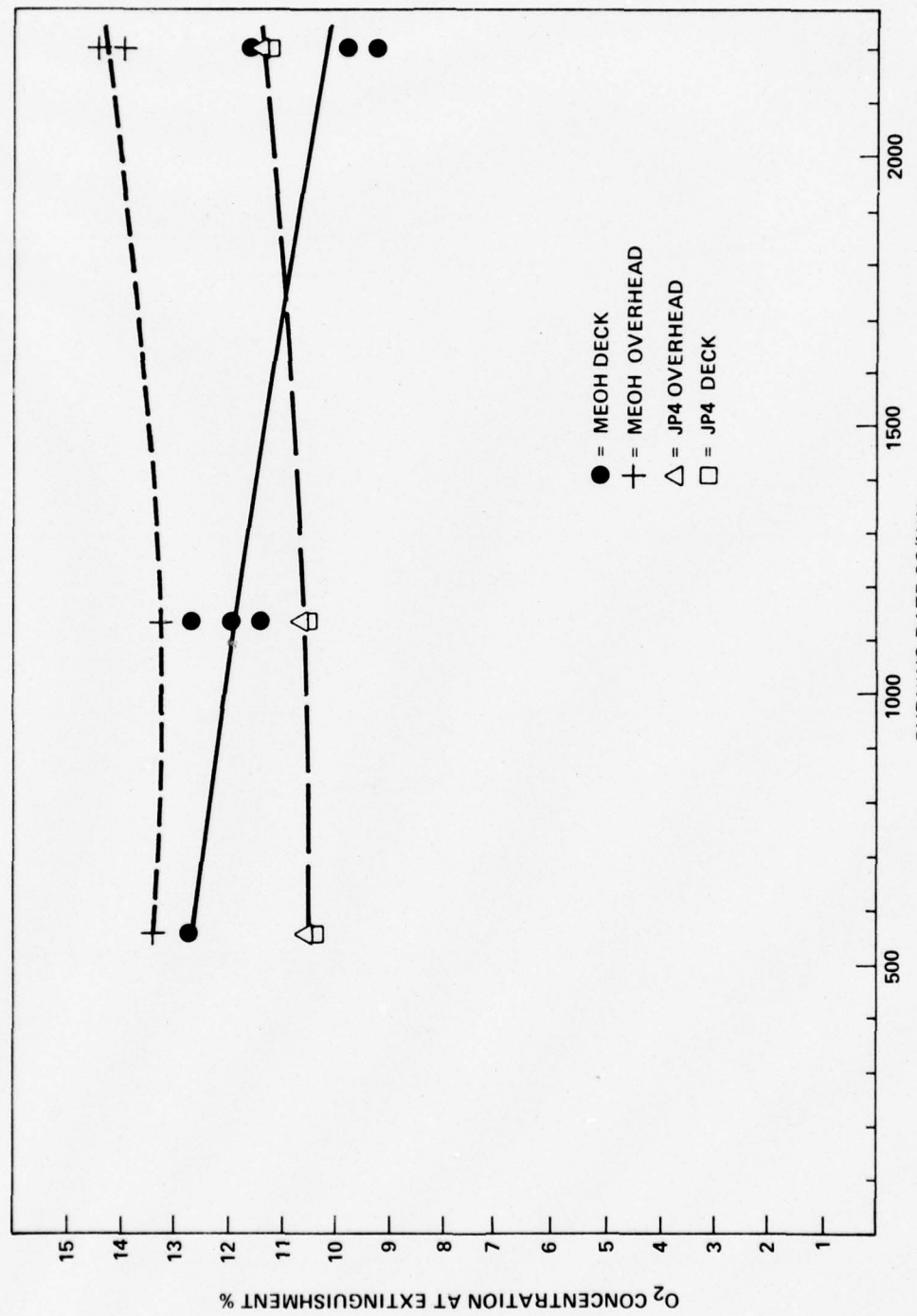


FIG. 3.8 EFFECT OF NOZZLE LOCATION AND SPRAY RATE ON EXTINGUISHMENT
 O_2 CONCENTRATION FOR JP-4 AND METHANOL FIRES

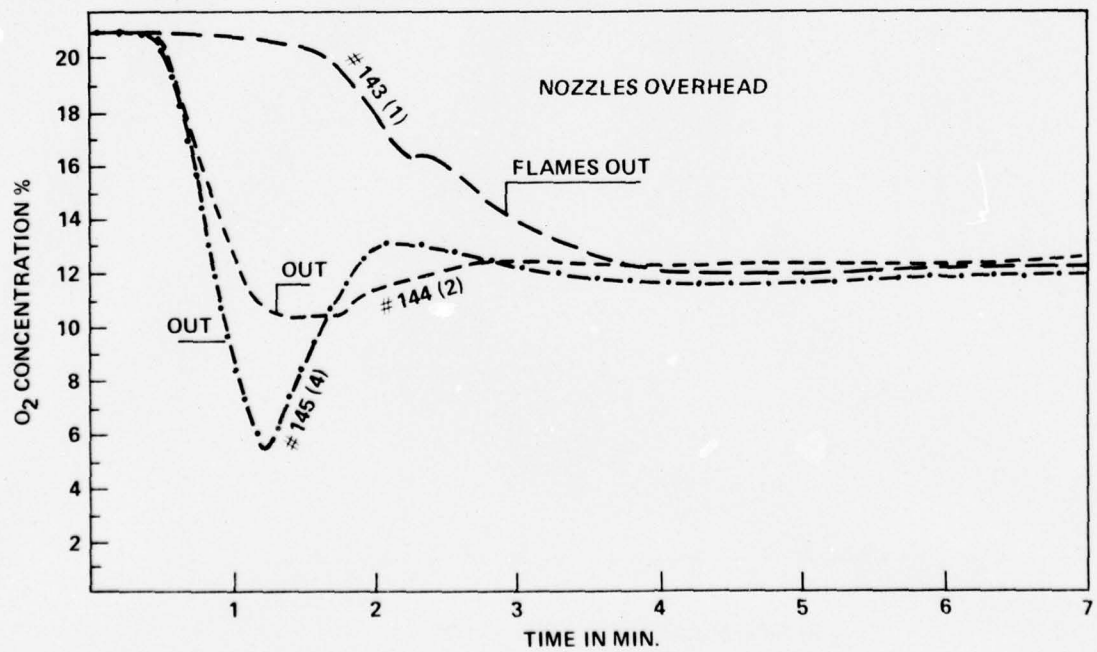
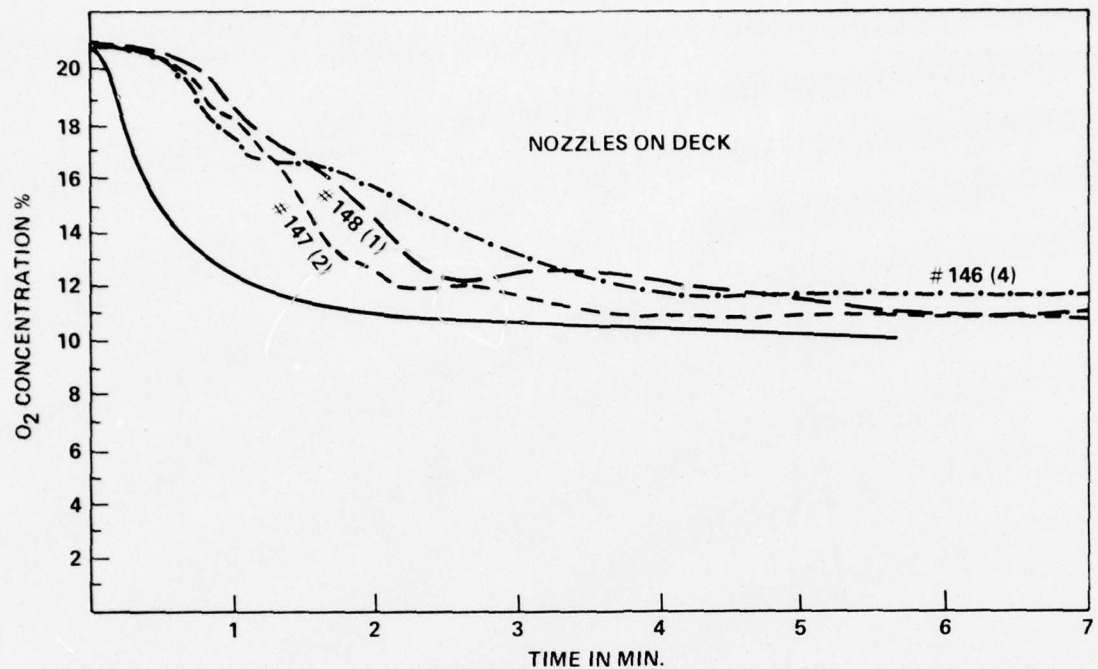


FIG. 3.9 VARIATION IN O₂ CONCENTRATION DURING JP-4 SPRAY FIRES IN 1050 FT³ SEALED TEST CELL

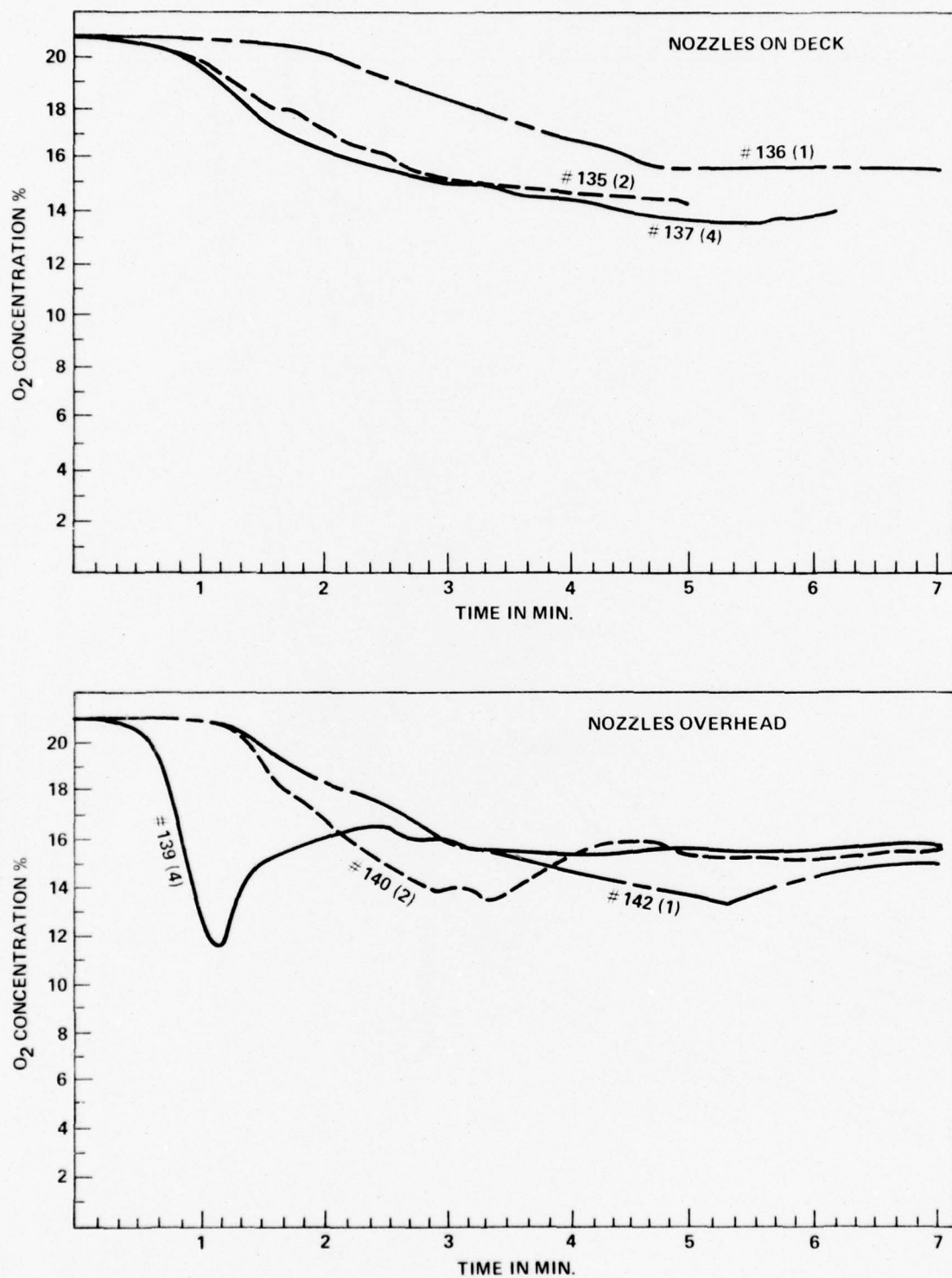


FIG. 3.10 VARIATION IN O₂ CONCENTRATION DURING METHANOL SPRAY FIRES
IN 1050 FT³ TEST CELL

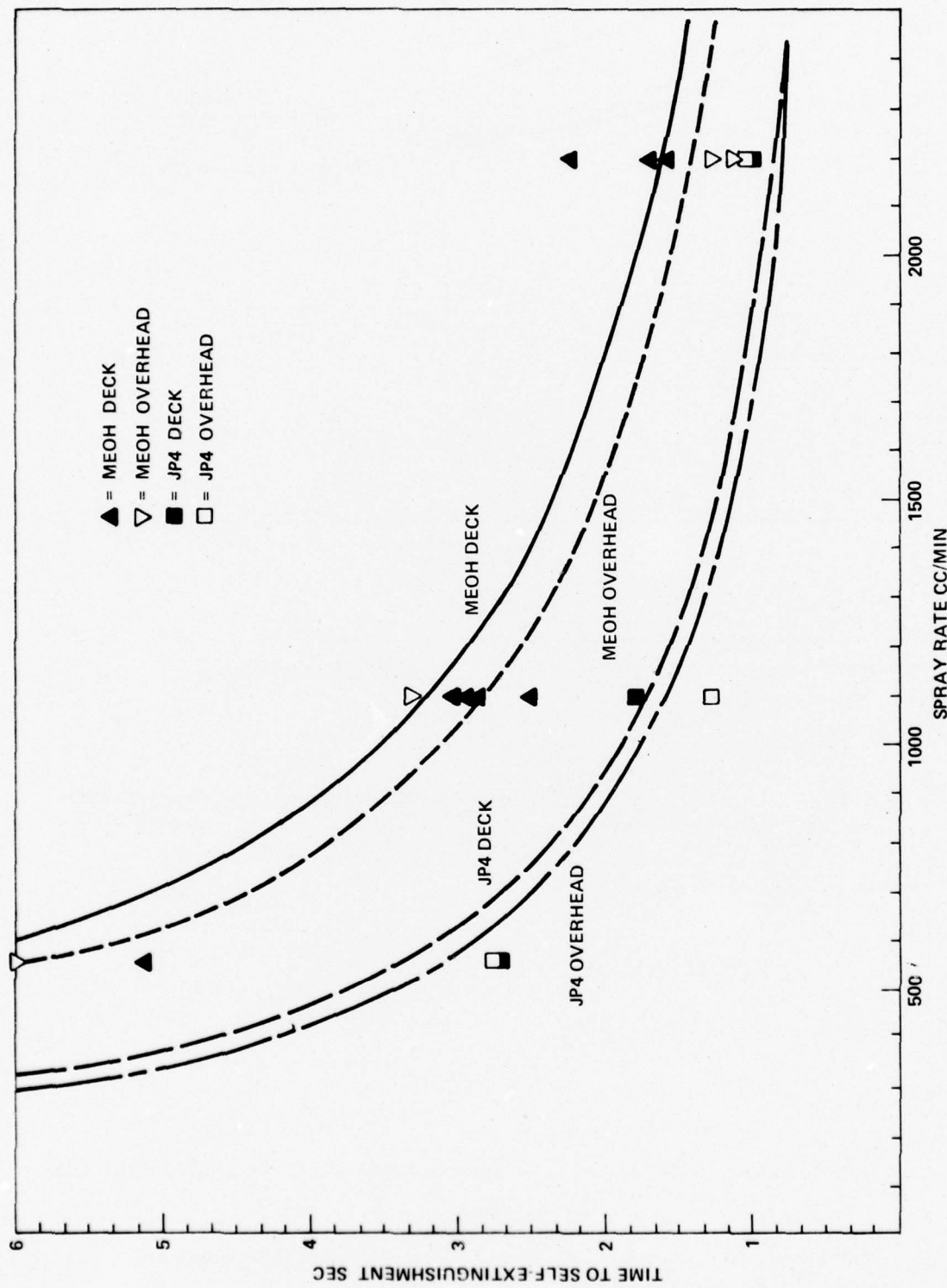


FIG. 3.11 EFFECT OF SPRAY RATE ON EXTINGUISHMENT TIME FOR JP-4 AND METHANOL FIRES IN SEALED 1050 FT³ TEST CELL

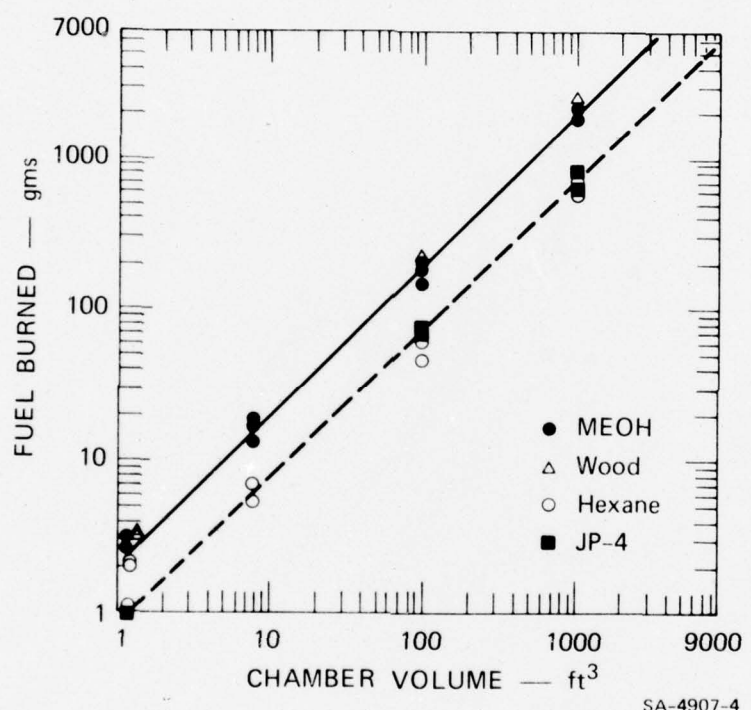


FIG. 3.12 FUEL BURNED IN A SEALED COMPARTMENT
AS A FUNCTION OF CHAMBER SIZE

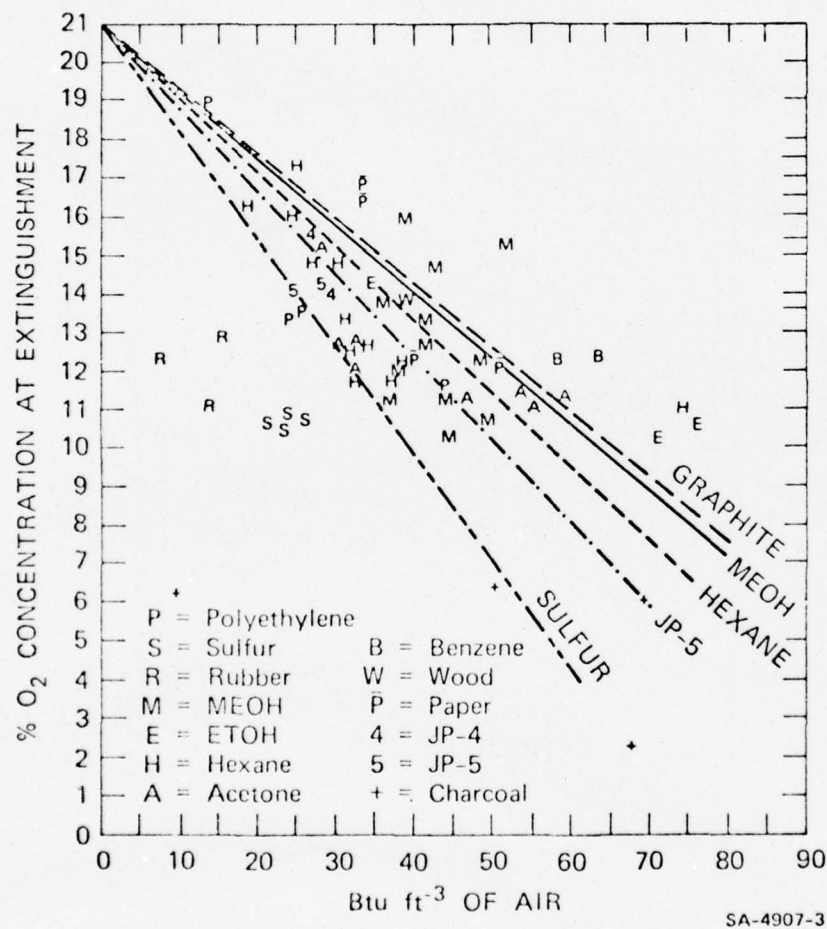


FIG. 3.13 COMPARISON OF THEORETICAL AND EXPERIMENTAL VALUES FOR THE AVAILABLE ENERGY PER FT³ OF AIR IN A SEALED COMPARTMENT WHEN BURNING VARIOUS FUELS

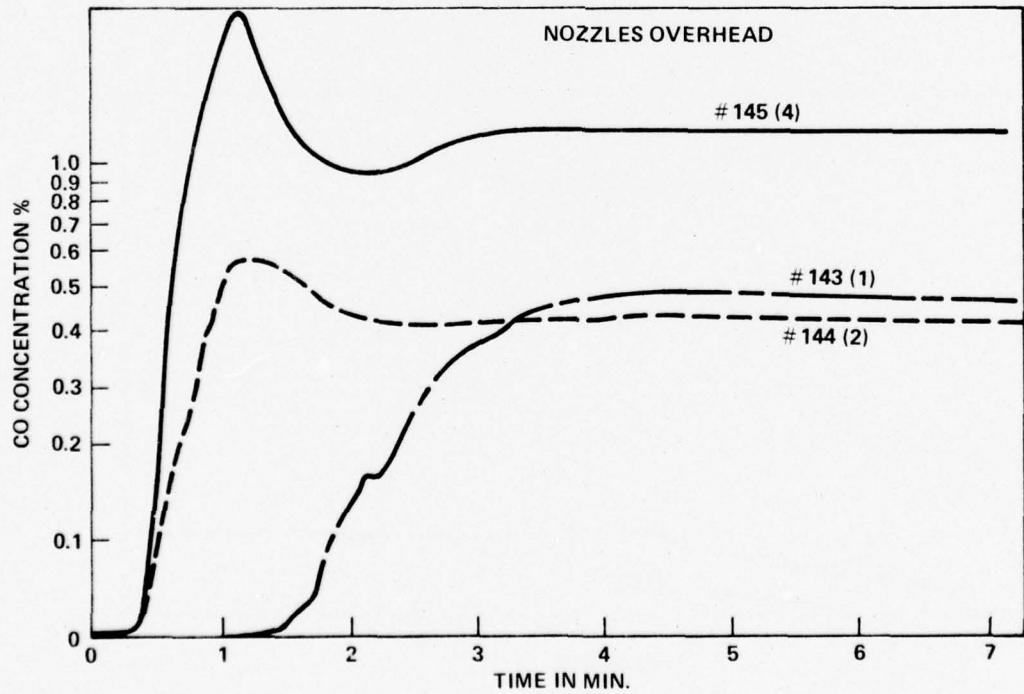
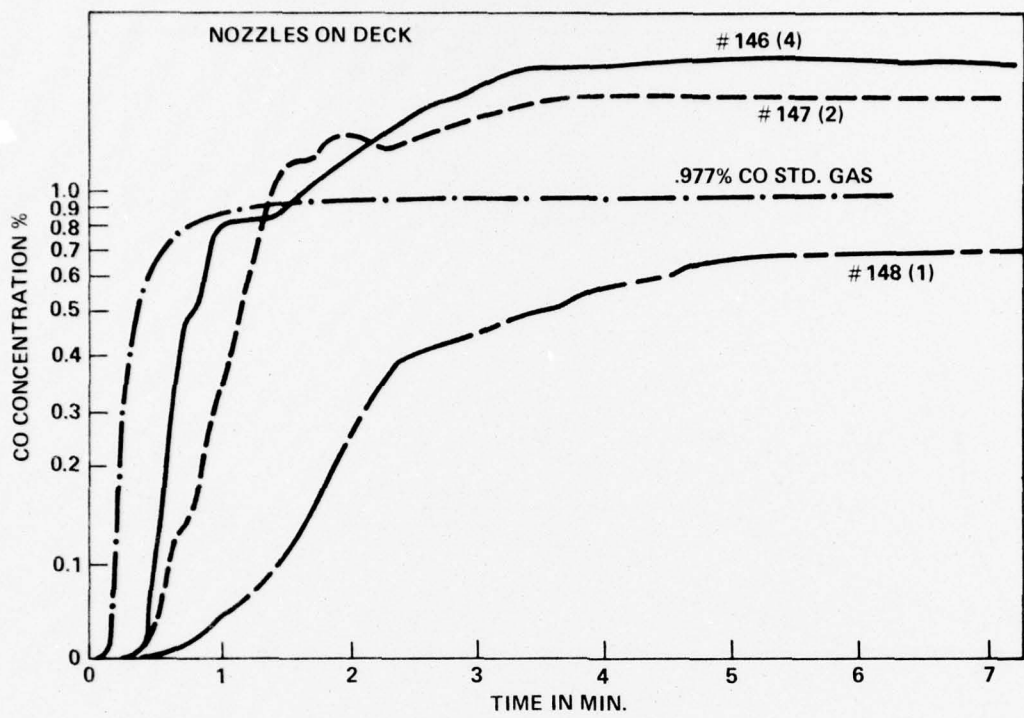


FIG. 3.14 VARIATION IN CO CONCENTRATION DURING JP-4 SPRAY FIRES
IN 1050 FT³ SEALED CHAMBER

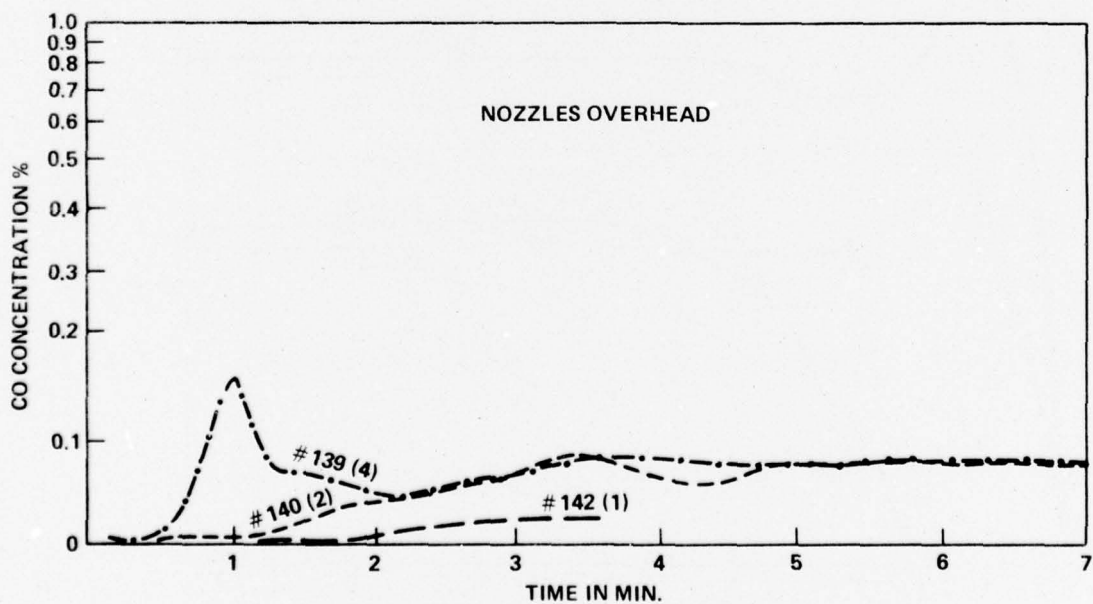
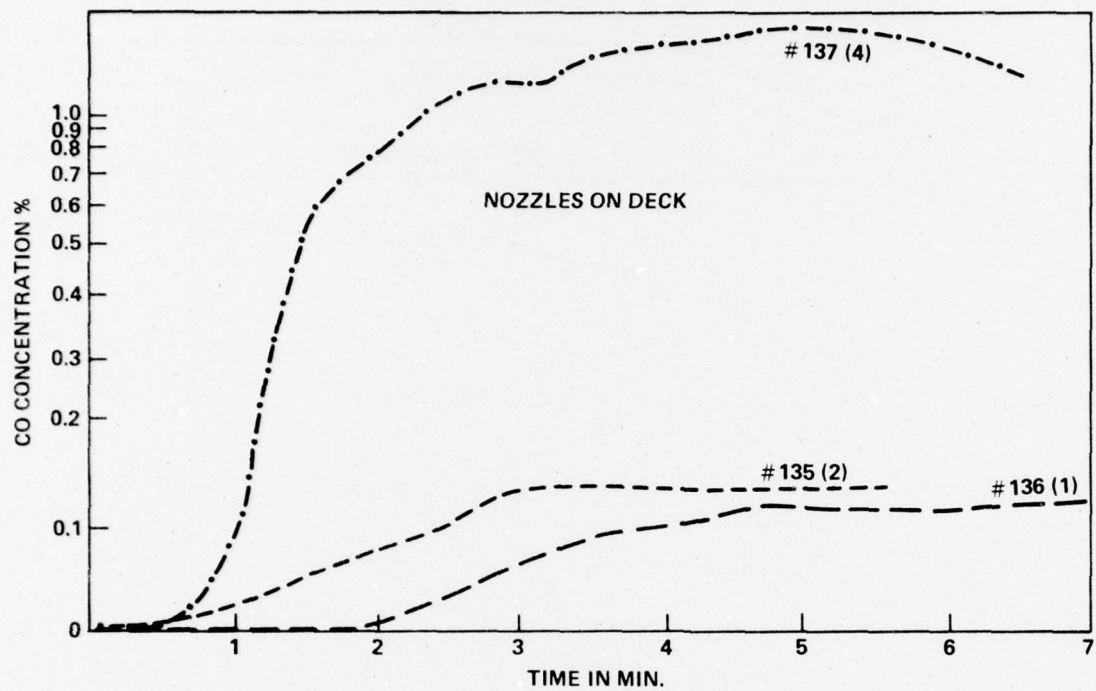


FIG. 3.15 VARIATION IN CO CONCENTRATIONS DURING MeOH SPRAY FIRES
IN 1050 FT³ SEALED CHAMBER

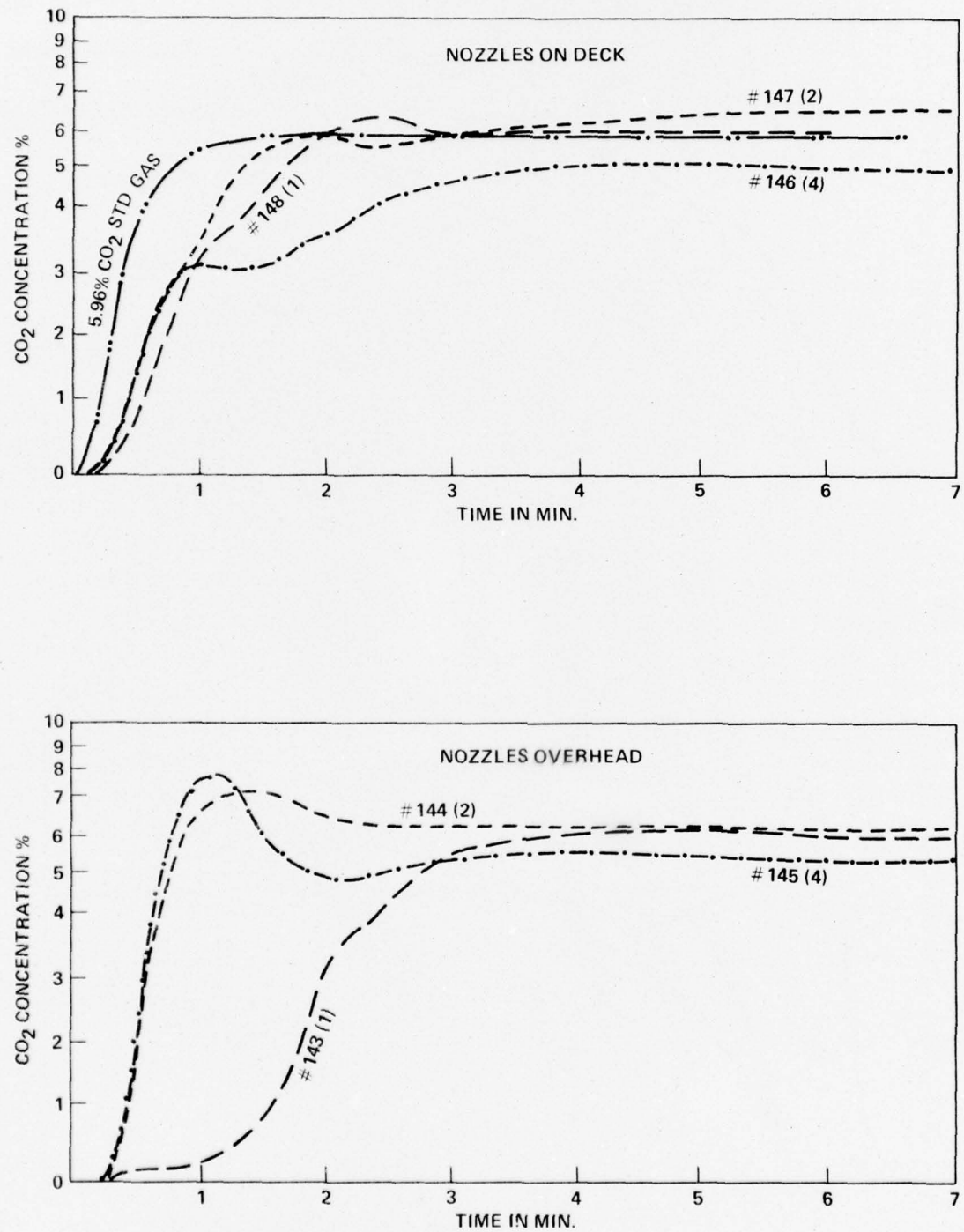


FIG. 3.16 VARIATION IN CO₂ CONCENTRATION DURING JP-4 SPRAY FIRES
IN 1050 FT³ SEALED CHAMBER

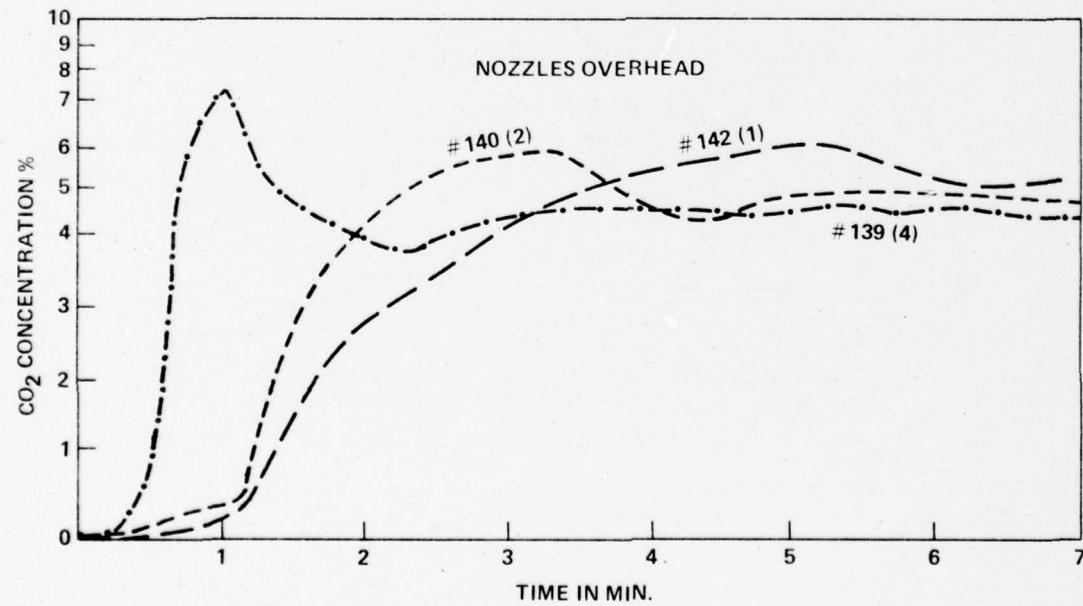
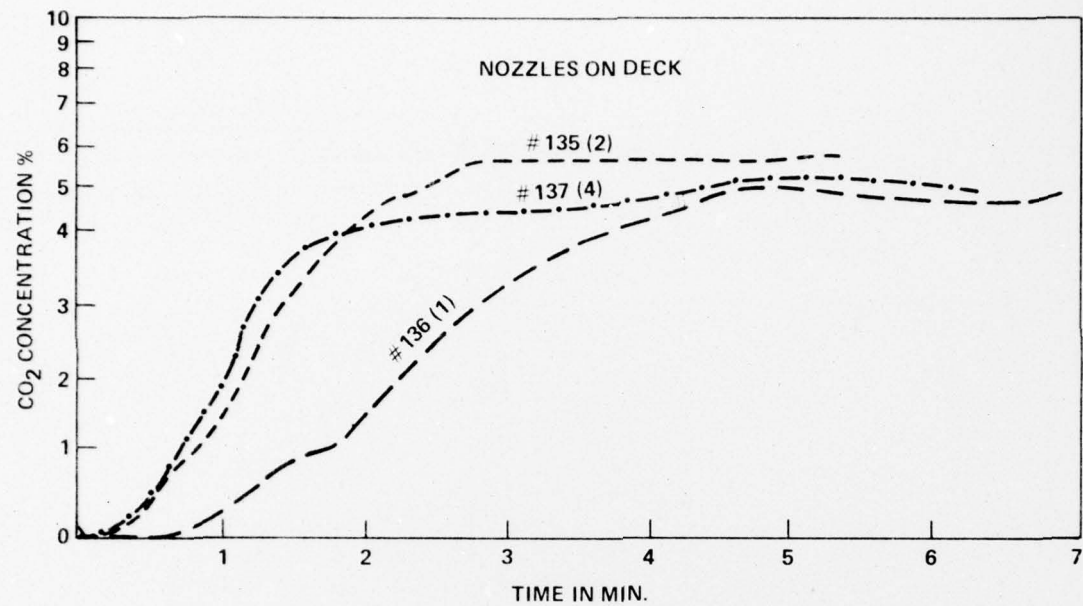


FIG. 3.17 VARIATION IN CO₂ CONCENTRATION DURING MeOH SPRAY FIRES
IN 1050 FT³ SEALED CHAMBER

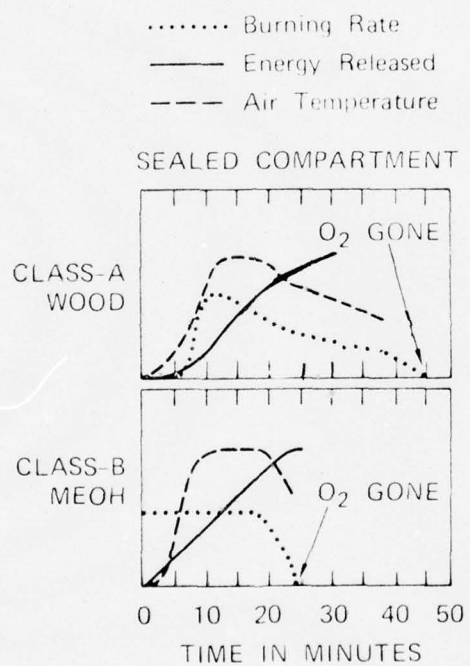
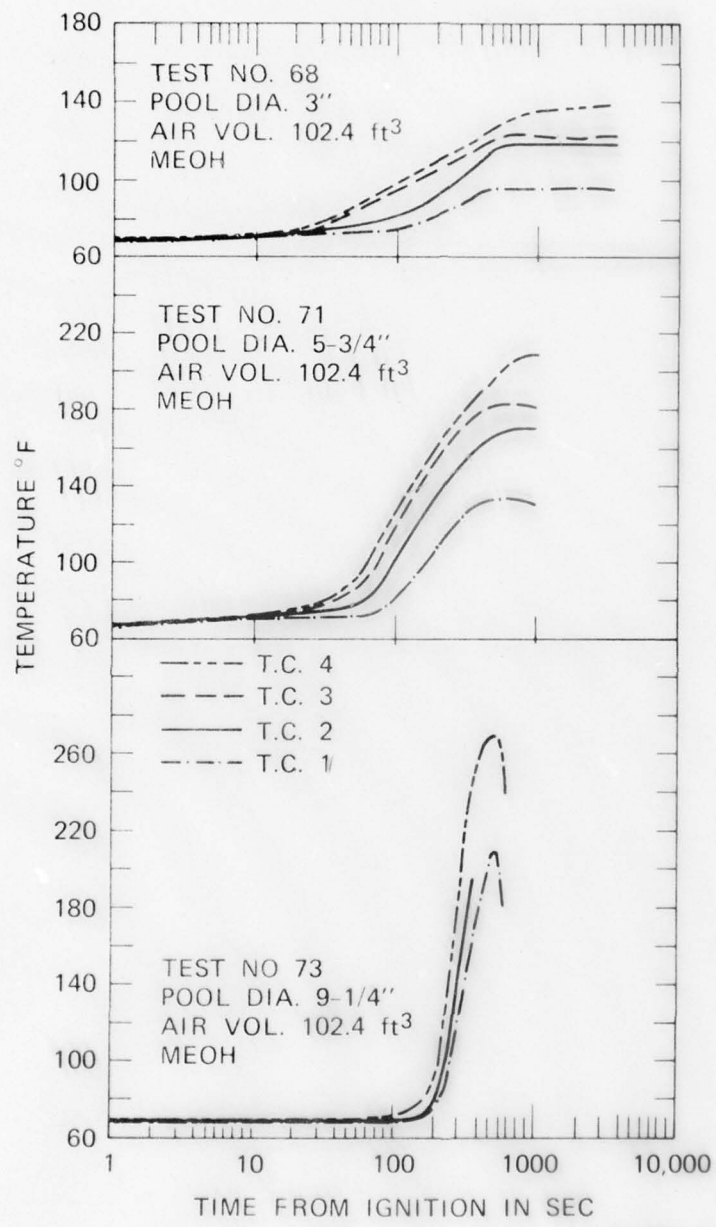
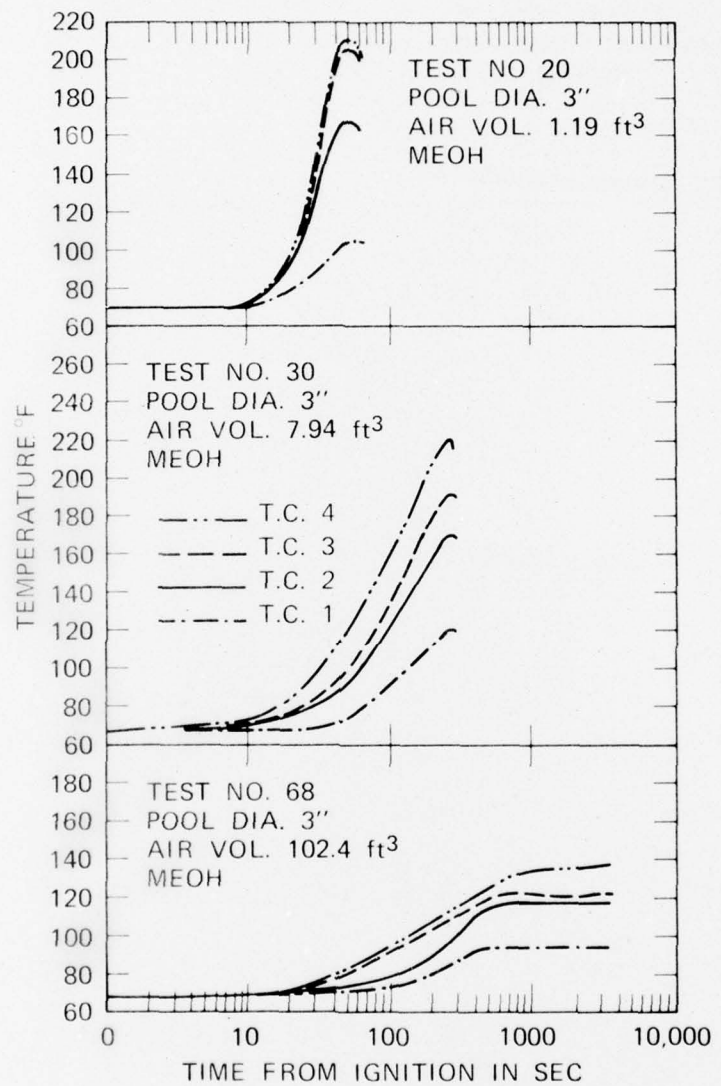


FIG. 3.18 BURNING RATES AND TOTAL ENERGY RELEASE AS OBTAINED FROM WEIGHT LOSS MEASUREMENTS



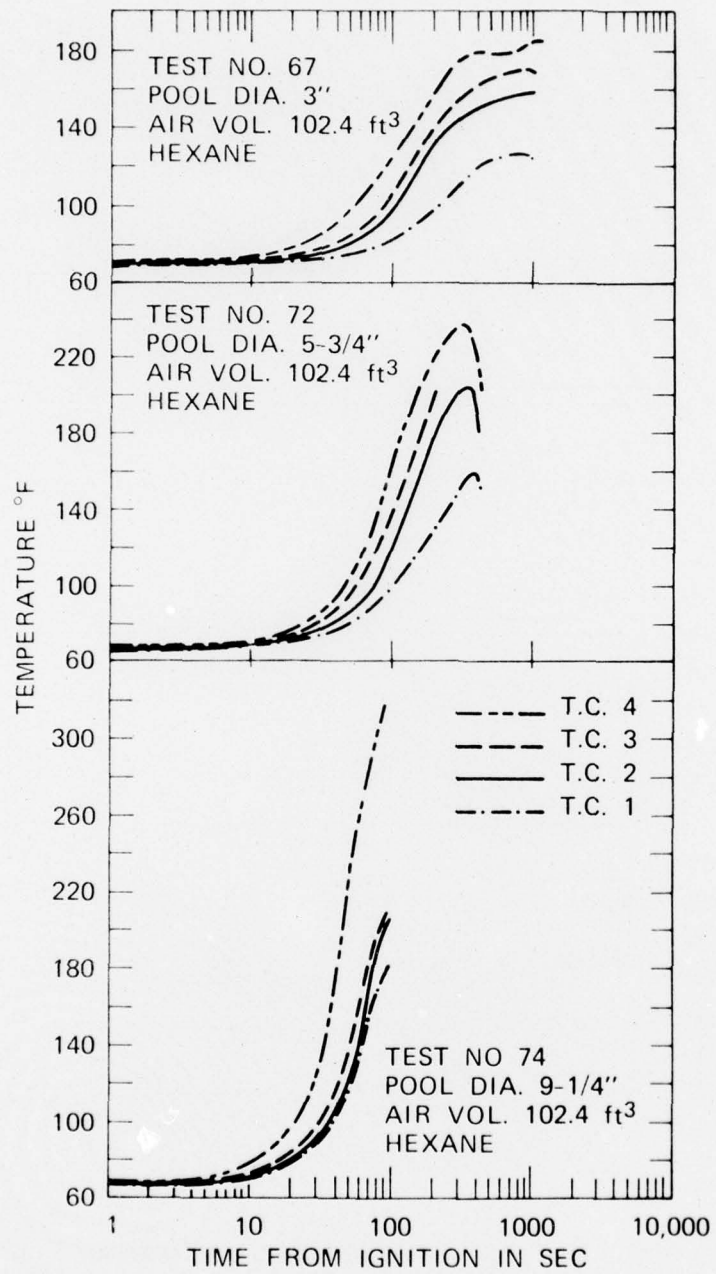
SA-4907-8

FIG. 3.19A SPATIAL AND TEMPORAL CHARACTERISTICS
OF VARIOUS SIZED METHANOL FIRES IN A
SEALED COMPARTMENT



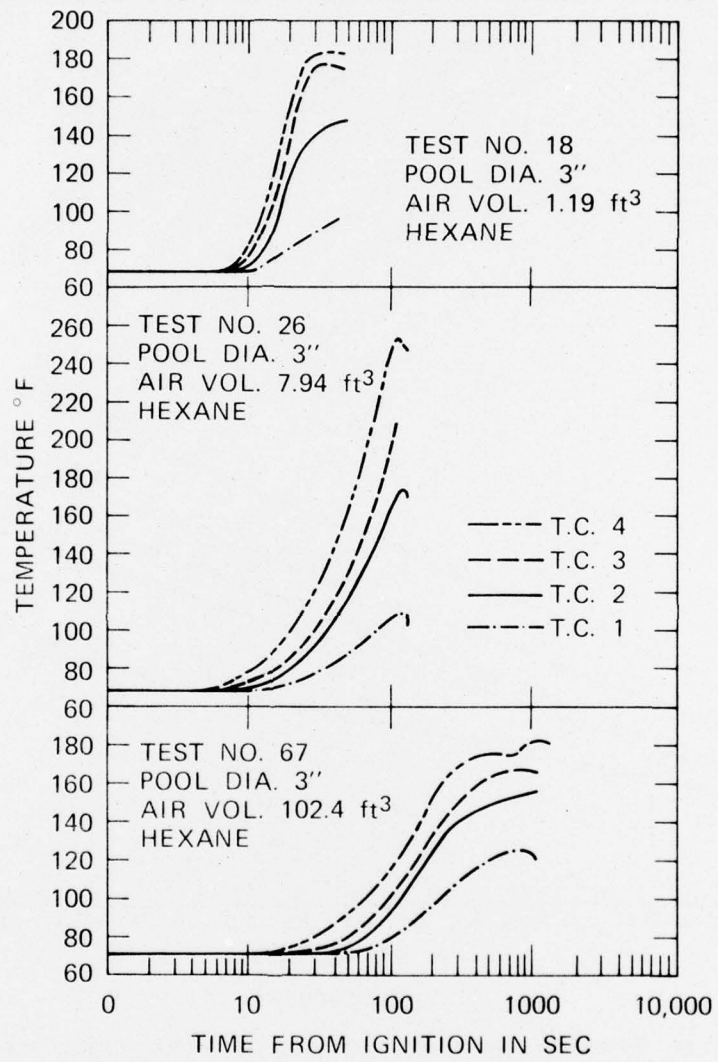
SA-4907-7

FIG. 3.19B SPATIAL AND TEMPORAL CHARACTERISTICS
OF CONSTANT AREA METHANOL FIRES IN
SEALED COMPARTMENTS



SA-4907-6

FIG. 3.20A SPATIAL AND TEMPORAL CHARACTERISTICS
OF VARIOUS SIZED HEXANE FIRES IN A SEALED
COMPARTMENT



SA-4901-9

FIG. 3.20B SPATIAL AND TEMPORAL CHARACTERISTICS
 OF CONSTANT AREA HEXANE FIRES IN SEALED
 COMPARTMENTS

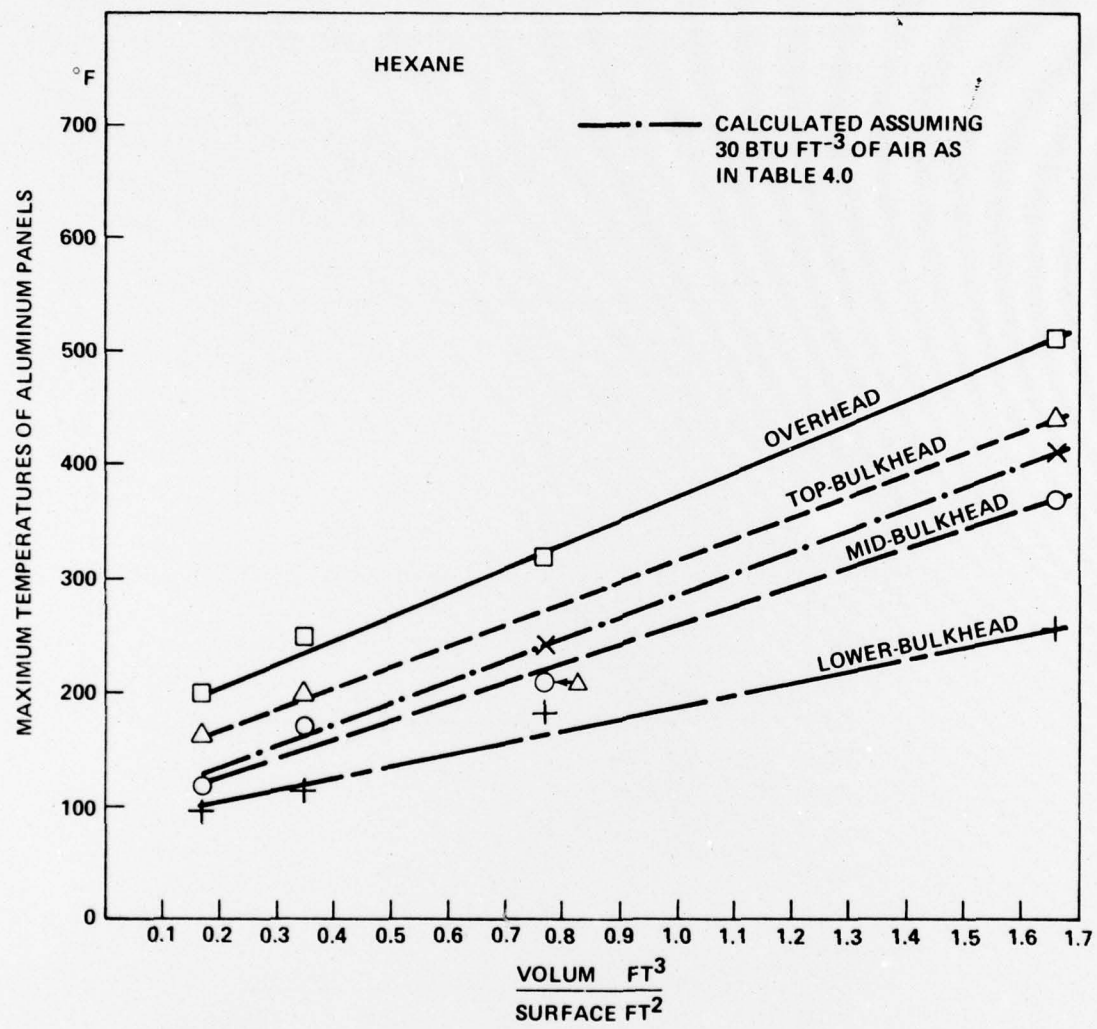


FIG. 3.21 EFFECT OF CHAMBER VOLUME TO SURFACE RATIO ON THE MAXIMUM TEMPERATURES REACHED BY THE VARIOUS ALUMINUM PANELS OF FIG. 2.5 AND 2.6 DURING HEXANE FIRES

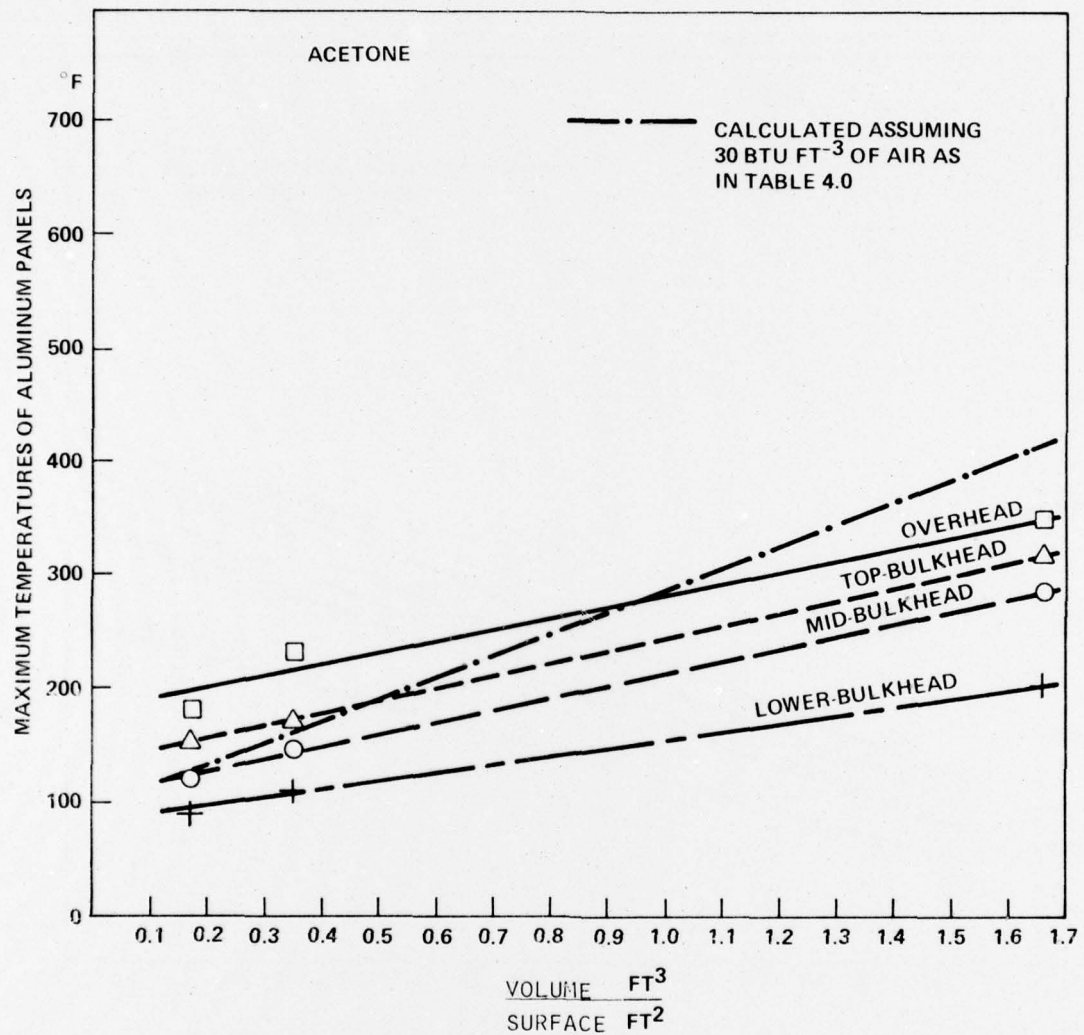


FIG. 3.22 EFFECT OF CHAMBER VOLUME TO SURFACE RATIO ON THE MAXIMUM TEMPERATURES REACHED BY THE VARIOUS ALUMINUM PANELS OF FIG. 2.5 AND 2.6 DURING ACETONE FIRES

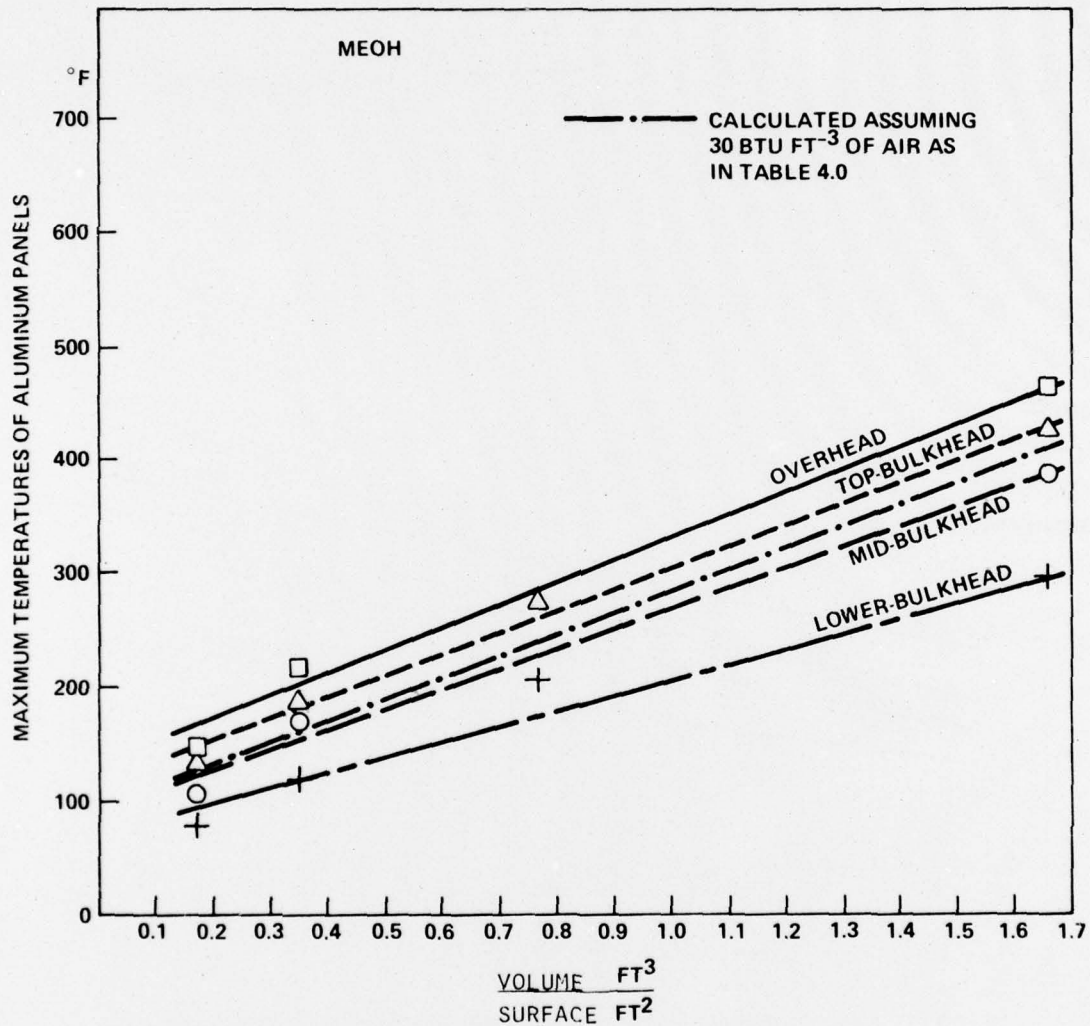


FIG. 3.23 EFFECT OF CHAMBER VOLUME TO SURFACE RATIO ON THE MAXIMUM TEMPERATURES REACHED BY THE VARIOUS ALUMINUM PANELS OF FIG. 2.5 AND 2.6 DURING METHANOL FIRES

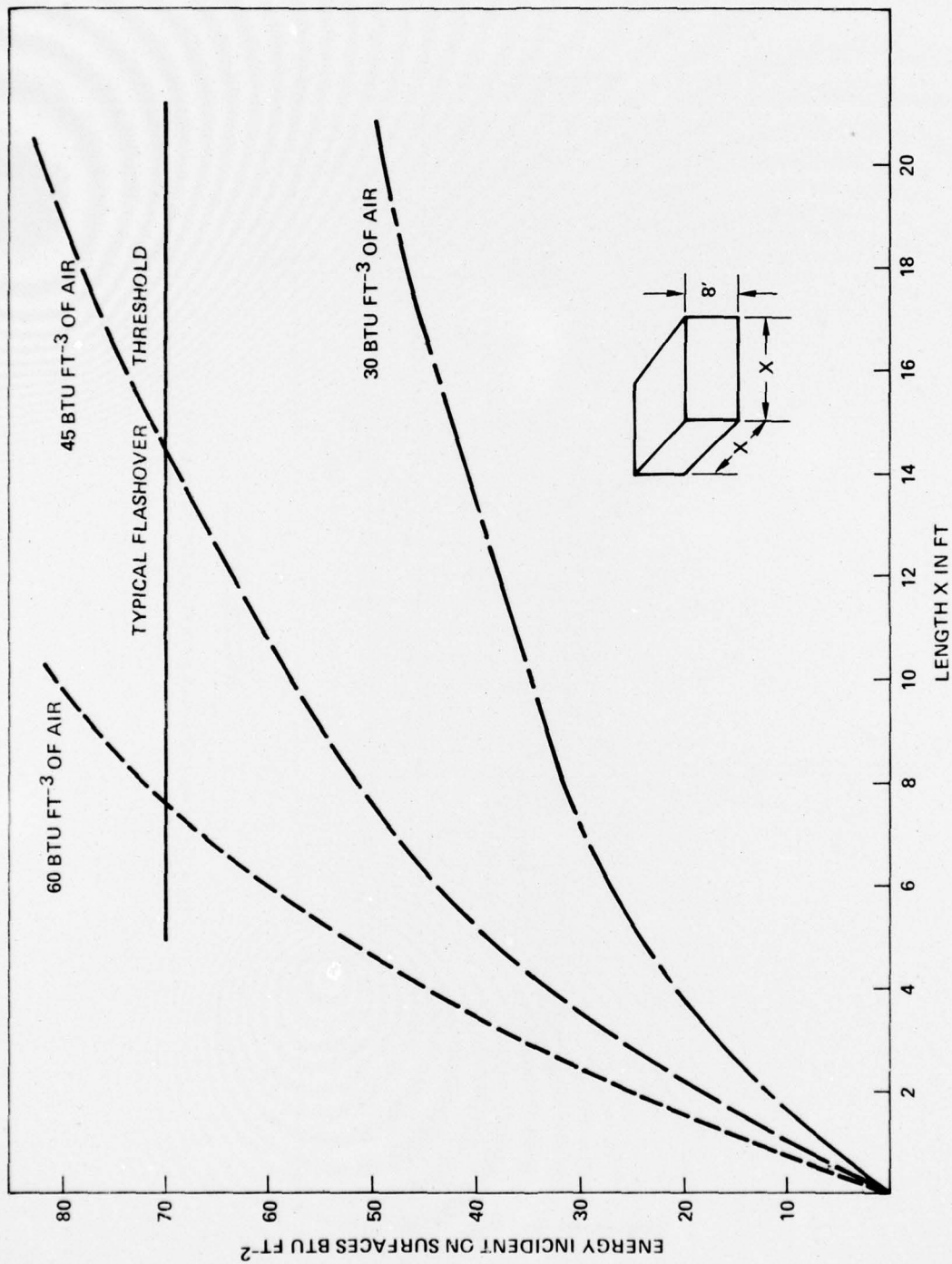


FIG. 4.0 EFFECT OF CHAMBER SIZE AND THE HEAT LIBERATED BY BURNING A CUBIC FOOT OF AIR ON THE THERMAL INSULT ARRIVING AT THE BOUNDARIES OF A SIMPLE ADIABATIC CHAMBER

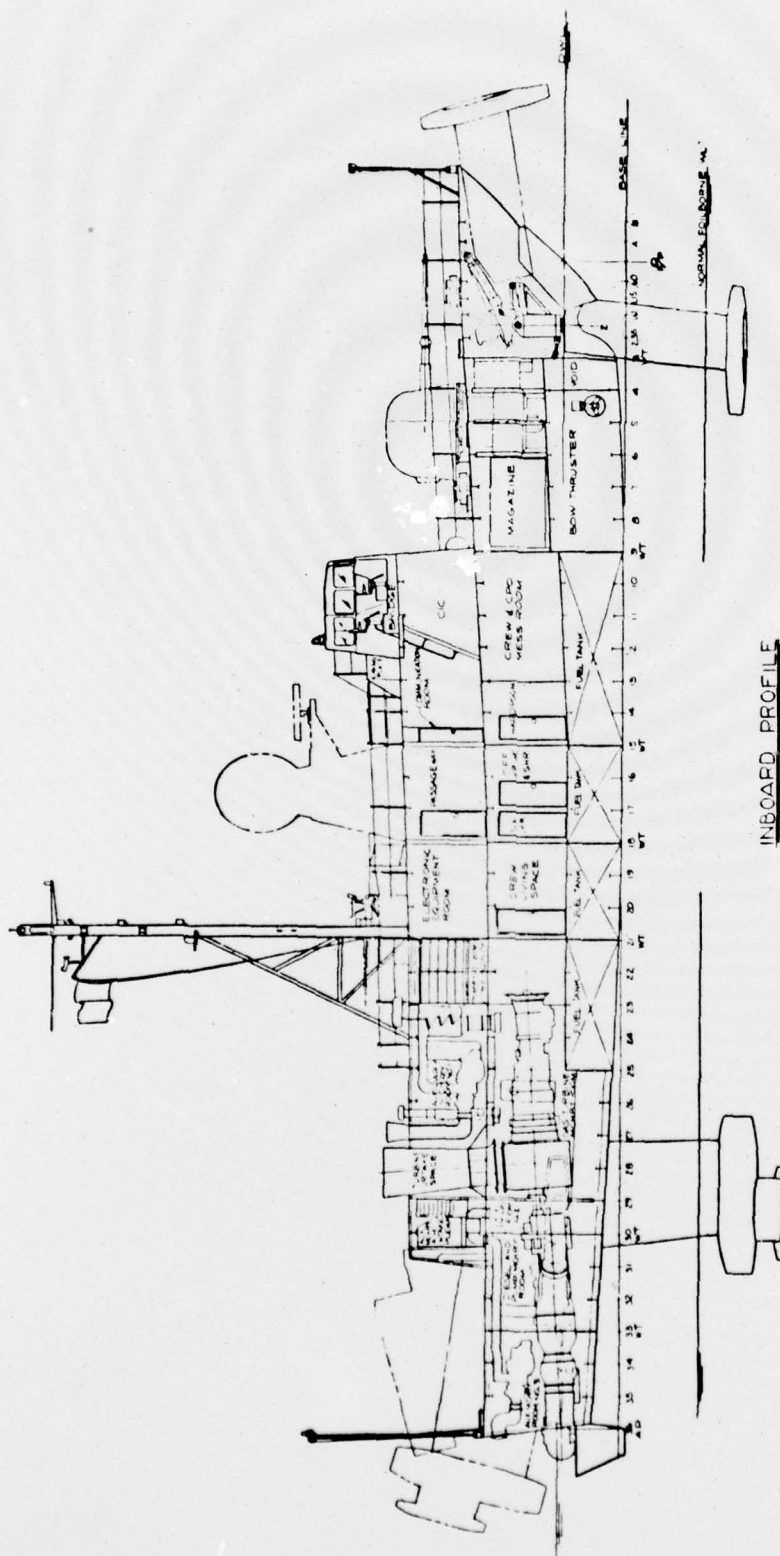


FIG. 4.1 COMPARTMENT ARRANGEMENTS FOR THE PHM-1

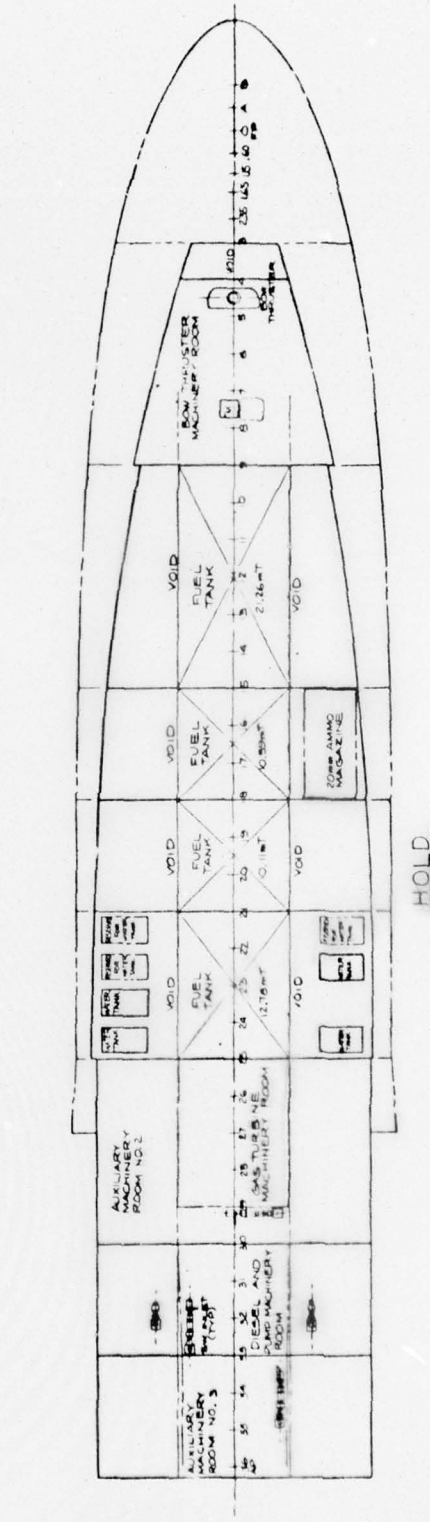
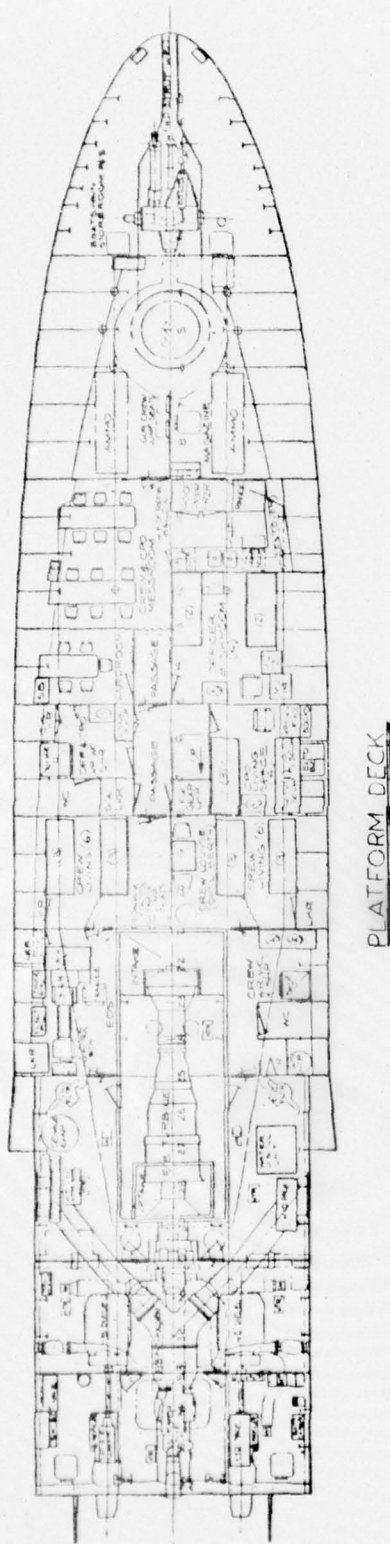
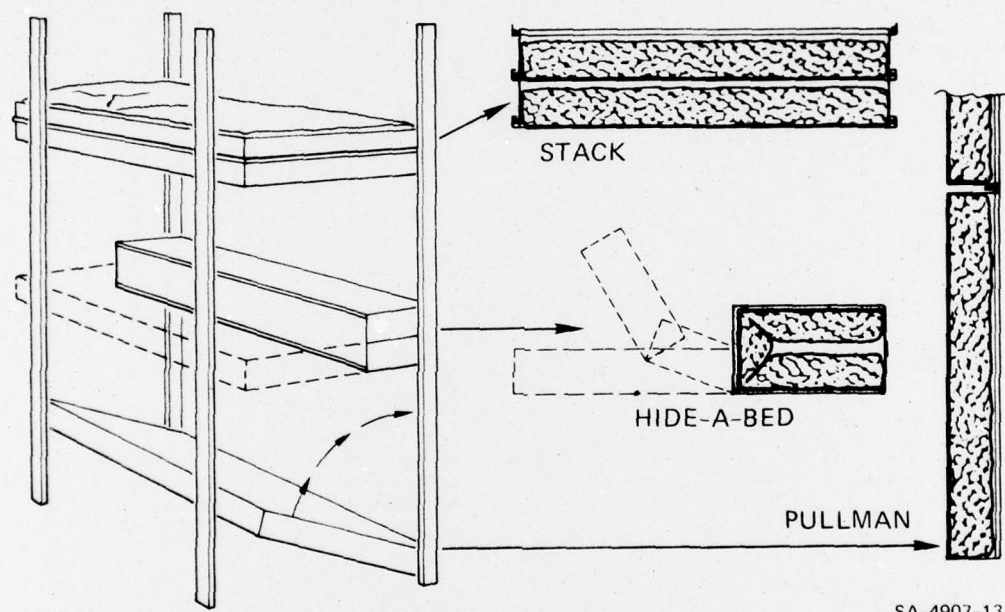


FIG. 4.1 COMPARTMENT ARRANGEMENTS FOR THE PHM-1 (CON'T)



SA-4907-13

FIG. 4.2 ENCLOSED BEDDING TECHNIQUES

DISTRIBUTION

	Copies
Naval Sea Systems Command Washington, D.C. 20362	
Attn: Mr. Carl H. Pohler, Code 0351	1
Mr. David Kay, Code 04H6	1
Dr. John Huth, Code 03C	1
Mr. S. R. Marcus, Code 03B	1
Technical Library, Code SEA-09G32	2
Naval Ship Engineering Center Center Building, Prince Georges Center Hyattsville, Maryland 20782	
Attn: Mr. Ben Leotta, Code 6105	1
Mr. Arthur Marchand, Code 6105E2	1
Mr. Robert McCann, Code 6154F	1
Mr. Edward Shedlock, Code 6154F	1
Naval Air Systems Command Washington, D.C. 20361	
Attn: Mr. Robert H. Krida, AIR-3034	1
Mr. R. E. Forman, Code 53433A	1
Chief of Naval Material Naval Material Command Department of the Navy Crystal Plaza #5 2211 Jefferson David Highway Arlington, Virginia 20360	
Attn: Capt. J. L. McVoy, Code 00F	1
Mr. R. L. Darwin, Code 00F1	1
Mr. O. J. Remson, MAT 033B	1
Naval Facilities Engineering Center 200 Stovall Street Alexandria, Virginia 22332	
Attn: Mr. Stephen M. Hurley, Code 0321B	1
Mr. Richard E. Richtmer, Code 10F	1
Mr. H. T. Anderson, Code IC55	1
Naval Facilities Engineering Center 1220 Pacific Highway San Diego, California 93132	
Attn: Don Sarrie, Area Fire Marshall	1

NSWC/WOL/TR 76-125

DISTRIBUTION (Continued)

	Copies
Naval Weapons Center China Lake, California 93555 Attn: Mr. John O'Malley, Code 4571	1
Applied Physics Laboratory Johns Hopkins University John Hopkins Road Laurel, Maryland 20810 Attn: Dr. Robert Fristrom Document Library	1 1
Naval Ships Research and Development Laboratory Annapolis, Maryland 21402 Attn: Mr. Alton Waldron Mr. Robert Fonsler	1 1
Naval Research Laboratory Chemical Dynamics Branch Chemistry Division Washington, D.C. 20390 Attn: Dr. Homer W. Carhart, Code 6180	1
Naval Civil Engineering Laboratory Port Hueneme, California 93041 Attn: Dr. Tim T. Fu	1
Air Force Weapons Laboratory Kirtland Air Force Base Albuquerque, New Mexico 87117 Attn: WLIL Technical Library	1 1
Institute for Defense Analyses 400 Army-Navy Drive Arlington, Virginia 22202 Attn: Dr. A. Sachs	1
National Bureau of Standards Washington, D.C. 20234 Attn: Mr. Dan Gross Dr. A. F. Robertson Mr. William Parker, Room B66, Technology Bldg.	1 1 1
Office of Assistant Secretary of Navy for Research and Development Pentagon Washington, D.C. 20301 Attn: Dr. Peter Waterman	1

NSWC/WOL/TR 76-125

DISTRIBUTION (Continued)

	Copies
Naval Medical Research Institute Bethesda, Maryland 20014 Attn: Dr. Seymour L. Friess	1
Federal Fire Council 19th and F Streets, N.W. Washington, D.C. 20405	1
Instructor of Fire Service Training Department of Education State of California P.O. Box 48 Igo, California 96047 Attn: Mr. Robert Shaw	1
National Academy of Sciences Advisory Committee on Civil Defense 2101 Constitution Avenue, N.W. Washington, D.C. 20418 Attn: Mr. Richard Park	1
National Academy of Sciences National Research Council Committee on Fire Research 2101 Constitution Avenue, N.W. Washington, D.C. 20418	1
National Science Foundation 1800 G Street, N.W. Washington, D.C. 20006 Attn: Dr. Ralph Long	1
International Association of Fire Fighters 815 16th Street, N.W. Washington, D.C. 20006 Attn: Mr. William D. Buck	1
International Association of Fire Chiefs 232 Madison Avenue New York, New York 10016 Attn: Mr. Donald O'Brien	1
General Services Administration Head, Fire Safety and Mobilization Planning Branch 7th and D Streets, S.W. Room 7922 Washington, D.C. 20405 Attn: Mr. Harold E. Nelson	1

NSWC/WOL/TR 76-125

DISTRIBUTION (Continued)

	Copies
National Fire Protection Association 60 Batterymarch Street Boston, Massachusetts 02110 Attn: Library	1
Science Information Exchange Suite 209 1730 M Street, N.W. Washington, D.C. 20036 Attn: Dr. Vincent Maturi	1
Southwest Research Institute Department of Structural Research Fire Research Section 8500 Culebra Road San Antonio, Texas 78206 Attn: Mr. C. H. Yuill	1
Gage-Babcock and Associates, Inc. 9836 W. Roosevelt West Chester, Illinois 60153 Attn: Mr. B. M. Cohn	1
National Fire Prevention and Control Administration 2400 M Street, N.W. Washington, D.C. 20036 Attn: Dr. Herman Wiseman	1
Factory Mutual Research Corporation 1151 Route 1 Norwood, Massachusetts 02062 Attn: Dr. David E. Breen Mr. M. Miller	1 1
Defense Documentation Center Cameron Station Alexandria, Virginia 22314	12
Stanford Research Institute Building 108 Menlo Park, California 94025 Attn: Mr. Raymond S. Alger	24